

Search for new physics in diphoton events

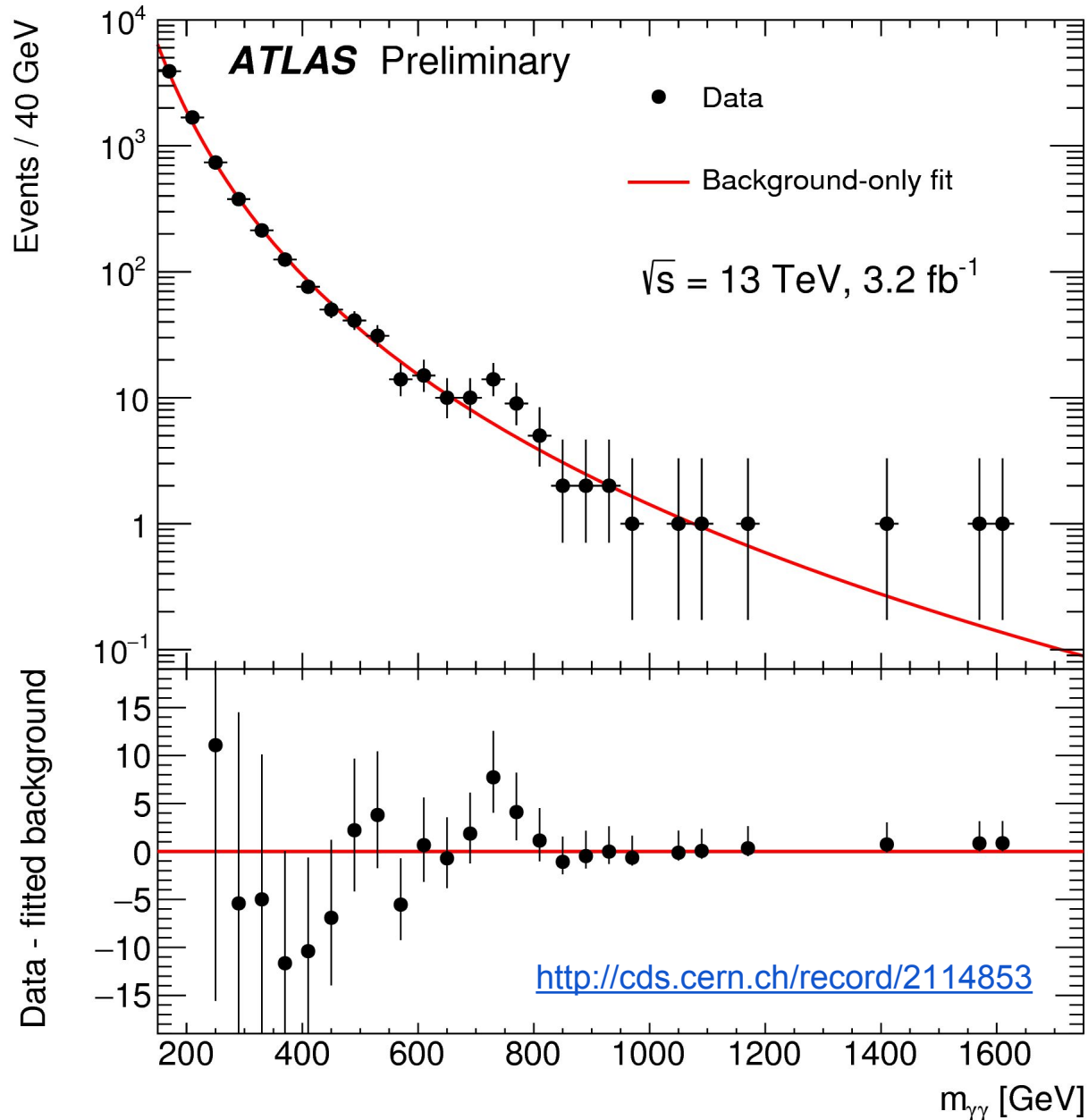
Wine & Cheese Seminar (April 15, 2016)

Chris Meyer

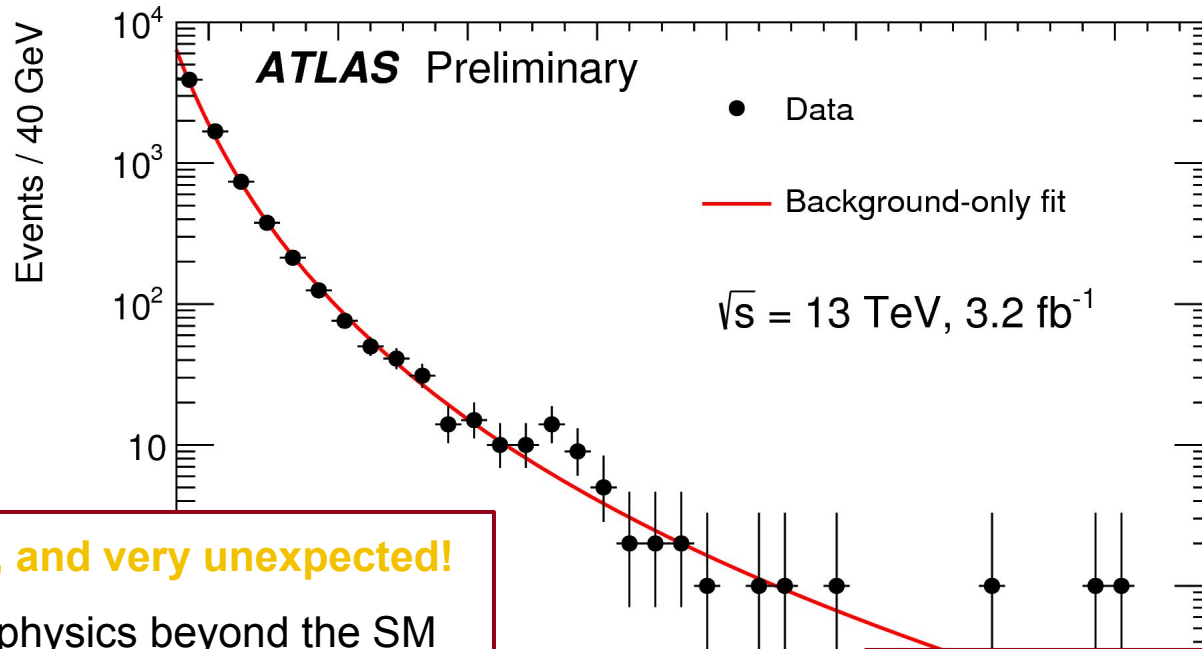
on behalf of the ATLAS Collaboration



You may recall the end of 2015...



You may recall the end of 2015...



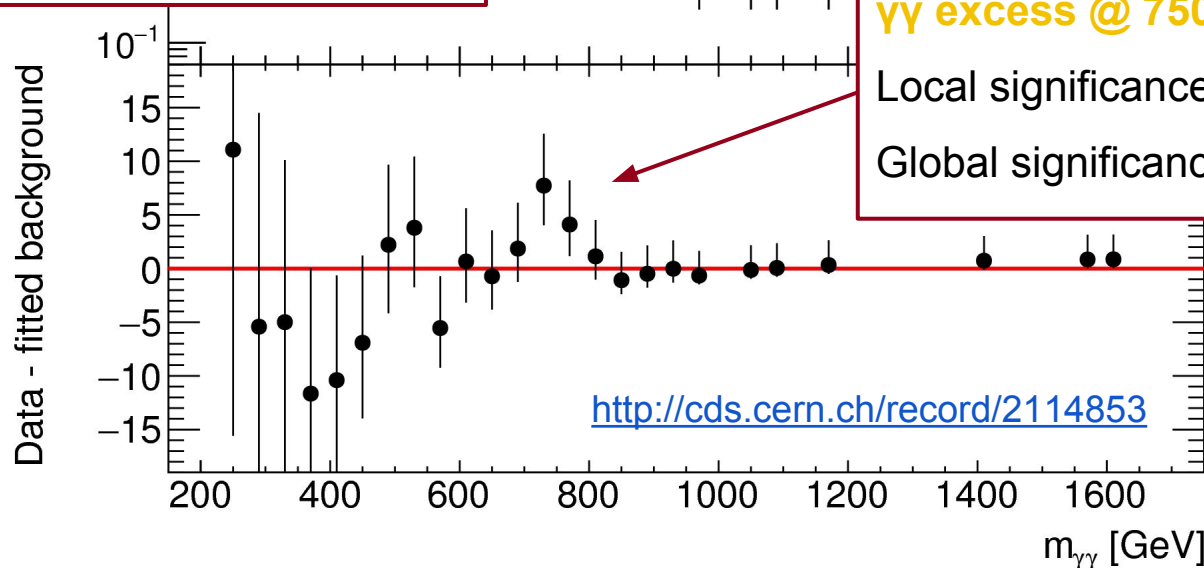
Very exciting, and very unexpected!

- Possible physics beyond the SM

$\gamma\gamma$ excess @ 750 GeV, 6% width

Local significance $p_0 = 3.9 \sigma$

Global significance $Z_0 = 2.3 \sigma$



Theory benchmarks

- Considering two benchmarks → **different kinematic behaviors**
- Spin-0 resonances from theories with extended Higgs sector
 - Isotropic decay in center-of-mass of resonance
 - Produces higher E_T photons than SM background

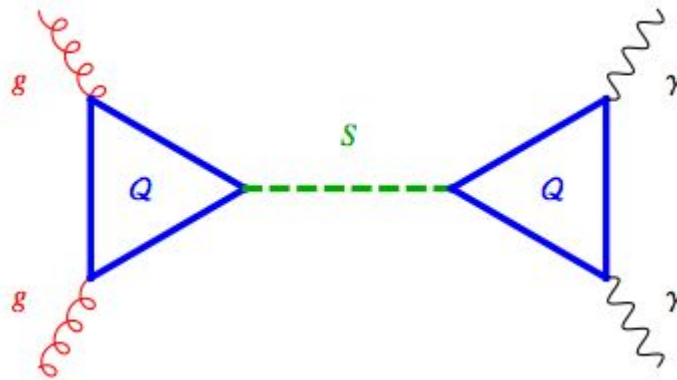
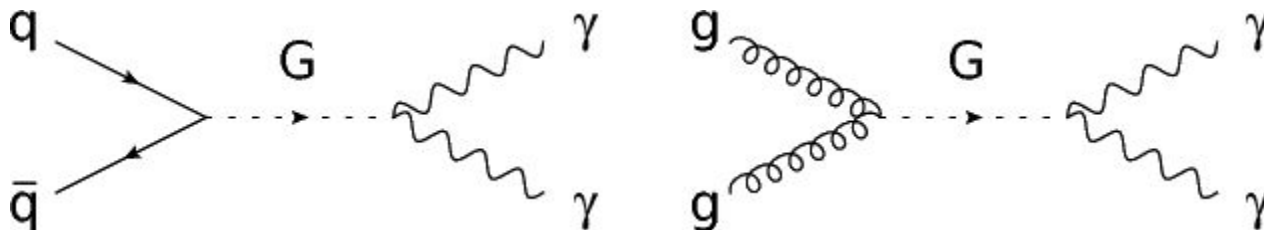


Figure from Résonances Blog

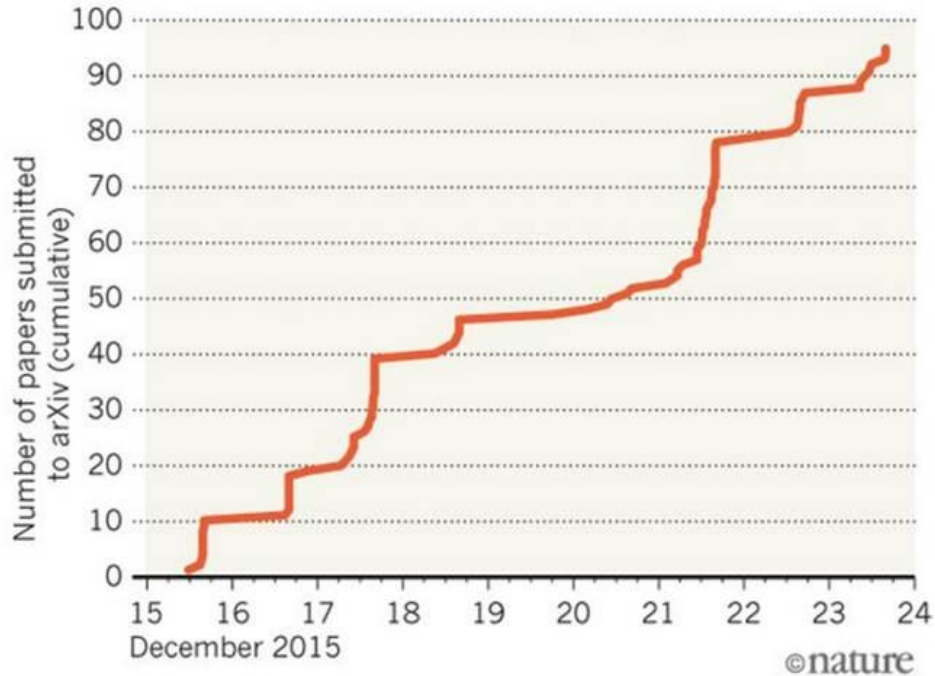
- Spin-2 resonances use Randall-Sundrum model graviton
 - Lightest Kaluza-Klein excitation
 - Dimensionless coupling k/M_{Pl}



Theory benchmarks

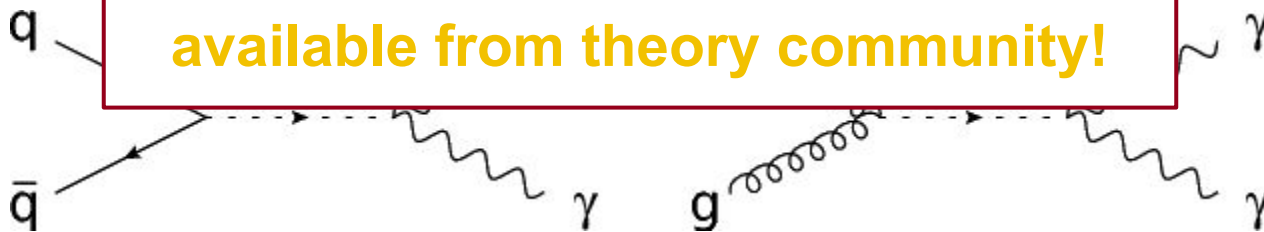
- Considering two benchmarks → **different kinematic behaviors**
- Spin-0 resonances from theories with extended Higgs sector

- Isotropic
- Produced



- Spin-2 resonance
- Lightest
- Dimensional

In reality, many other models available from theory community!

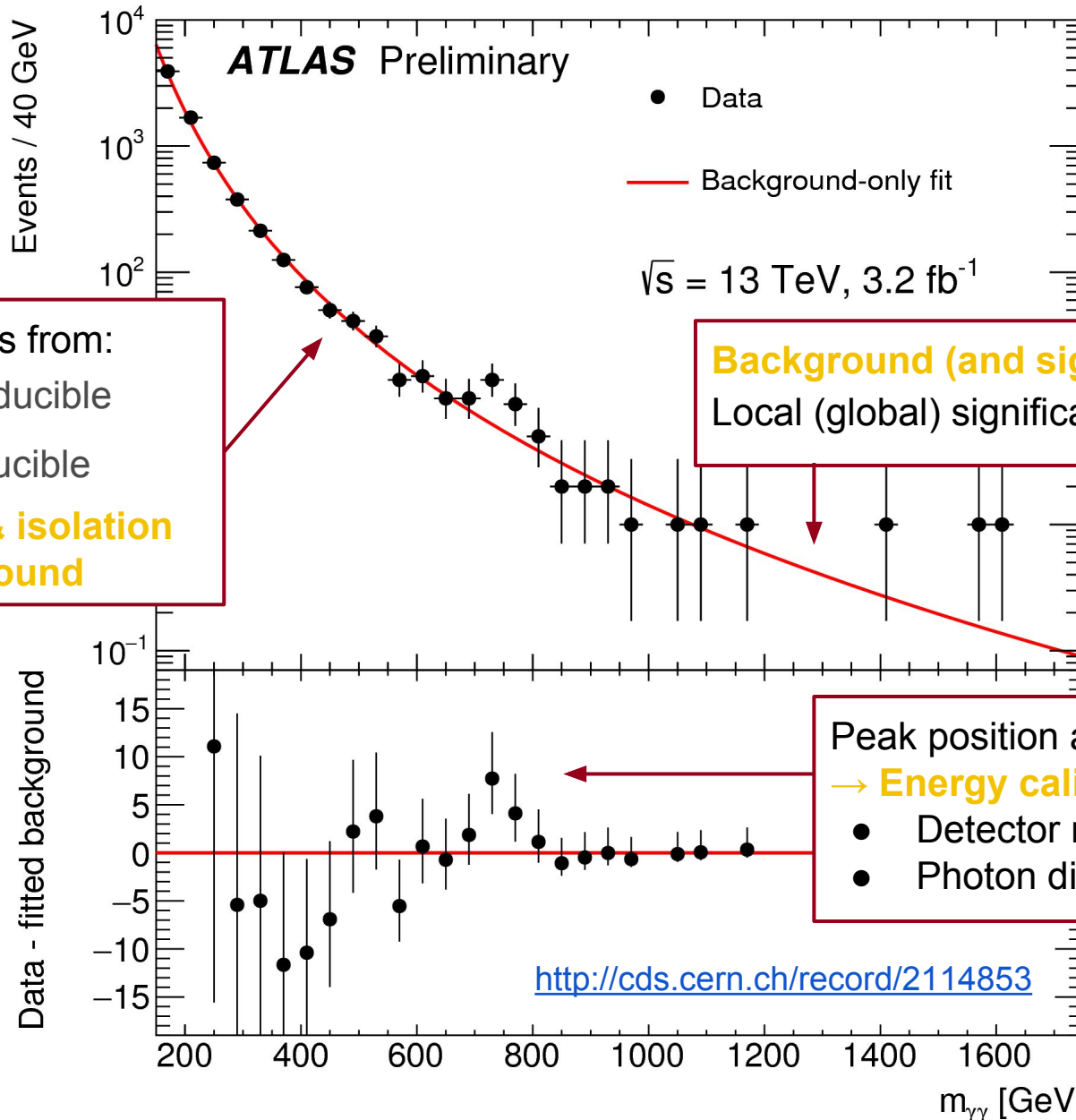


viton

Overview of talk

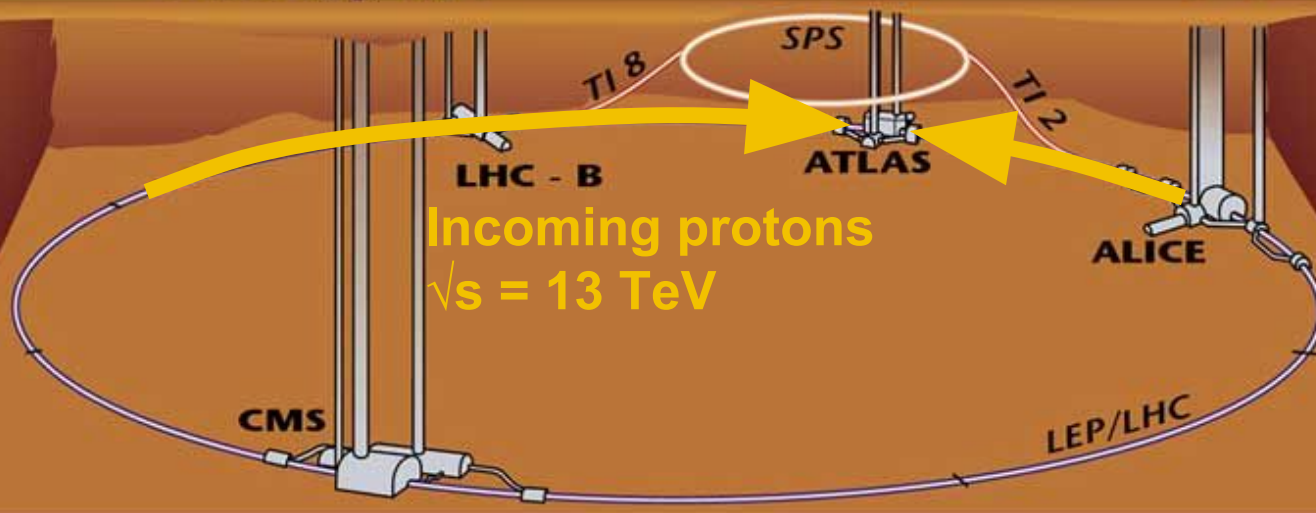
- Summary of recent diphoton search
 - [ATLAS-CONF-2016-018](#)
- Overview of photon performance
 - Identification and isolation
 - Calibration and energy resolution uncertainty
- Signal and background modeling
- Results of updated 13 TeV analysis
 - Spin-0 analysis → same selection as December
 - Spin-2 analysis → prepared, but not released in December
- What are the next steps?

Important points from 2015



Recording the dataset

- Proton-proton collisions at 13 TeV with 25 ns bunch spacing
 - Average interactions / bunch crossing: $\langle \mu \rangle = 13.7$
 - This level of “pileup” events well understood from 2012 running
- Diphoton trigger decides which events to record
 - Close to 99% efficient for events passing final selection



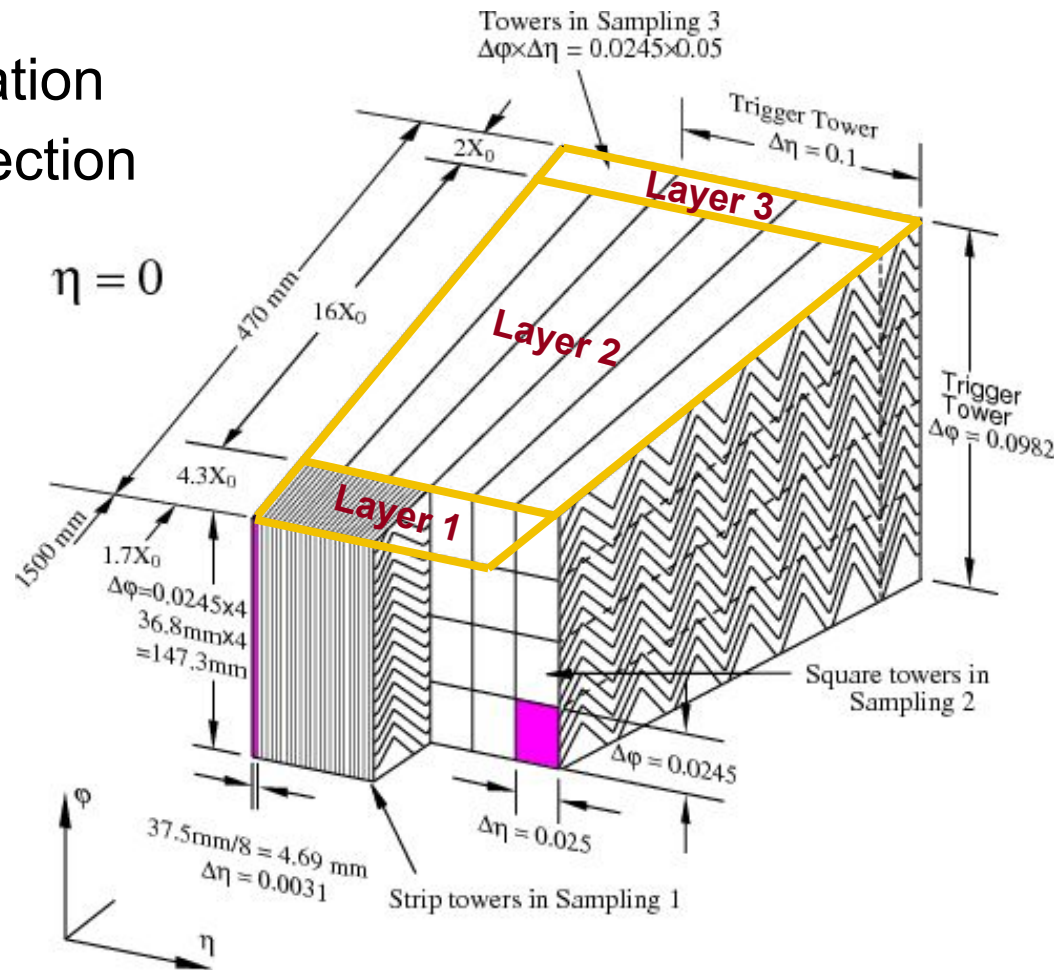
Electromagnetic calorimeters

- Liquid Argon (LAr) sampling calorimeter **designed for this!**
- 4 longitudinal layers
 - Thin pre-sampling (PS) layer in front
 - 3 sampling layers

- Shower shapes → identification
- Provides coarse photon direction
- Resolution follows:

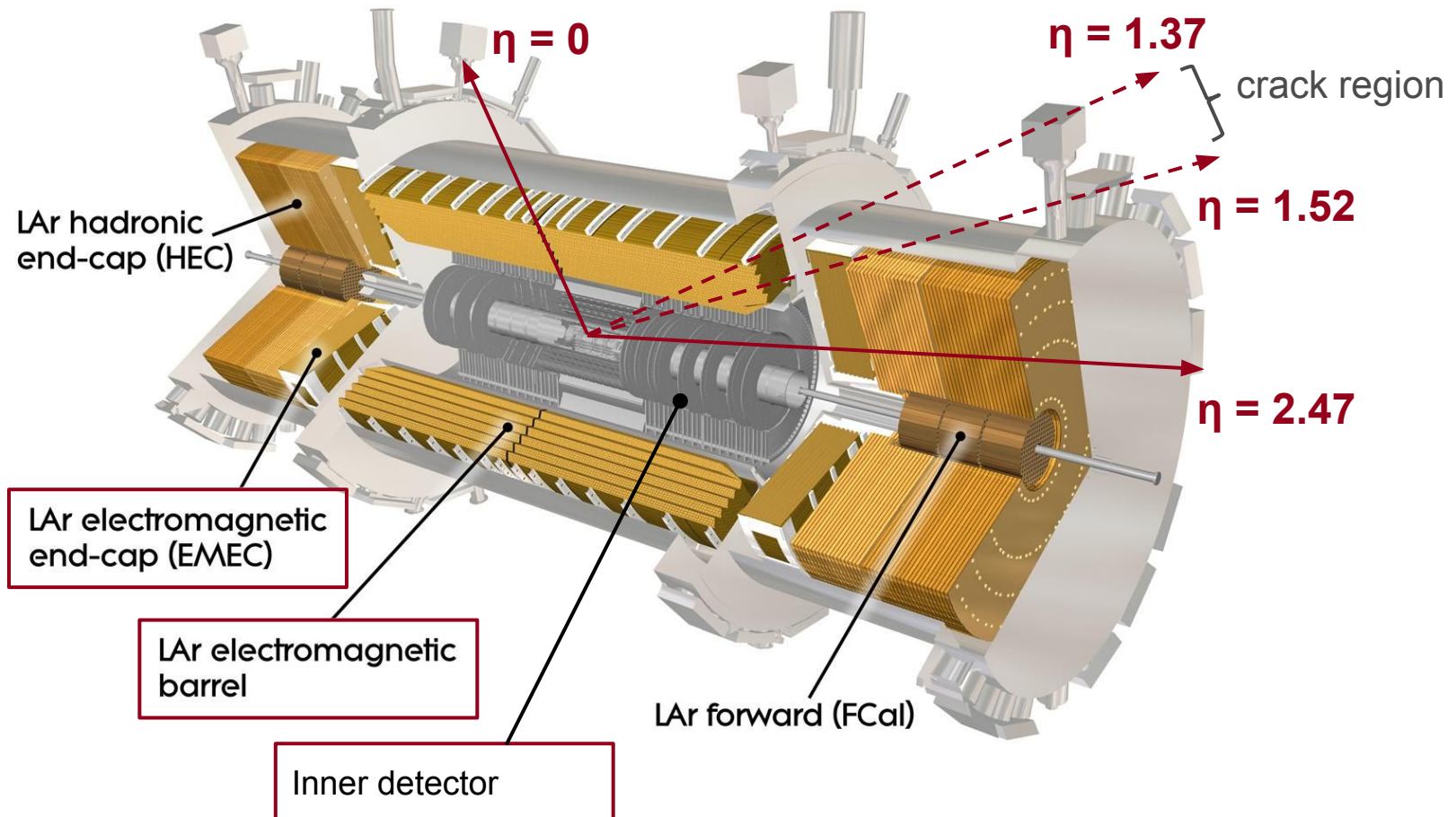
$$\frac{\sigma}{E} = \frac{a}{\sqrt{E}} \oplus \frac{b}{E} \oplus c$$

- At large photon E_T dominated by $c = 0.6-1.5\%$



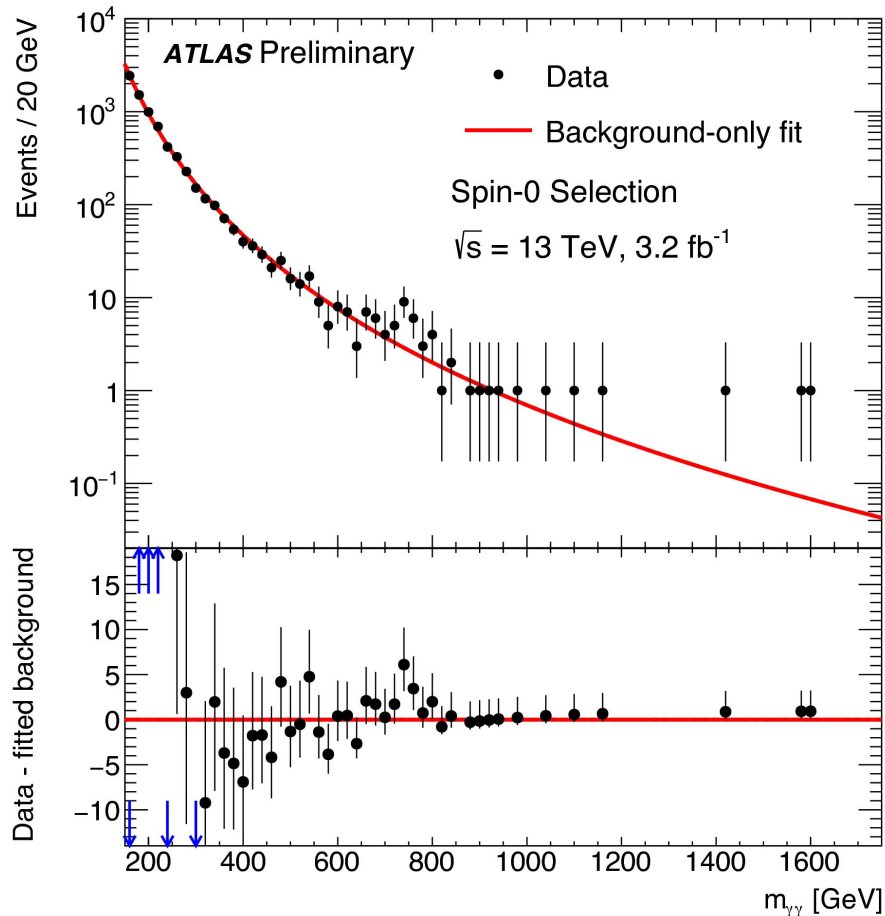
Electromagnetic calorimeters

- Dead material in crack region leads to poor photon reconstruction
 - Photons in this region are excluded from the result
- Inner detector provides tracking for electrons / photon conversions

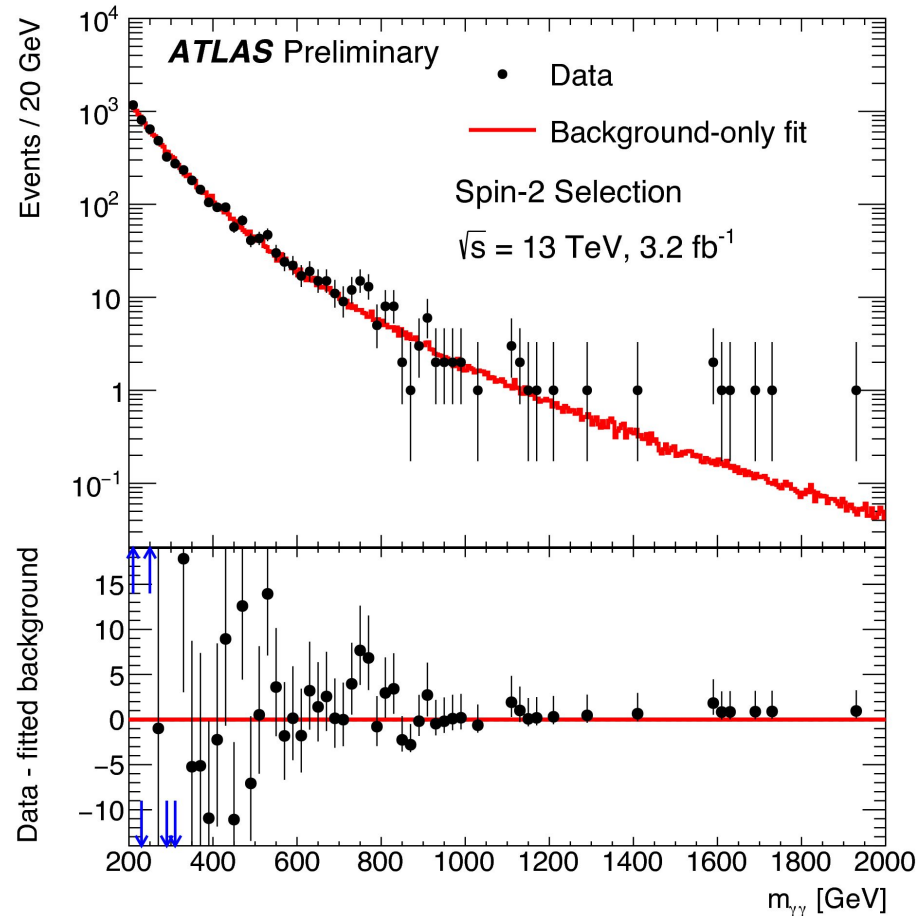


Current results

Spin-0 selections

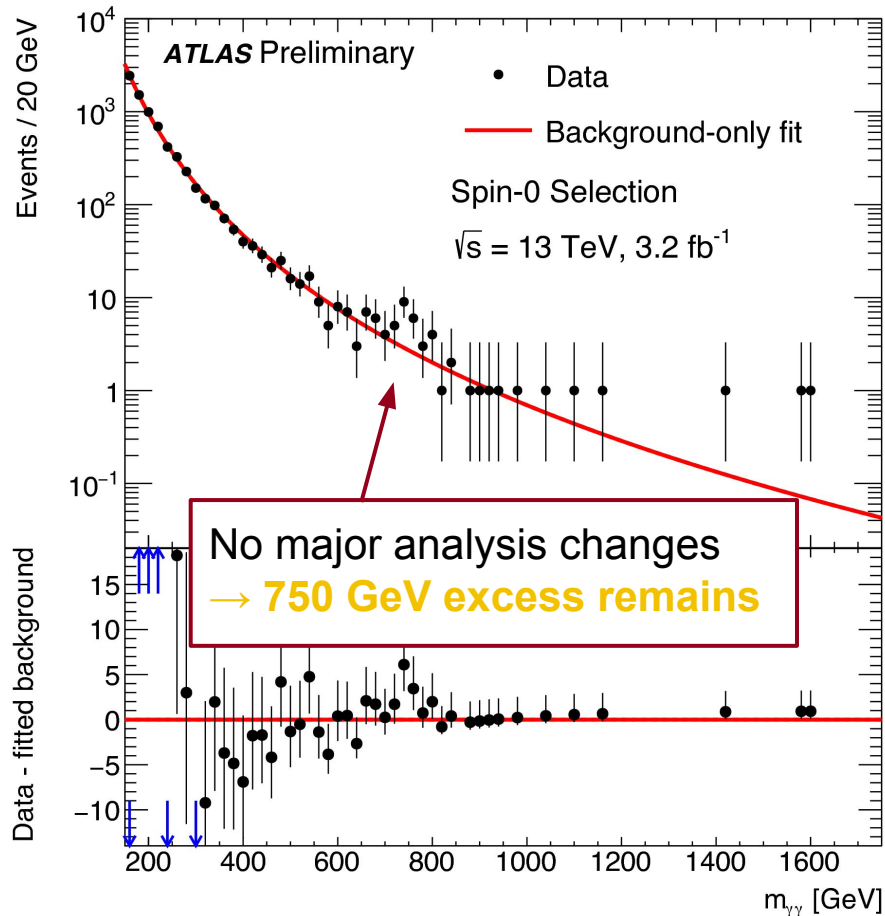


Spin-2 selections

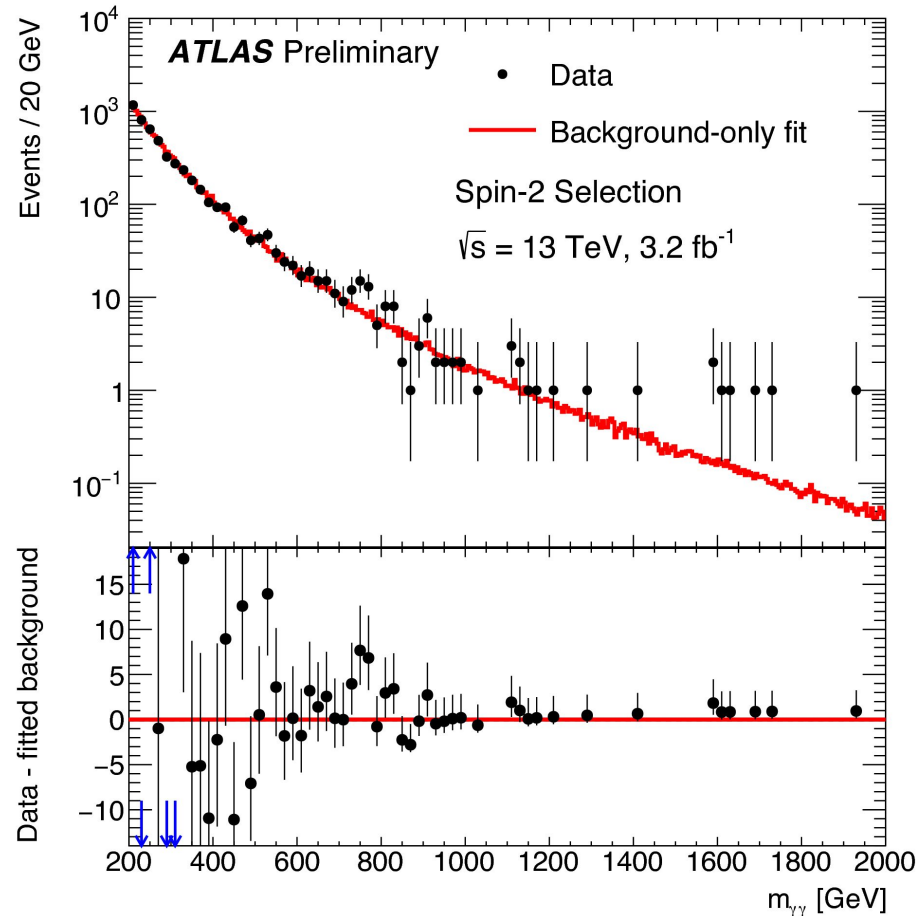


Current results

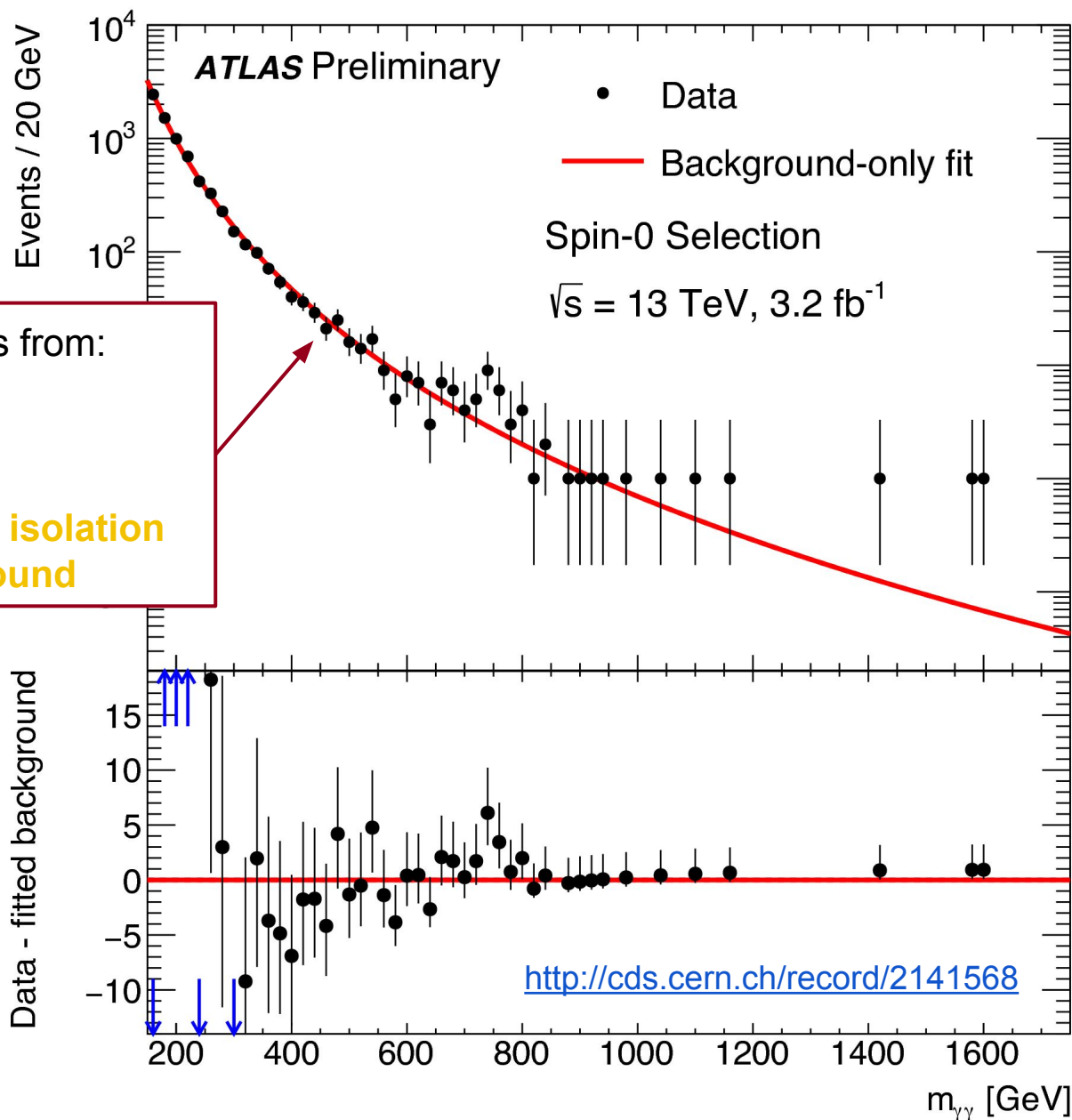
Spin-0 selections



Spin-2 selections



Current result



Photon reconstruction

- Clustering of LAr calorimeter cells in 4 sampling layers
 - Sliding window algorithm over projective towers
- Center of cluster calculated separately for each layer
 - Allows for coarse photon pointing
- Provides depth and lateral shower shapes
 - Discrimination between photons and jets
 - Attached track \rightarrow electron or conversion

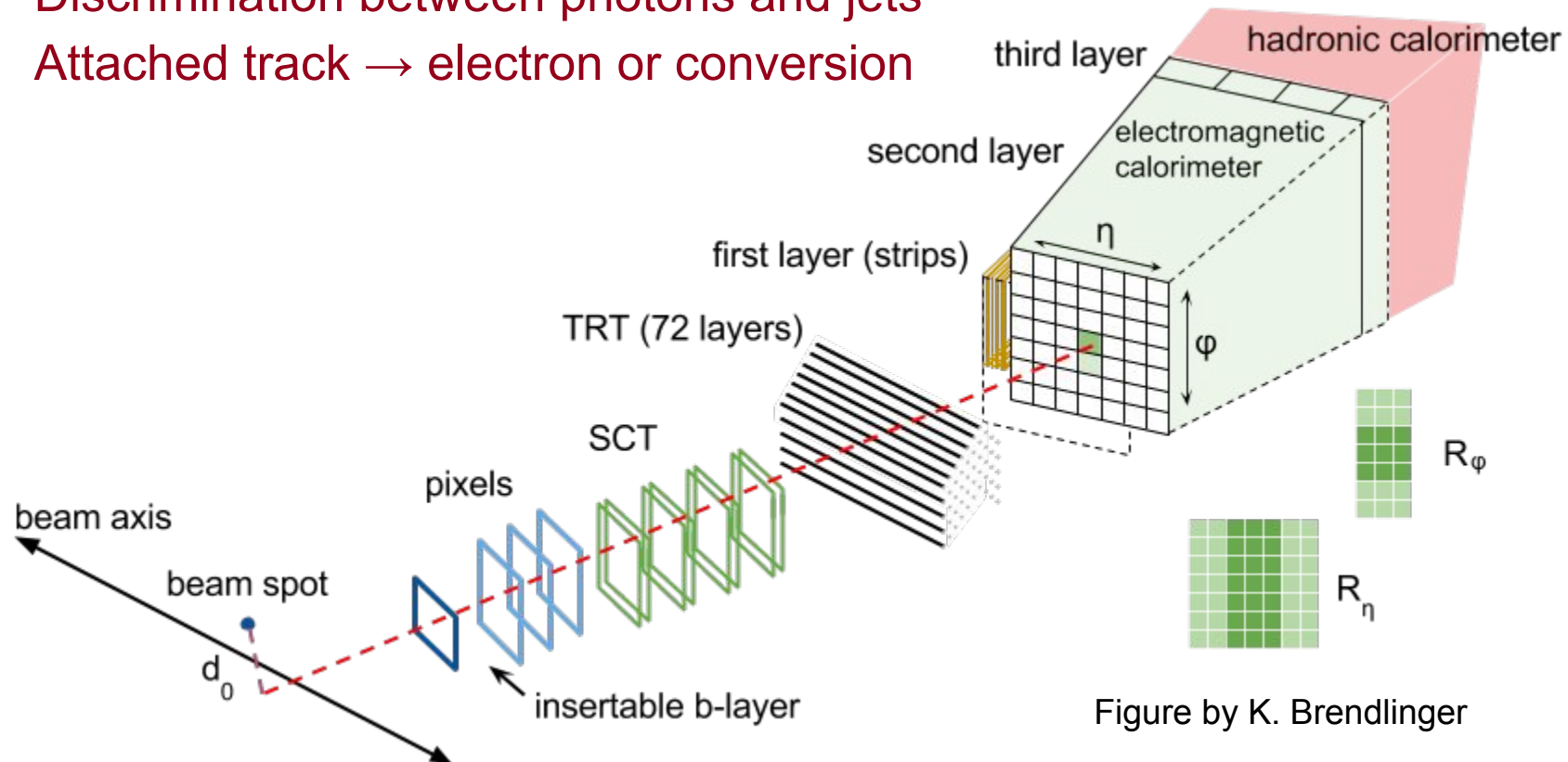
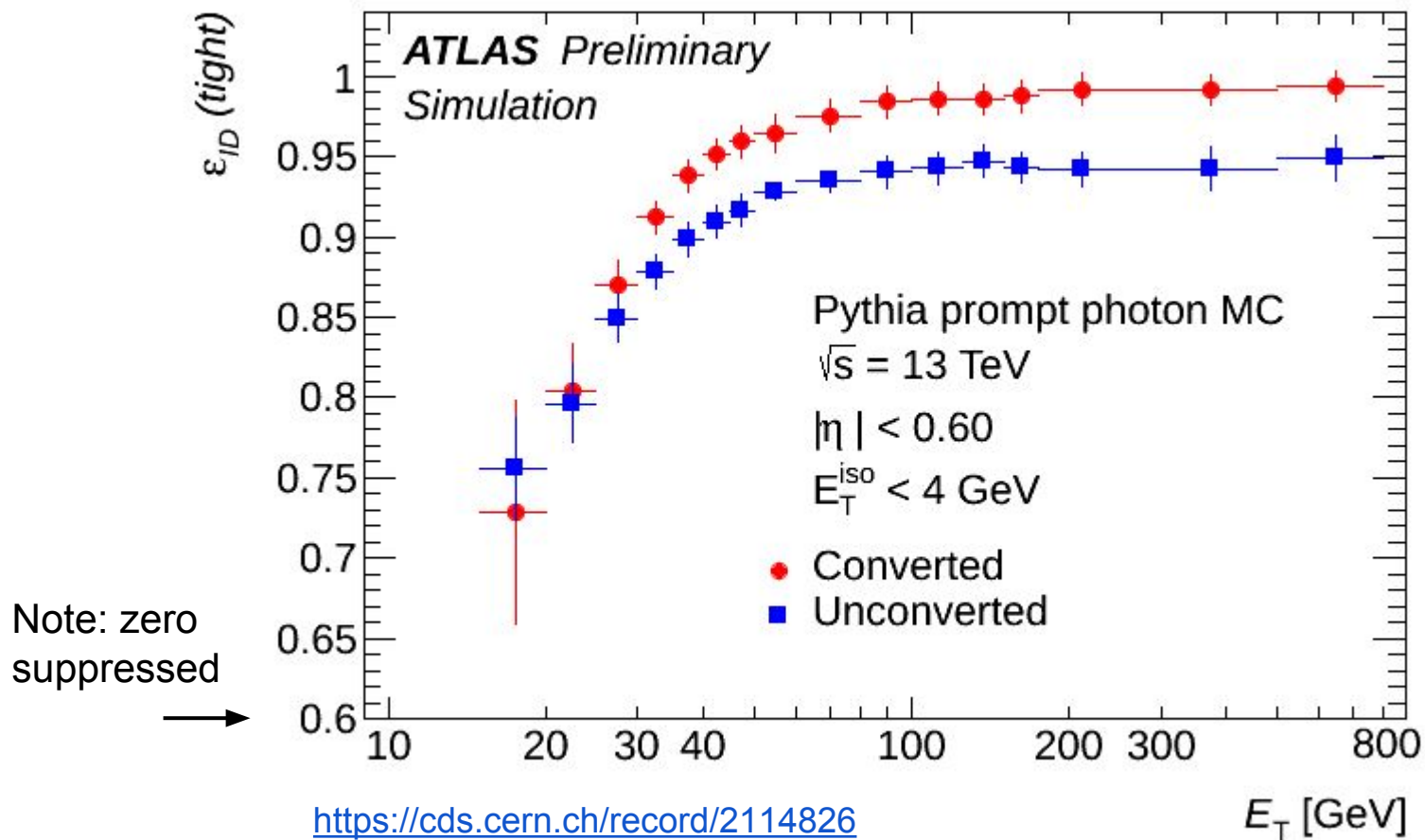


Figure by K. Brendlinger

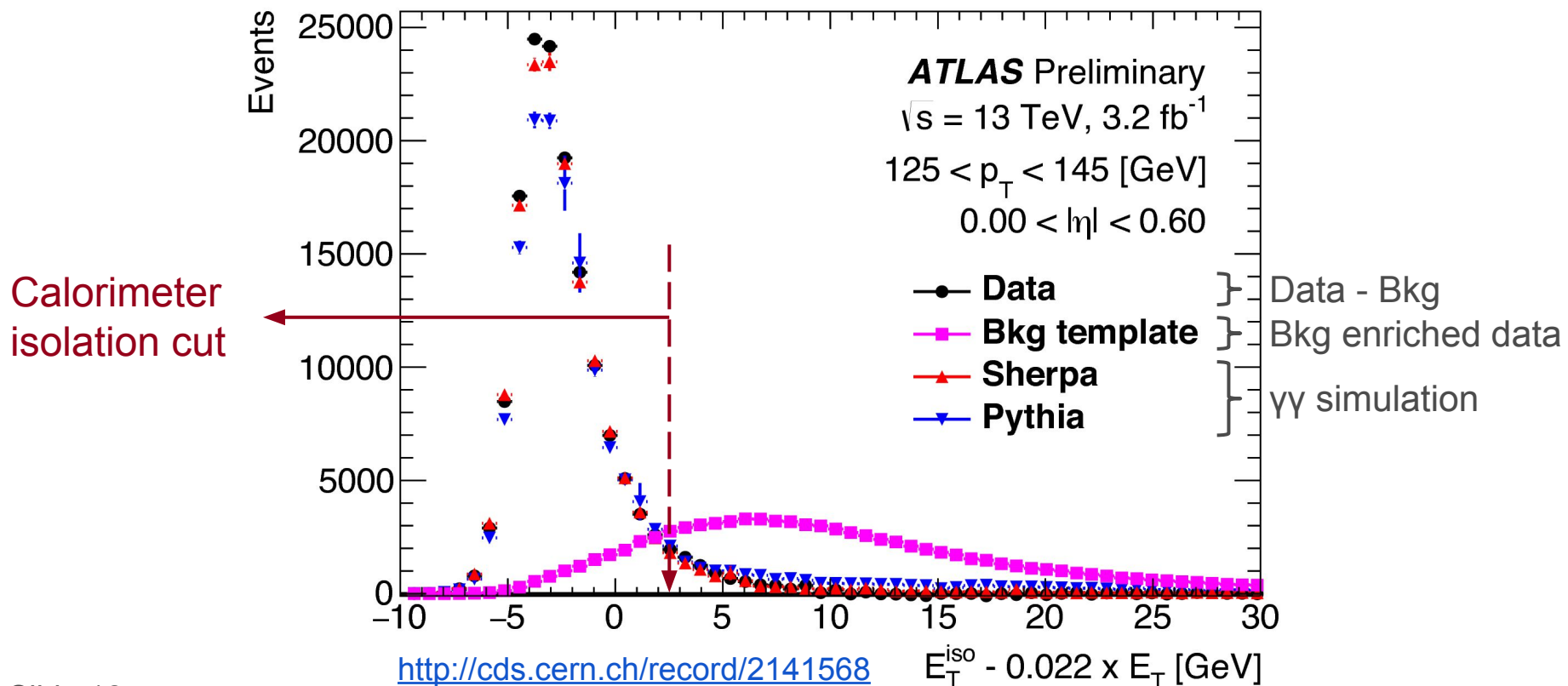
Photon identification efficiency

- Based on shower shapes in electromagnetic calorimeter
- Tracker provides improved efficiency for converted photons

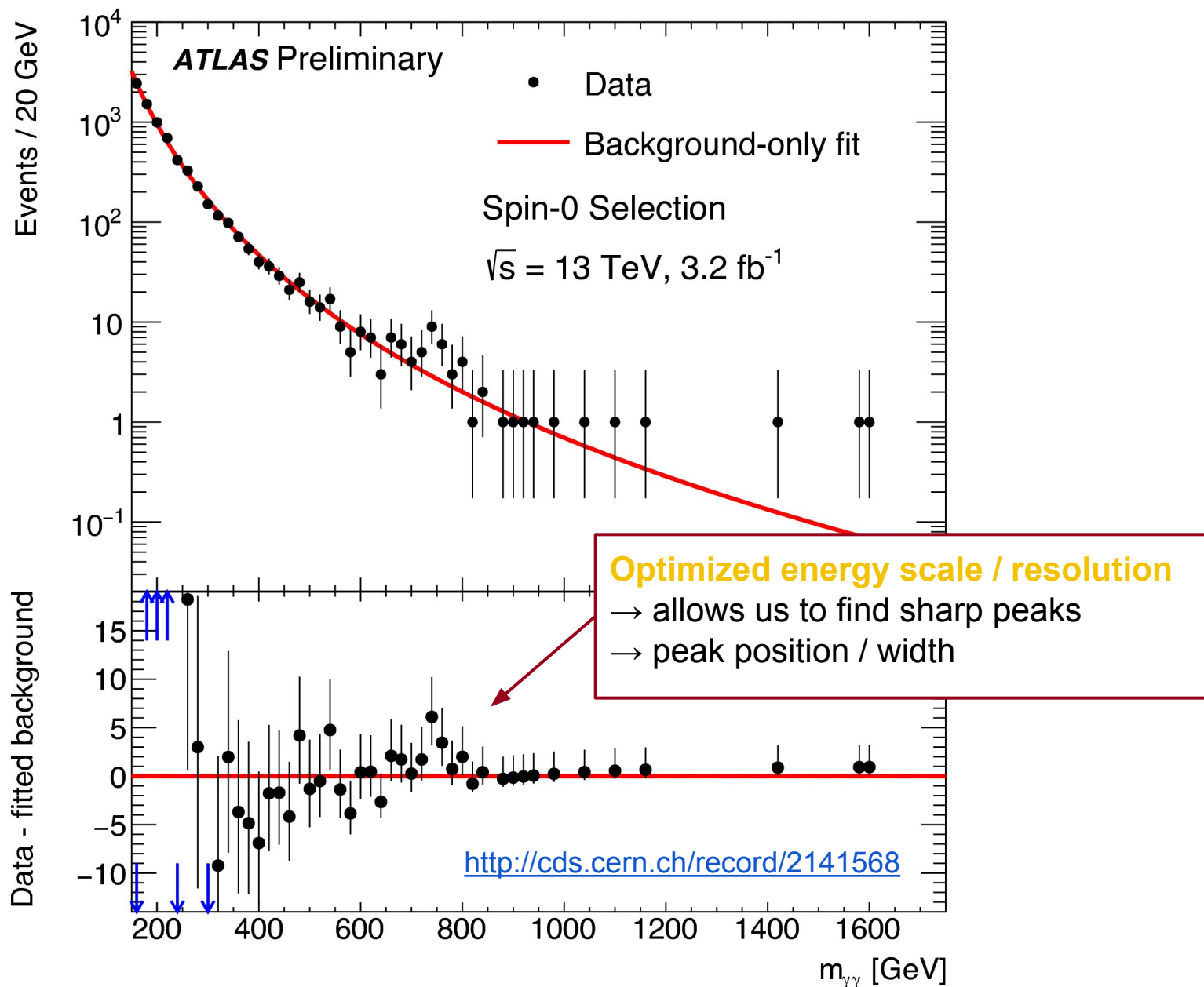


Photon isolation

- Important for purity determination, background rejection
- Both calorimeter and track isolation required
 - Calo isolation $\rightarrow \Sigma E_T$ of energy clusters within $\Delta R = 0.4$
 - Track isolation $\rightarrow \Sigma p_T$ of tracks within $\Delta R = 0.2$
- Optimized for 2015 running conditions

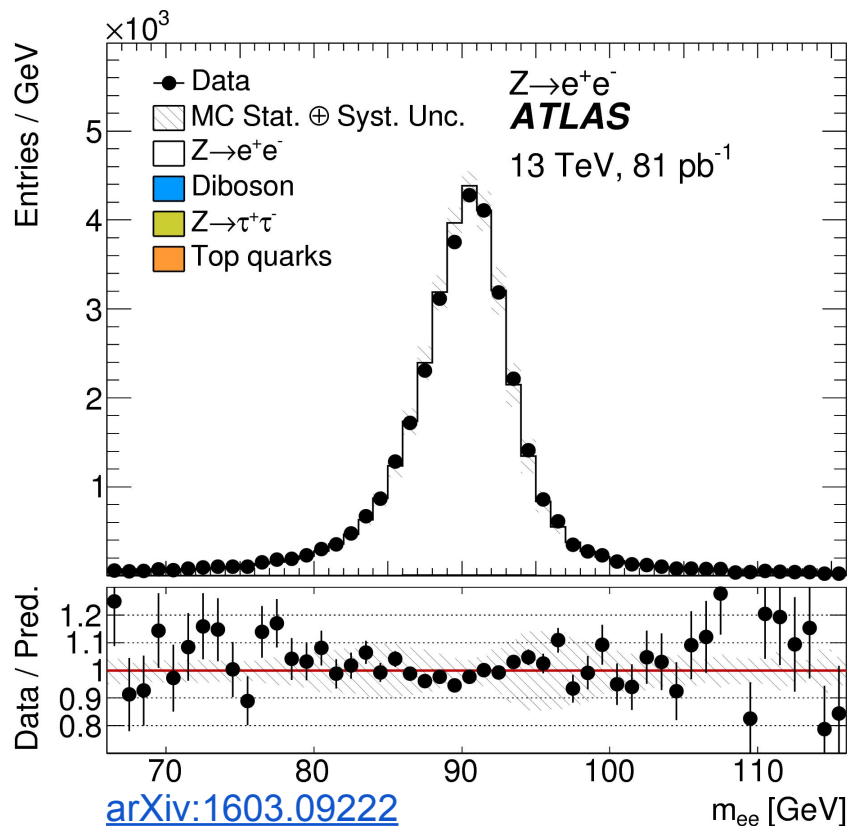


Current result

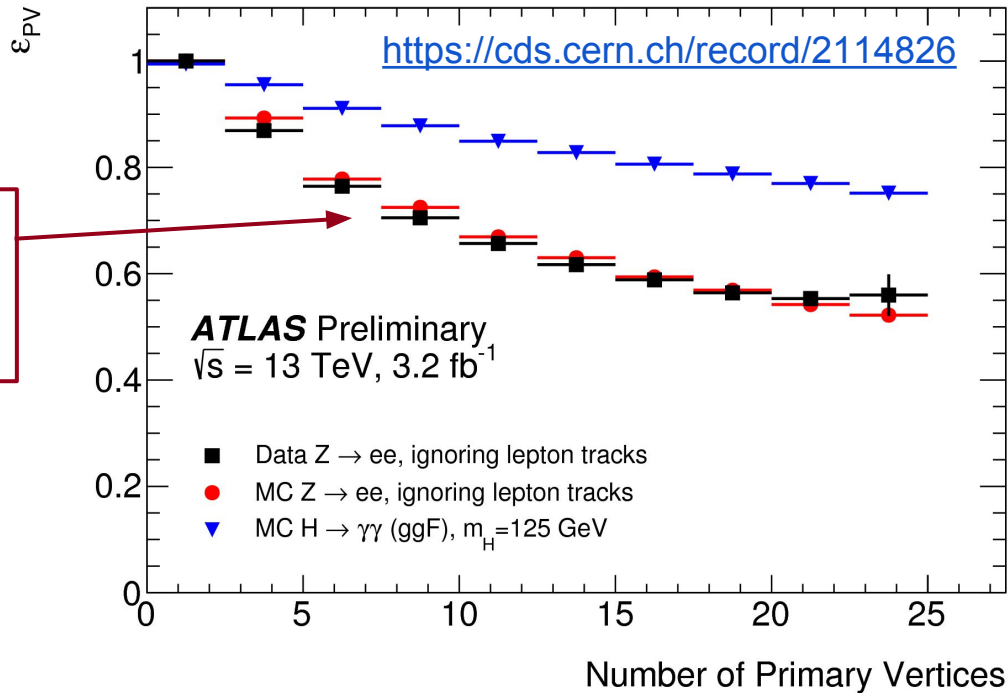


Photon calibration

- Multivariate analysis used for photon calibration
 - Optimized using MC simulation
 - Correct for energy outside cluster / in front of calorimeter
 - Longitudinal layer energy inter-calibration from 2012 data
- Overall calibration validated with $Z \rightarrow ee$ events
- Scale uncertainty:
 - $\pm(0.4 - 0.2)\%$
- Resolution uncertainty:
 - 300 GeV $\rightarrow \pm(80-100)\%$



Primary vertex important for resolution

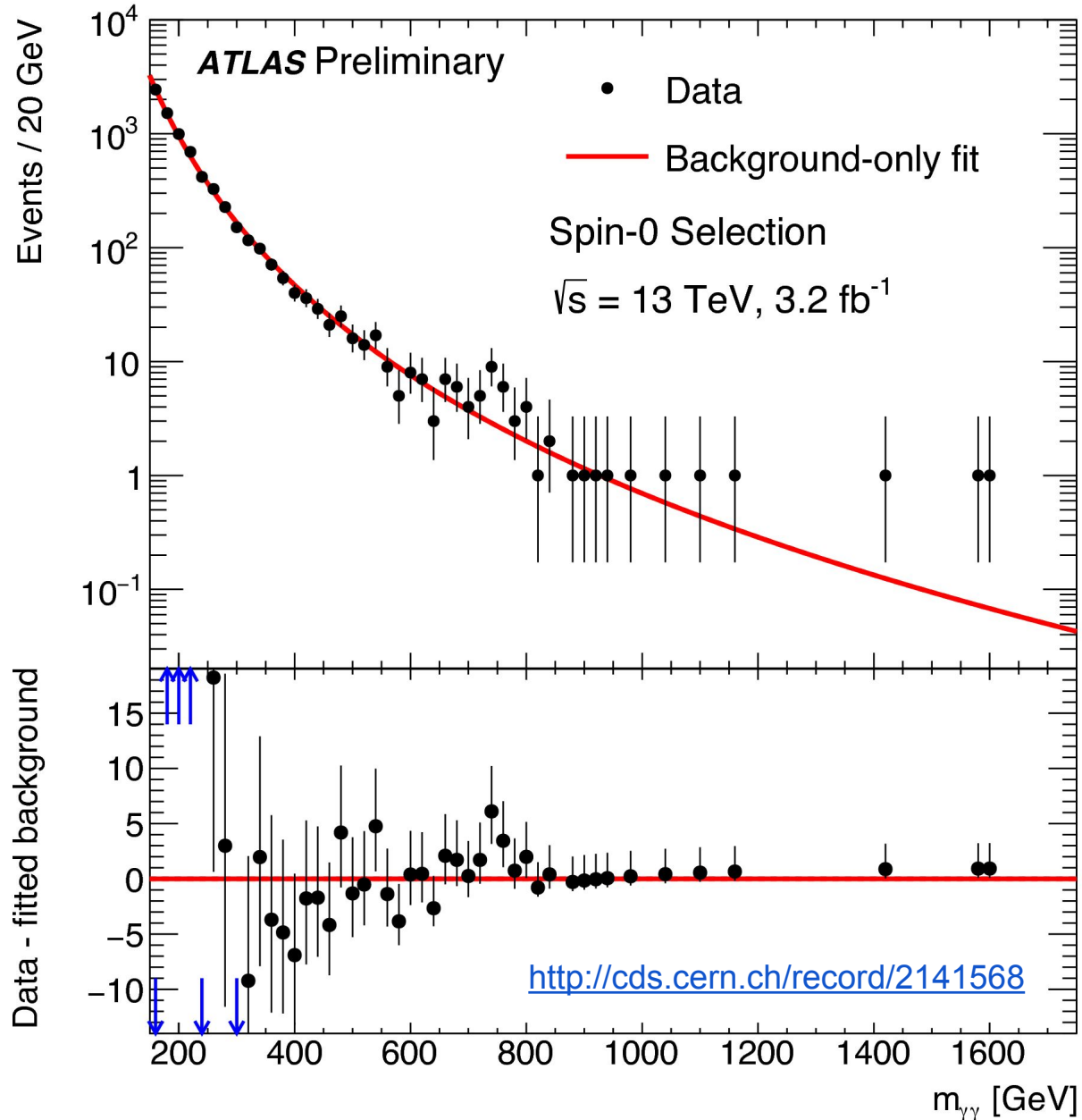


Non-optimal vertex
→ slightly worse mass resolution

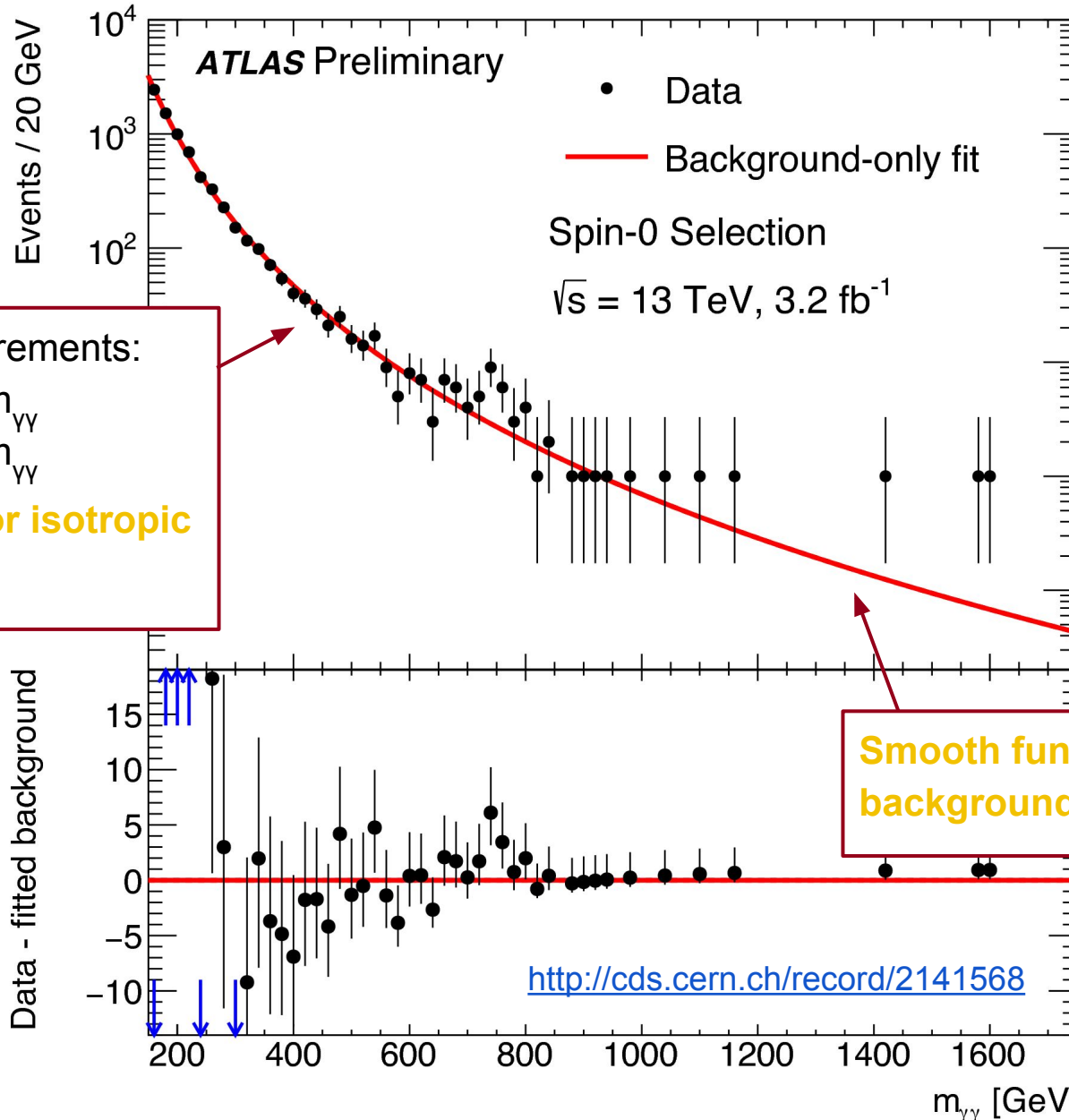
Diphoton vertex used

- Important to select vertex which produced diphoton system
- Position of different calorimeter layers points at diphoton vertex
 - Combined with average beamspot, conversion vertex (if available)
- Makes mass resolution dependence on opening angle negligible
- Provides correct tracks for calculating $p_{T,iso}$

Spin-0 selections



Spin-0 selections



Background estimate

- Consider family of functional forms from dijet searches:

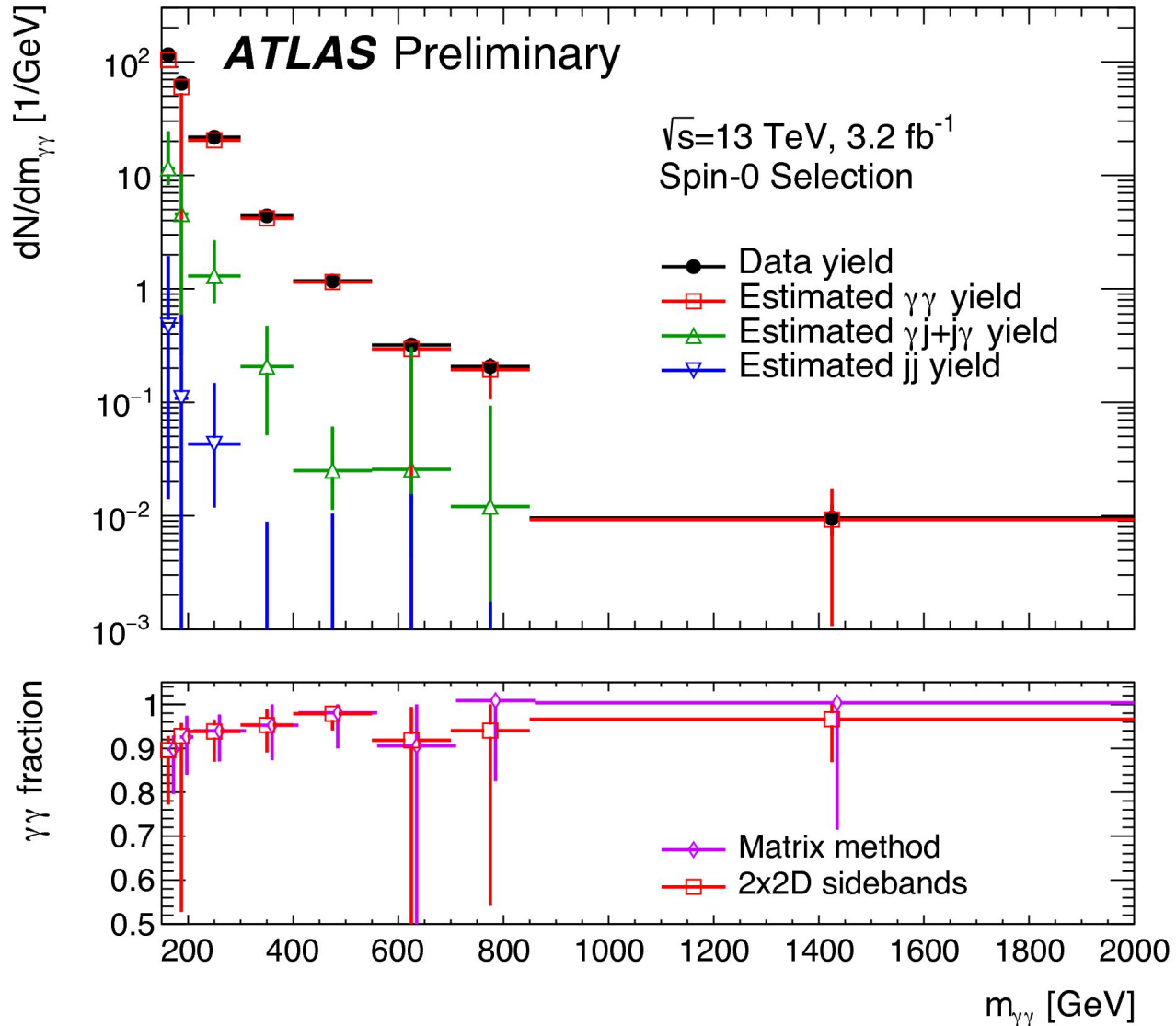
$$f_{(k)}(x; b, \{a_k\}) = N(1 - x^{1/3})^b x^{\sum_{j=0}^k a_j (\log x)^j}$$

$x = m_{\gamma\gamma} / \sqrt{s}$

- Optimized for middle range of diphoton mass
 - Shape constrained by events above/below signal
- **Test family of functions on large sample of pseudo-data**
 - DIPHOX NLO smeared with detector resolution
 - $\gamma\gamma$ and jj shape estimated from background enriched data sample
- Background only shape → **no expected signal events**
 - Any signal that is extracted is a “spurious” yield

Background estimate

$\gamma\gamma$ purity is $93 \pm 3\%$



- Cons

f

- Optim

○ S

- Test

○ D

○ y_j

- Backg

○ A

$x)^j$

$\gamma\gamma / \sqrt{s}$

ata

ample

Background checks

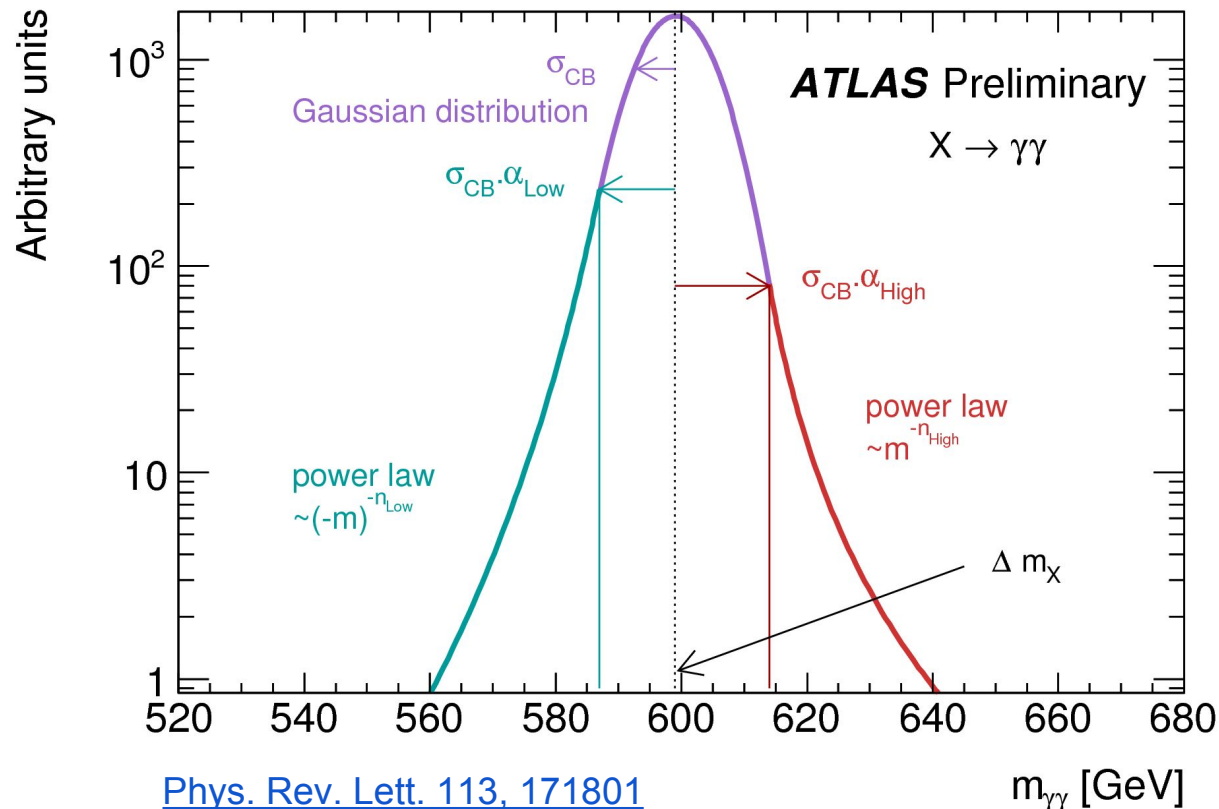
$$f_{(k)}(x; b, \{a_k\}) = N(1 - x^{1/3})^b x^{\sum_{j=0}^k a_j (\log x)^j}$$

- Require fitted spurious yield < 20% stat. unc. on background
 - Choose function with fewest degrees of freedom → $k = 0$
 - Uncertainty from envelope of # fitted spurious yield
- Possibility that data needs more degrees of freedom in fit
 - F-test using background fit of data shows that $k = 0$ is sufficient

$$F = \frac{\frac{\sum_i (y_i - f_1(x_i))^2}{p_1} - \frac{\sum_i (y_i - f_2(x_i))^2}{p_2}}{\frac{\sum_i (y_i - f_2(x_i))^2}{n - p_2}}$$

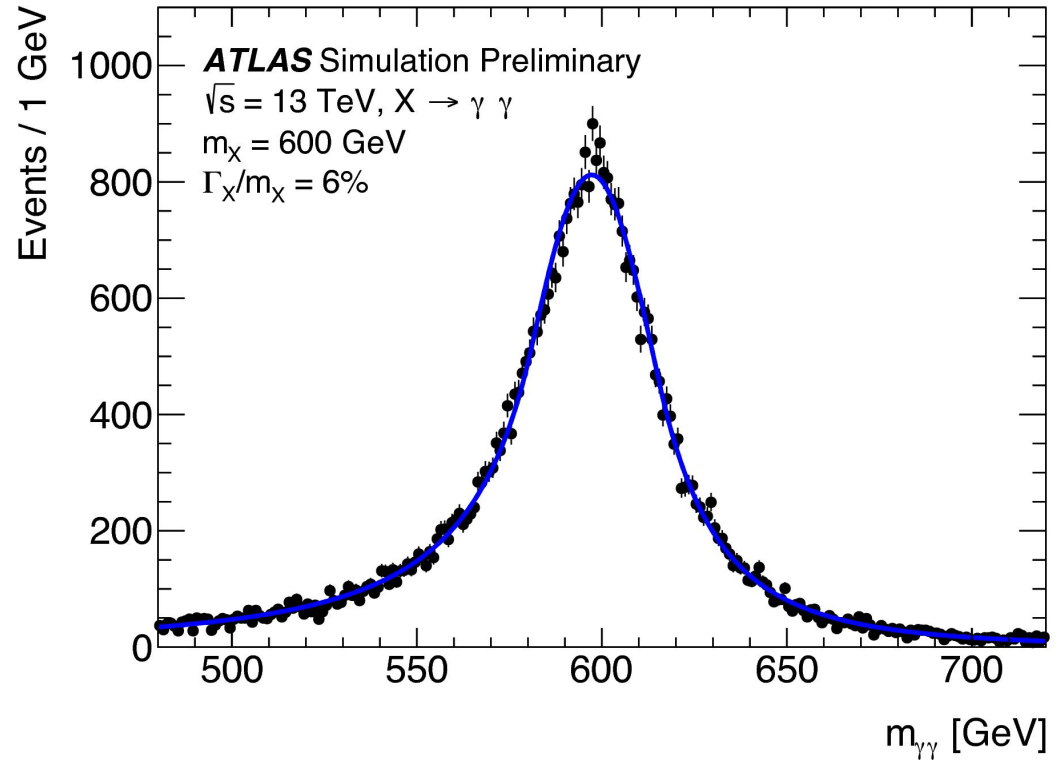
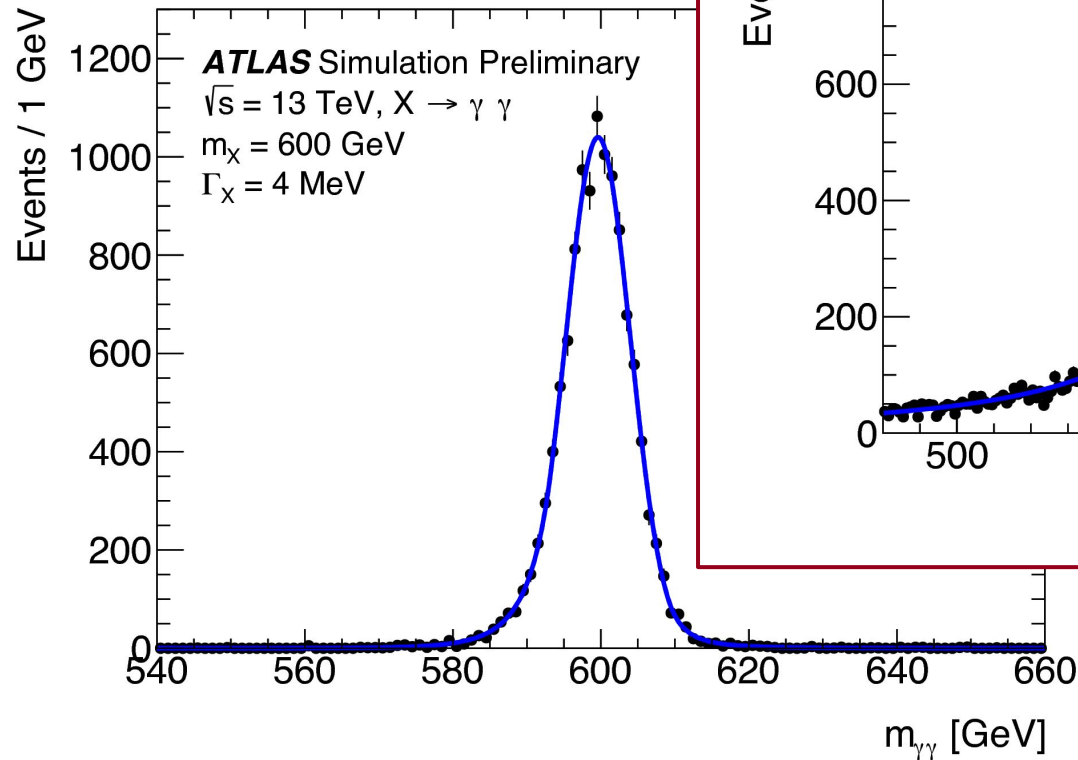
Signal modeling

- Double-sided Crystal Ball function
 - Line-shape of spin-0 resonance follows a Breit Wigner function
 - Detector resolution is also asymmetric
- Spin-0 with narrow width varies from $\sigma_{\text{CB}} = 2 \text{ GeV}$ to 13 GeV
 - Over a mass range of 200 GeV to 2 TeV



Spin-0 signal shape

- Signal shape with narrow width \rightarrow detector resolution



<http://cds.cern.ch/record/2141568>

Signal extraction / statistical method

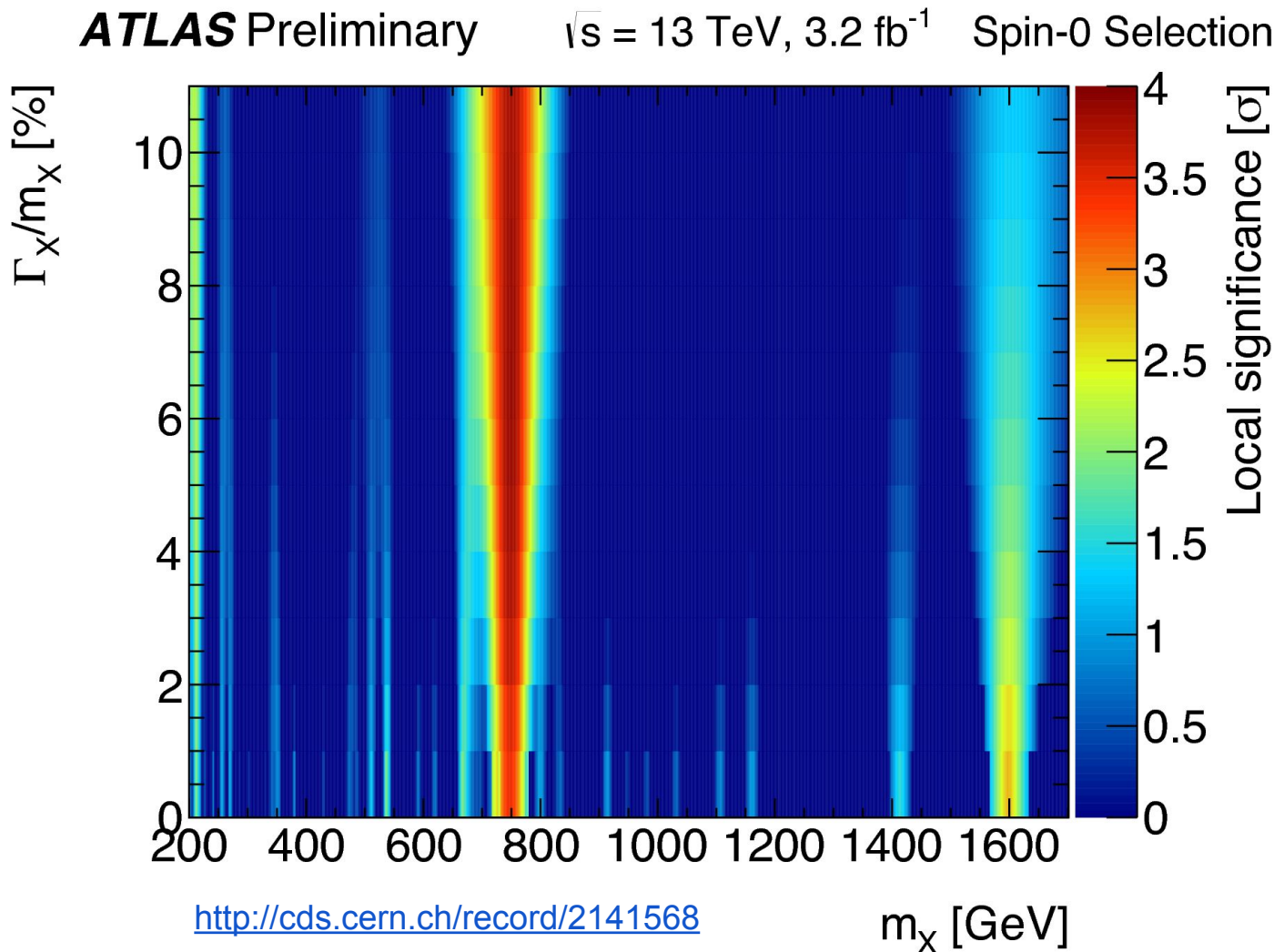
- Maximum likelihood fit using the function:

$$N_S f_S(m_{YY}) + N_B f_B(m_{YY})$$

- $N_{S(B)}$ is the number of fitted signal (background) events
- $f_{S(B)}$ is the mass dependent form of the signal (background)
- Uncertainties included through nuisance parameters
 - Gaussian constraint terms in likelihood equation
- Scan log-likelihood ratio to determine local significance

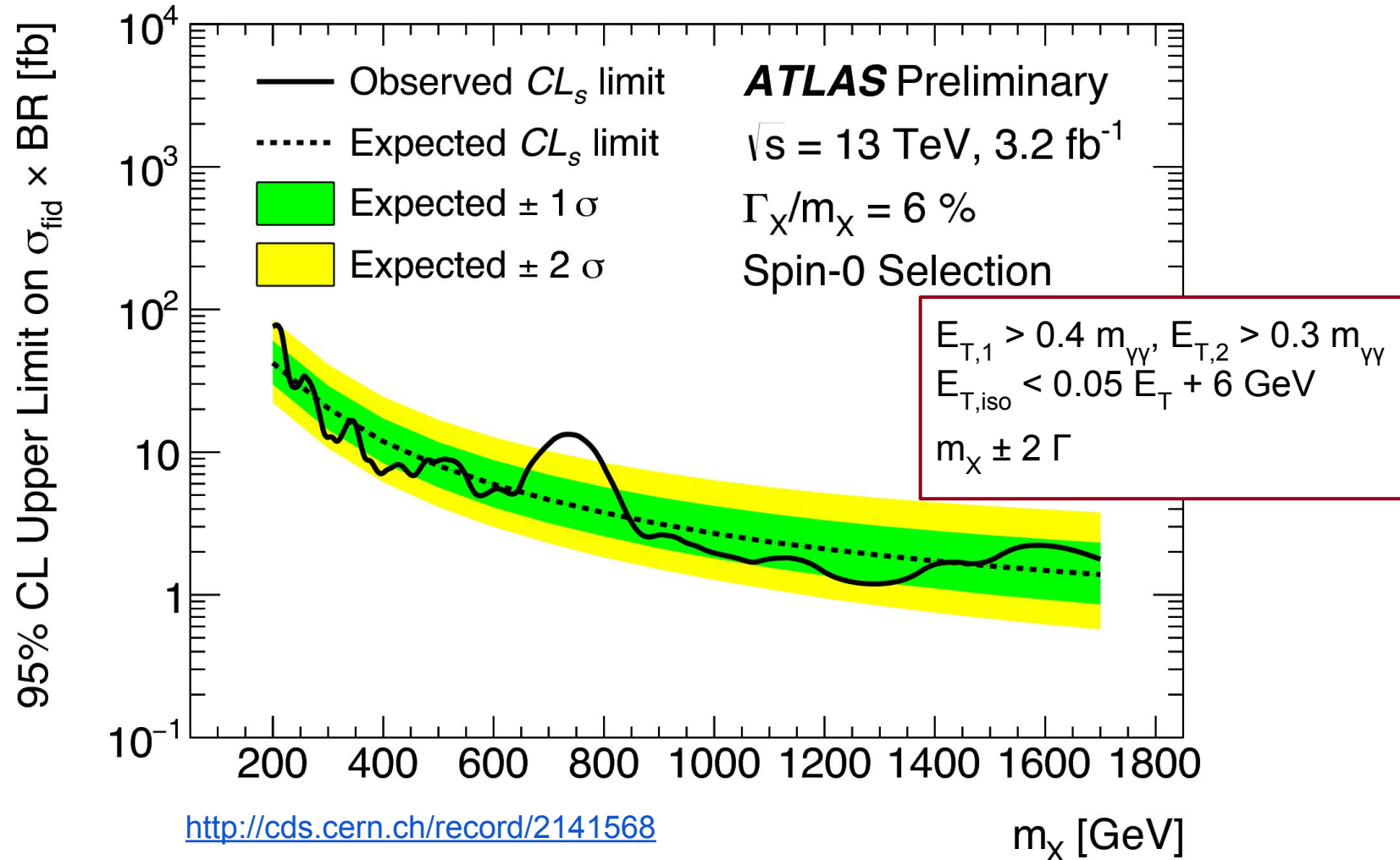
Local significance for spin-0 analysis

- Largest local significance (3.9σ) around 750 GeV, width of 6%
- Global significance of this excess is **2.0σ**

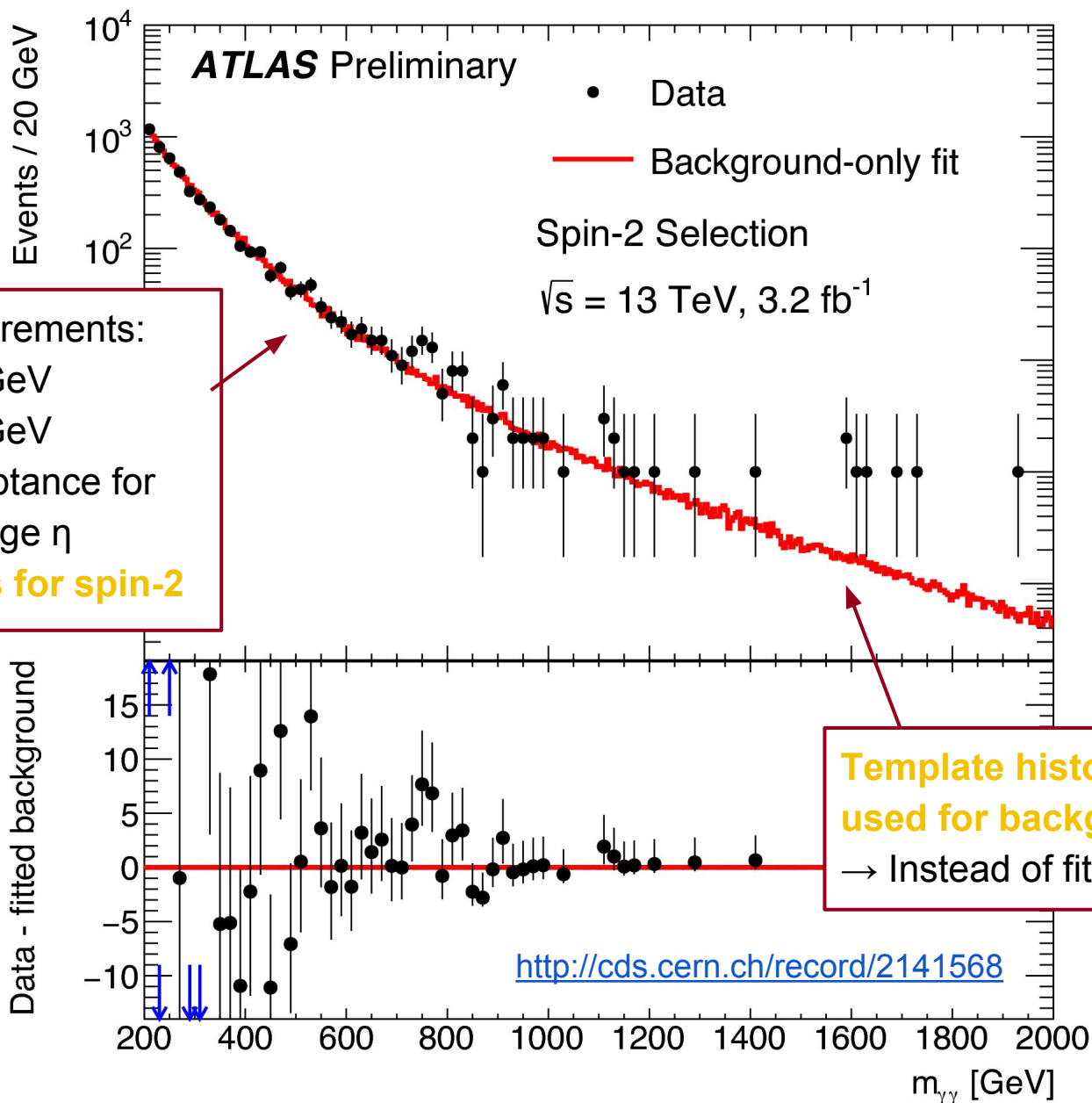


Cross section limits for spin-0 analysis

- Observed cross section limits in agreement with expected limits
 - Except for excess around 750 GeV



Spin-2 selections



Background estimate

- Background template → data doesn't constrain high $m_{\gamma\gamma}$ shape
 - Fully simulated Sherpa $\gamma\gamma$ sample
 - Weighted with parton-level NLO DIPHOX prediction of $\gamma\gamma$
 - Uncertainties due to PDF and QCD scale choice
 - Background enriched data used for γj and jj
 - Uncertainties due to background identification definition
- Weight by sample composition between 200-500 GeV

Background estimate

- Background

○ Full

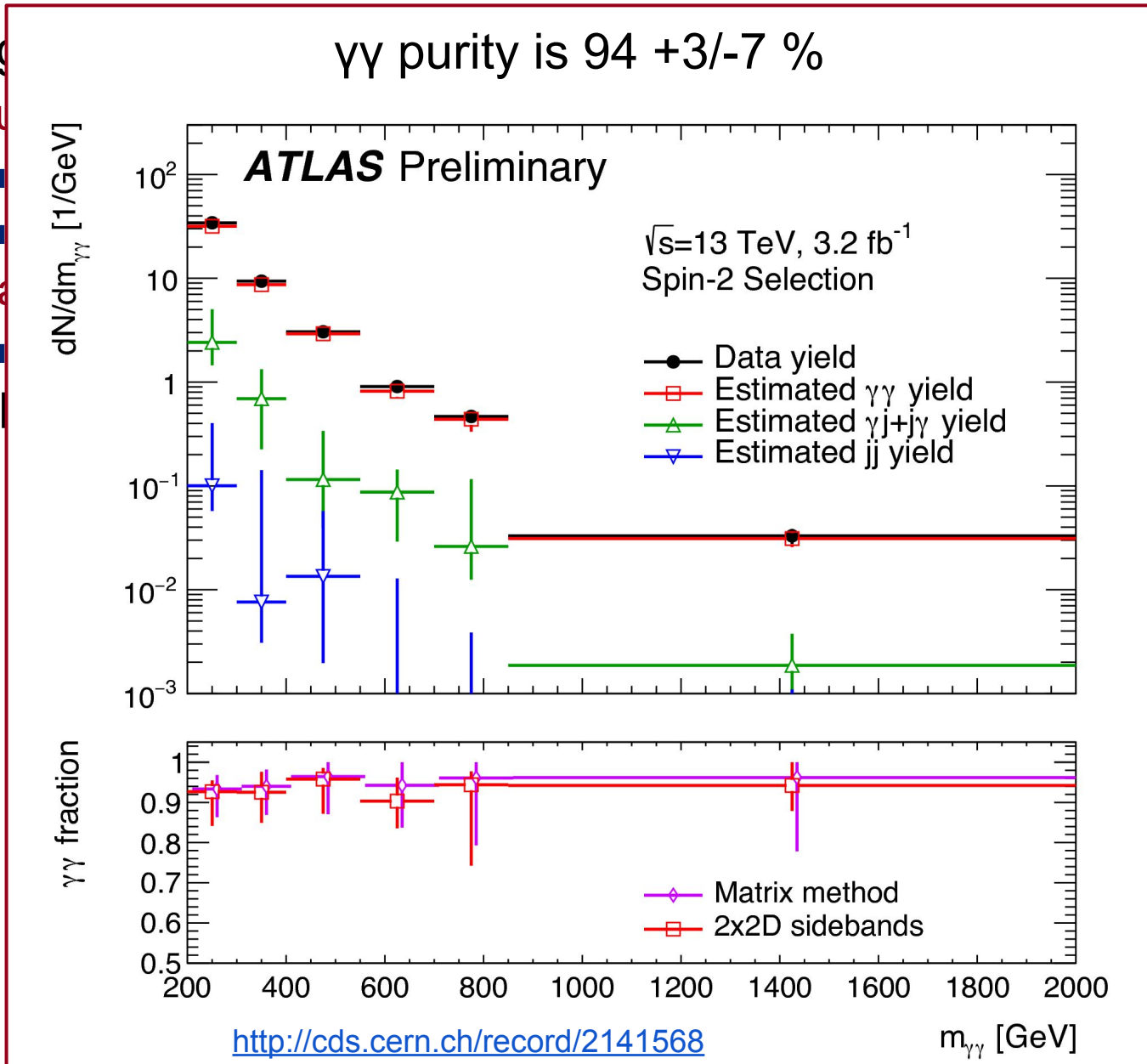
■ Background

○ Background

■ Background

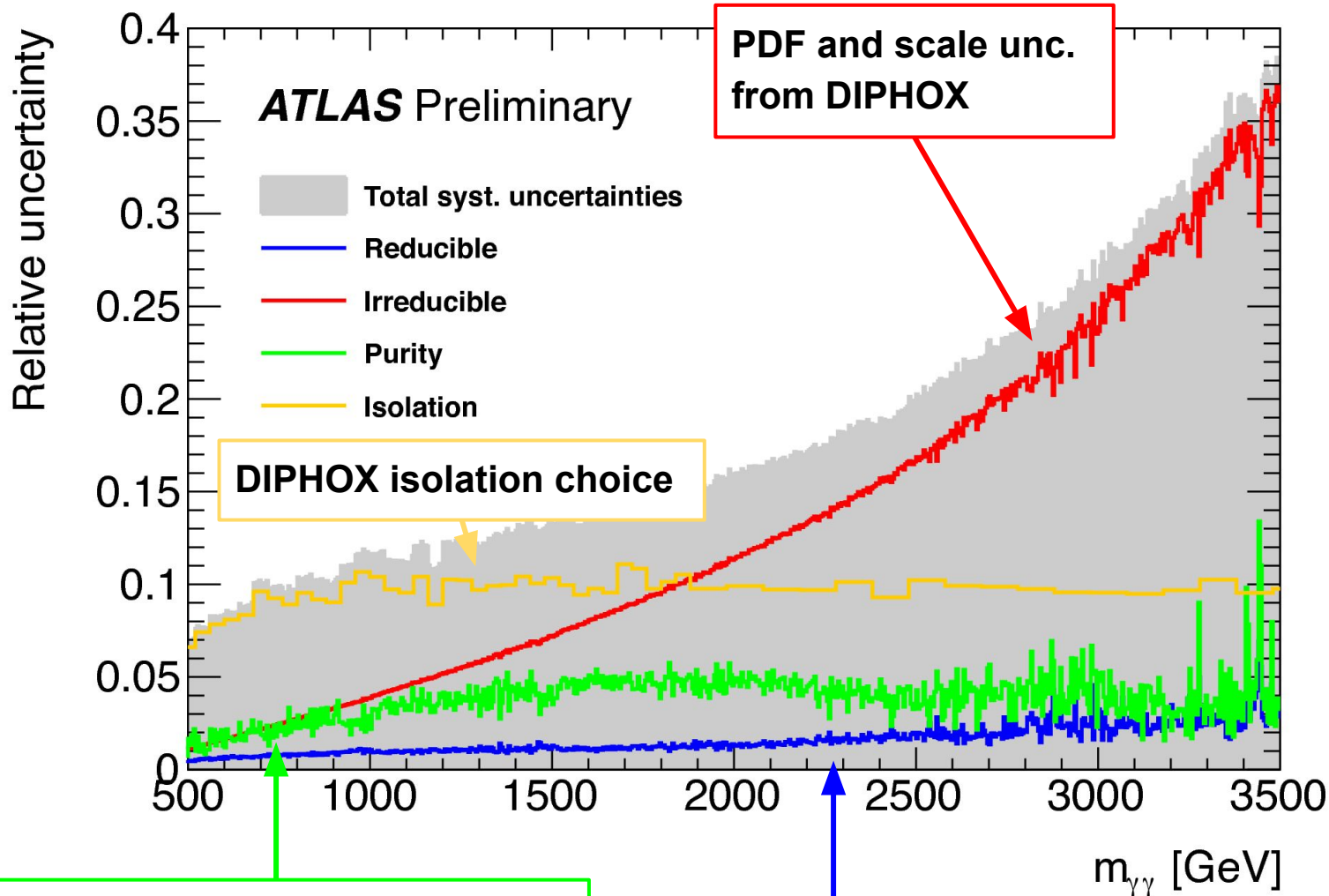
- Weight

shape



Background uncertainties

<http://cds.cern.ch/record/2141568>

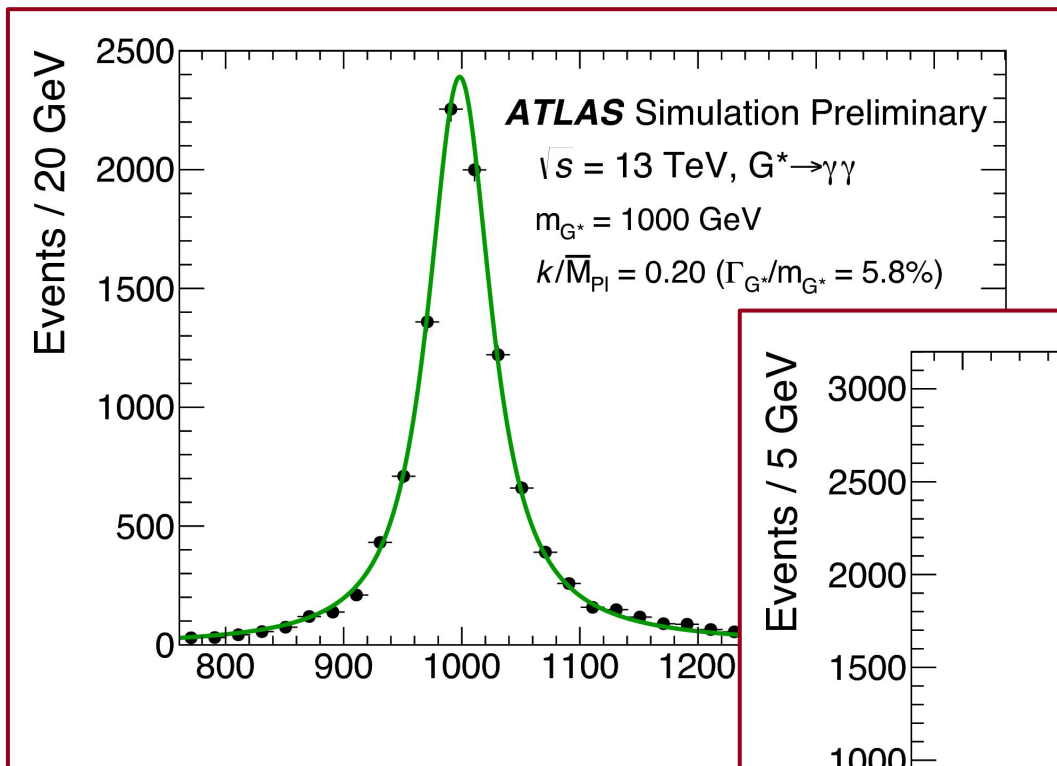


$\gamma\gamma, \gamma j, jj$ composition uncertainty

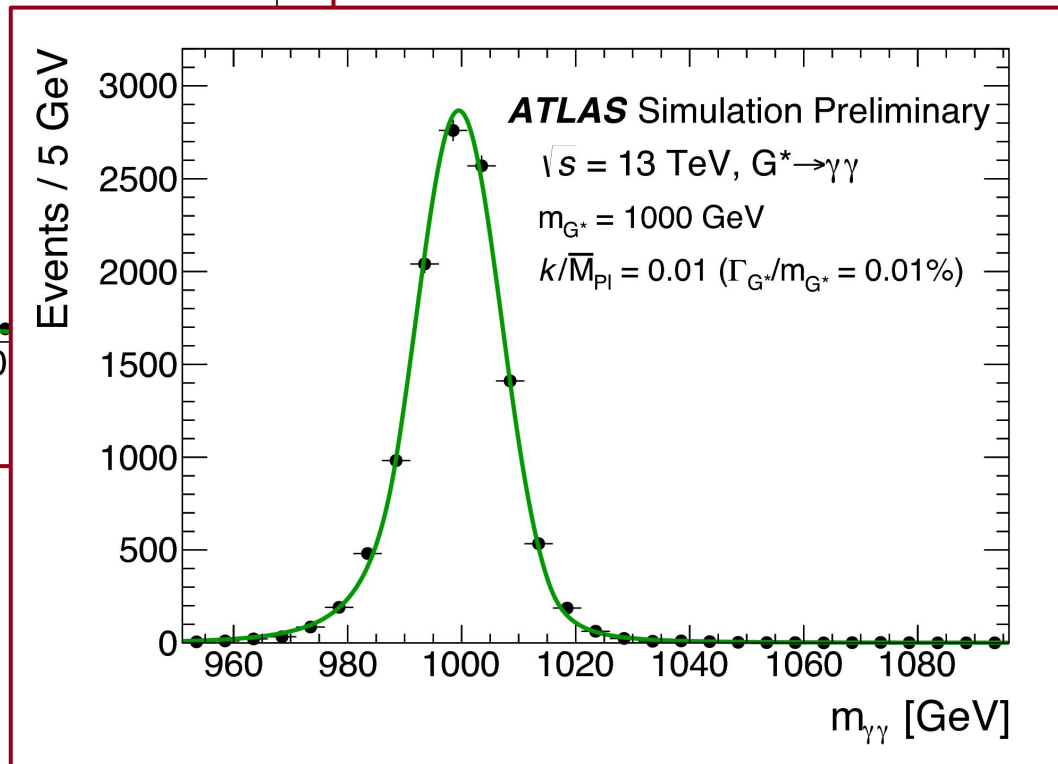
Definition of enriched- background identification for $\gamma j, jj$ shape

Spin-2 signal shape

- Convolution of double sided Crystal Ball + theoretical line-shape
- Signal shapes for spin-2 model → note asymmetry of tails



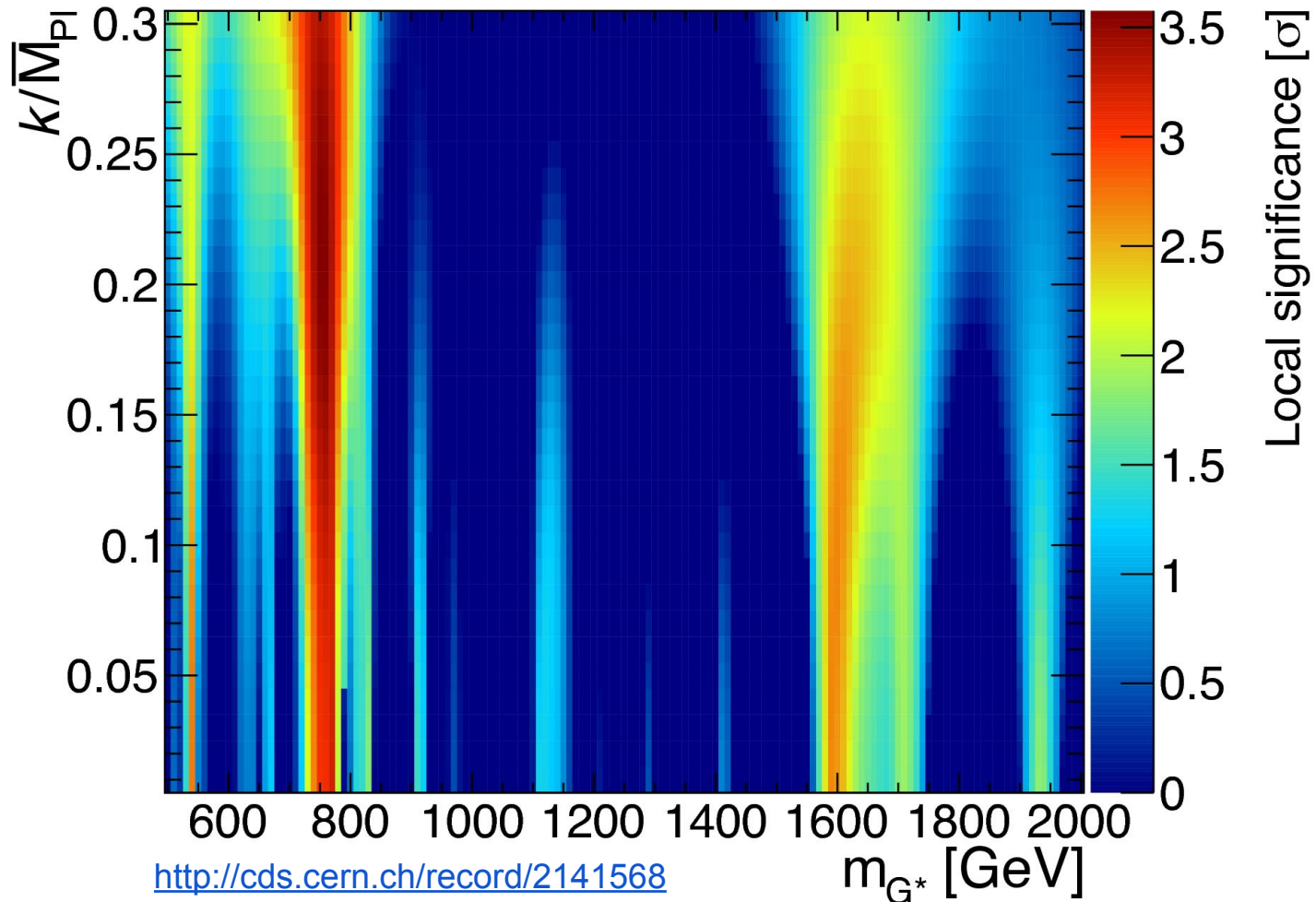
<http://cds.cern.ch/record/2141568>



Spin-2 selections local significance

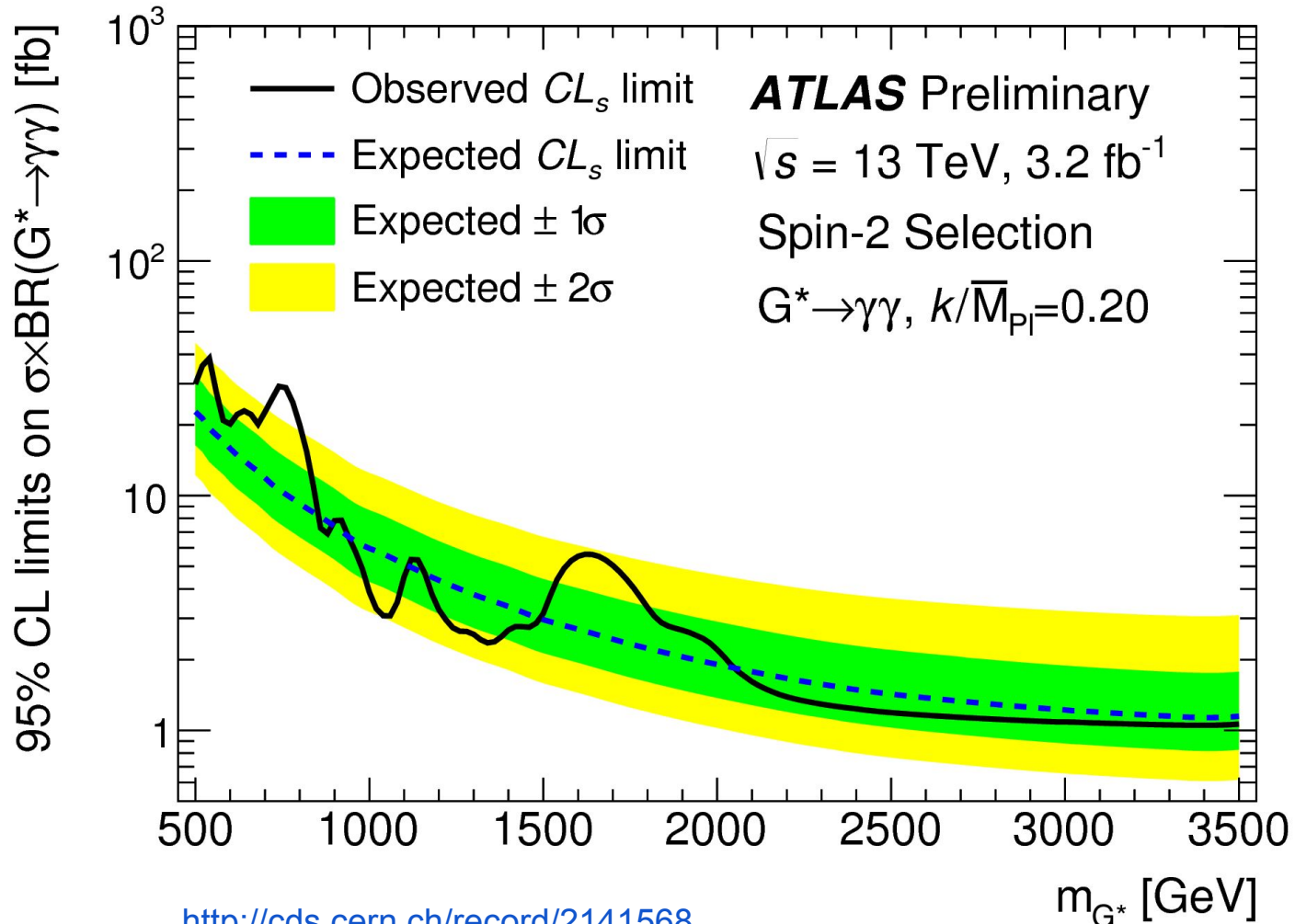
- Largest local significance (3.6σ) around 750 GeV, $k/\overline{M}_{\text{Pl}} = 0.21$
- Global significance of this excess is **1.8σ**

ATLAS Preliminary $\sqrt{s} = 13 \text{ TeV}, 3.2 \text{ fb}^{-1}$ Spin-2 Selection



Cross section limits for spin-2 analysis

- Observed cross section limits in agreement with expected limits
 - Except for excess around 750 GeV



Summary of results

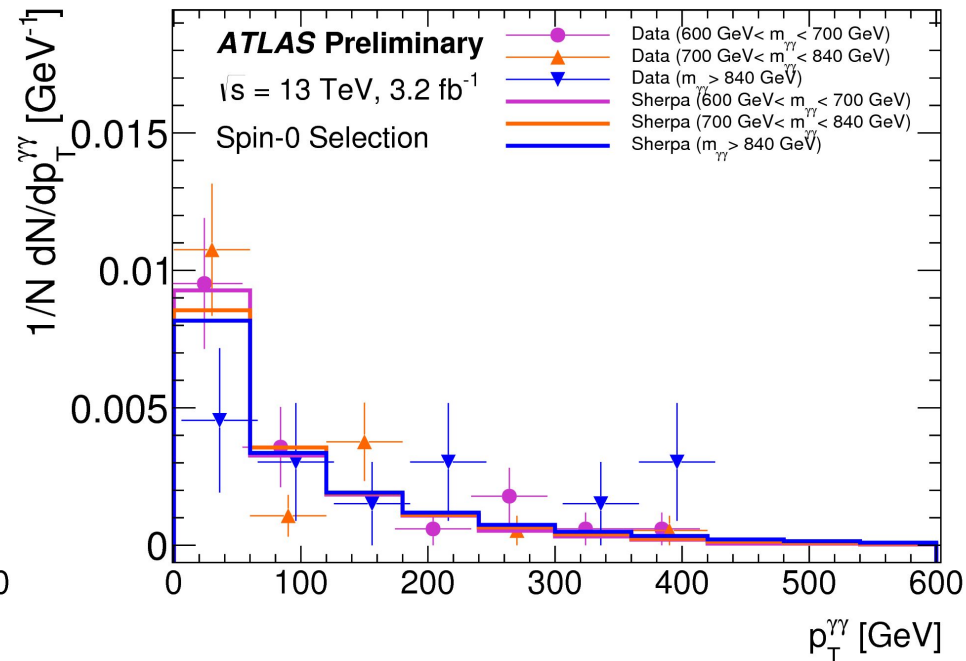
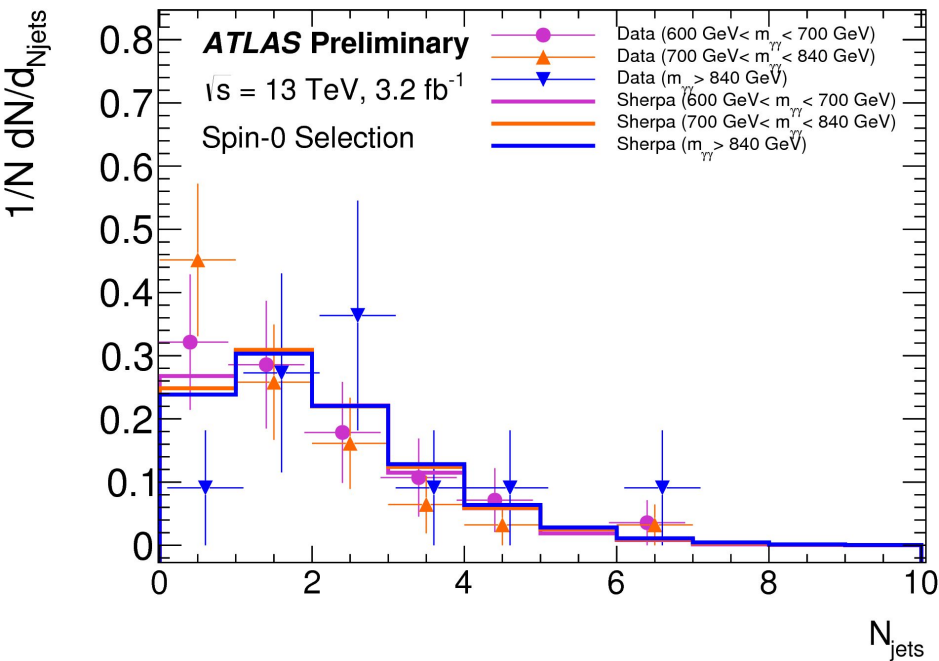
- Summary of largest local significance (near 750 GeV)
 - Both results fully compatible with one another
- Global significance considering look elsewhere effect
 - Done using fits of background pseudo-data

| Selections | Local p_0 | Global Z_0 | Best fit width |
|------------|--------------|--------------------------------|----------------|
| Spin-0 | 3.9 σ | 2.0 σ | 45 GeV |
| Spin-2 | 3.6 σ | 1.8 σ | 48 GeV |

- Note: global significance is lower than initial result
 - Due to improved method which uses pseudo-data
- How consistent are this results with the previous 8 TeV analyses

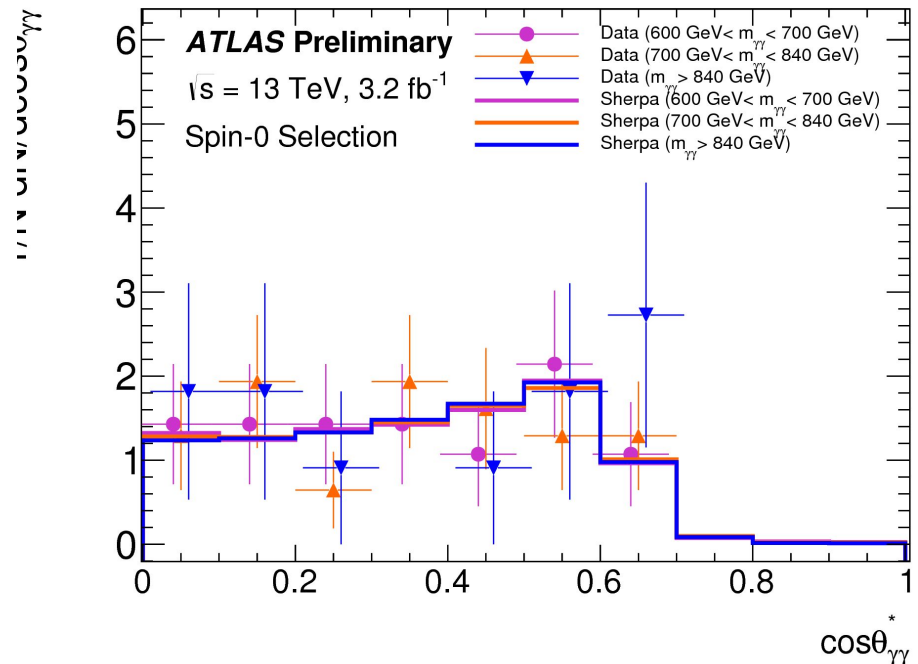
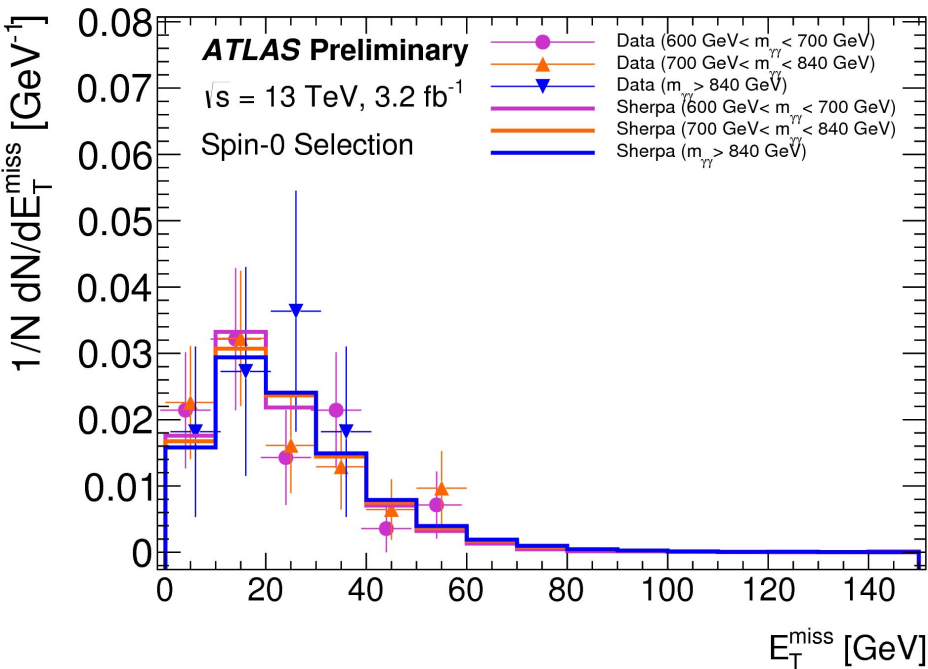
Kinematic distributions for 13 TeV

- Examine properties of events in different mass regions
 - Low side-band: 600-700 GeV
 - Excess region: 700-840 GeV
 - High side-band: >840 GeV
- No significant difference observed in different mass regions



Kinematic distributions for 13 TeV

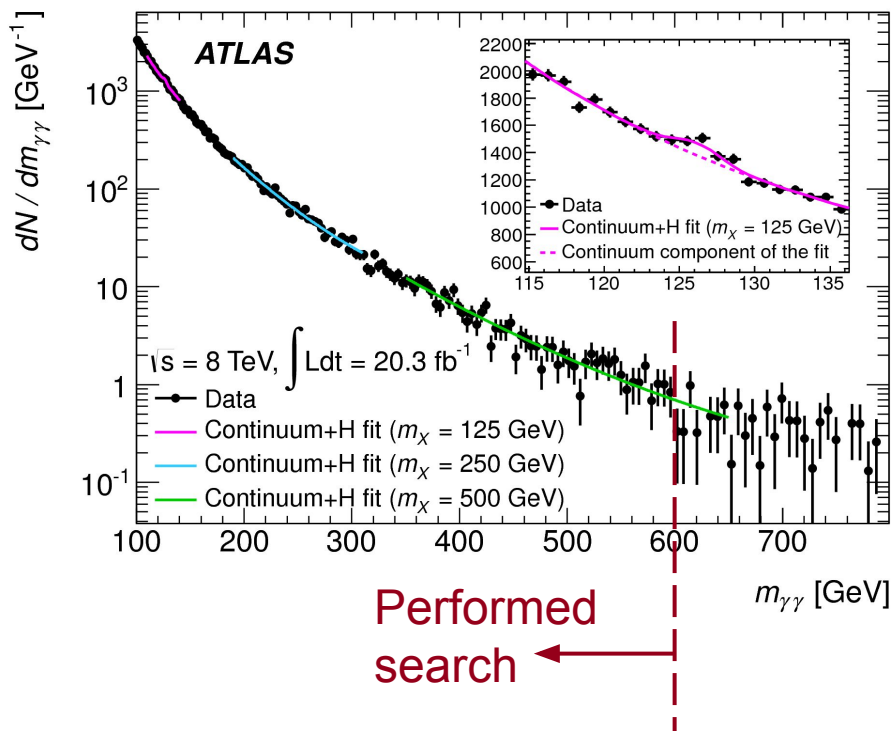
- Examine properties of events in different mass regions
 - Low side-band: 600-700 GeV
 - Excess region: 700-840 GeV
 - High side-band: >840 GeV
- No significant difference observed in different mass regions



Run 1 diphoton searches

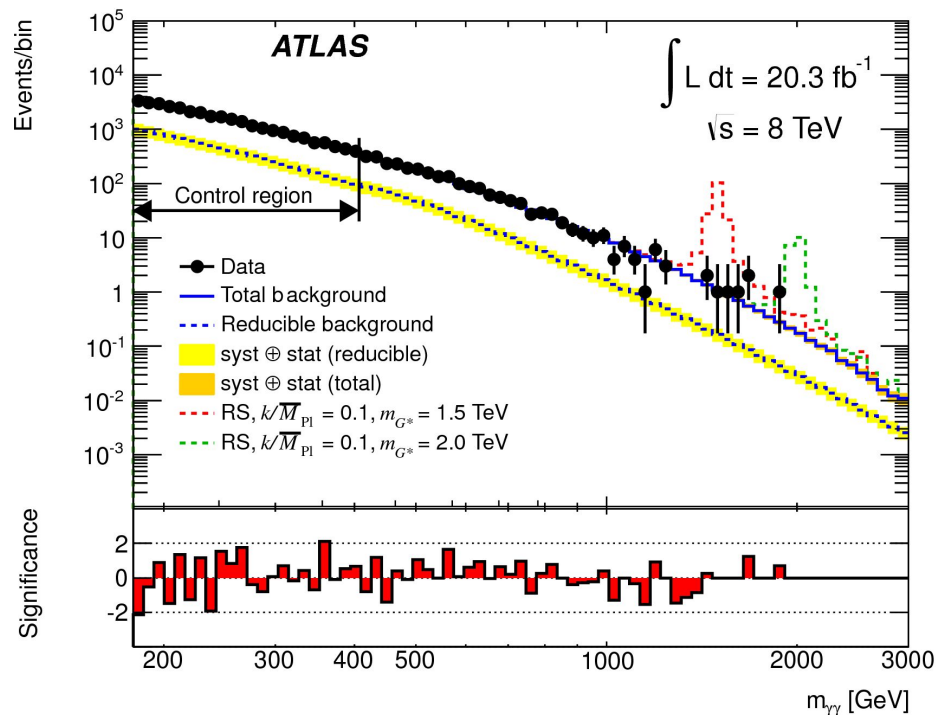
Spin-0 selections

[Phys. Rev. D 92, 032004 \(2015\)](#)



Spin-2 selections

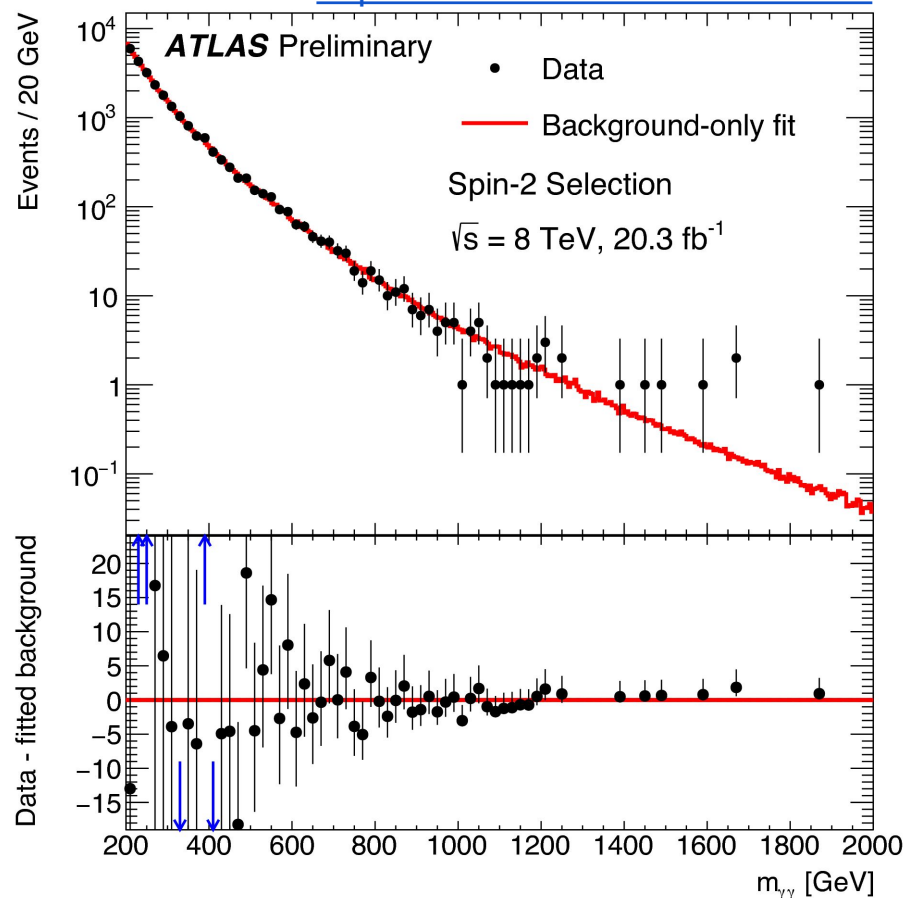
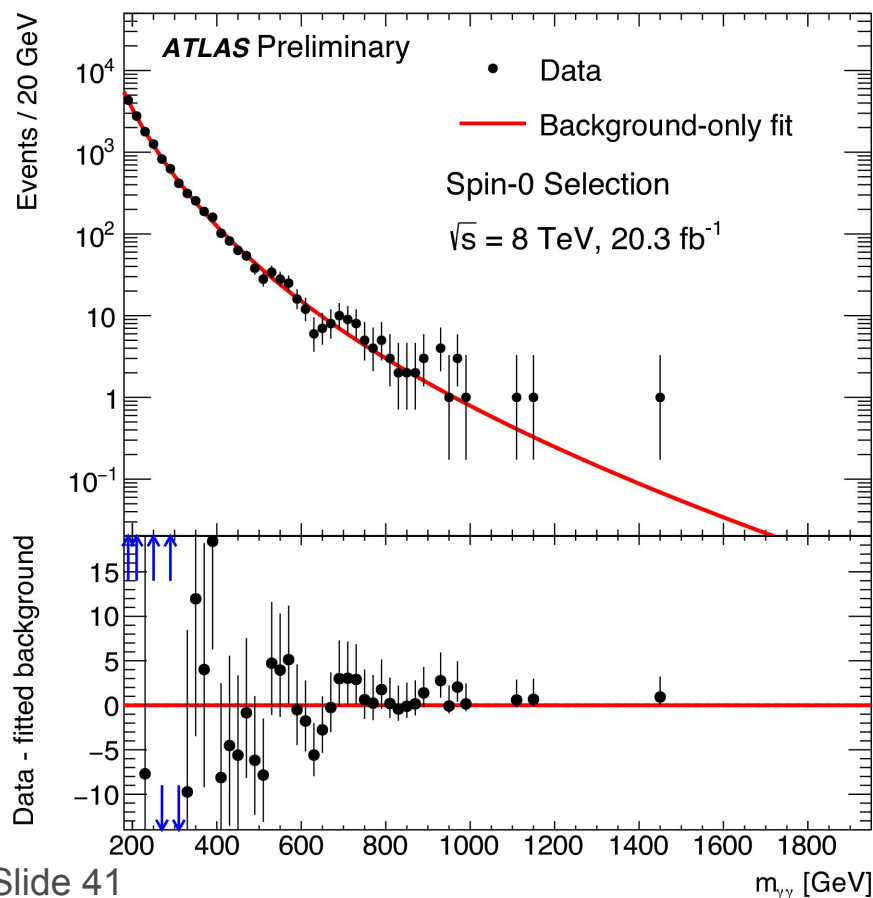
[Phys. Rev. Lett. 113, 171801](#)



Re-analysis / extension of 8 TeV data

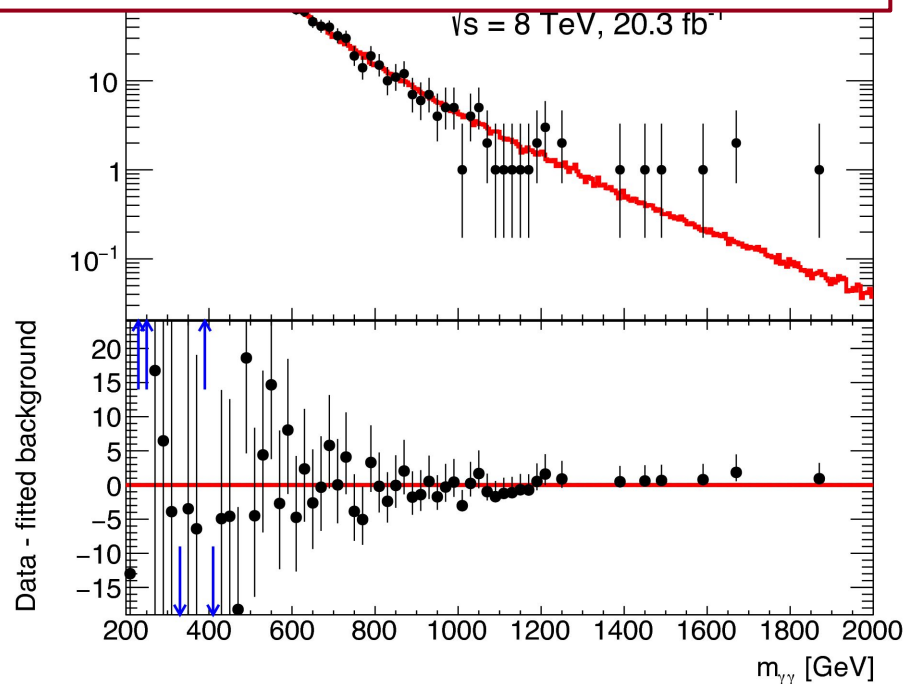
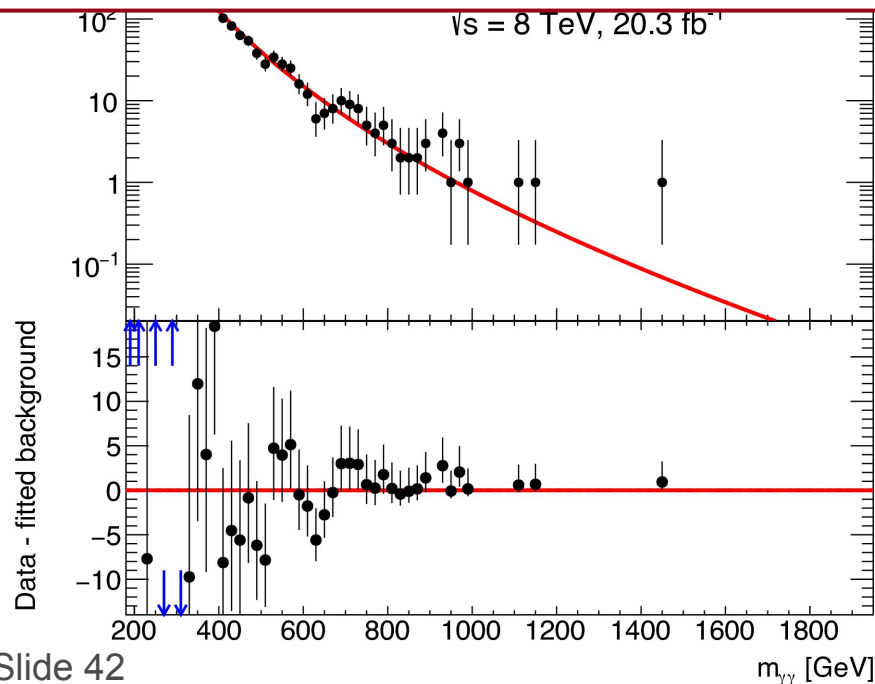
- Updated analysis of 8 TeV data from 2012 (20 fb⁻¹)
 - Final 2012 calibration → correlated uncertainties with 13 TeV
 - Signal + background modeling coherent with 13 TeV analysis
- Selections, identification, isolation remain unchanged

<http://cds.cern.ch/record/2141568>



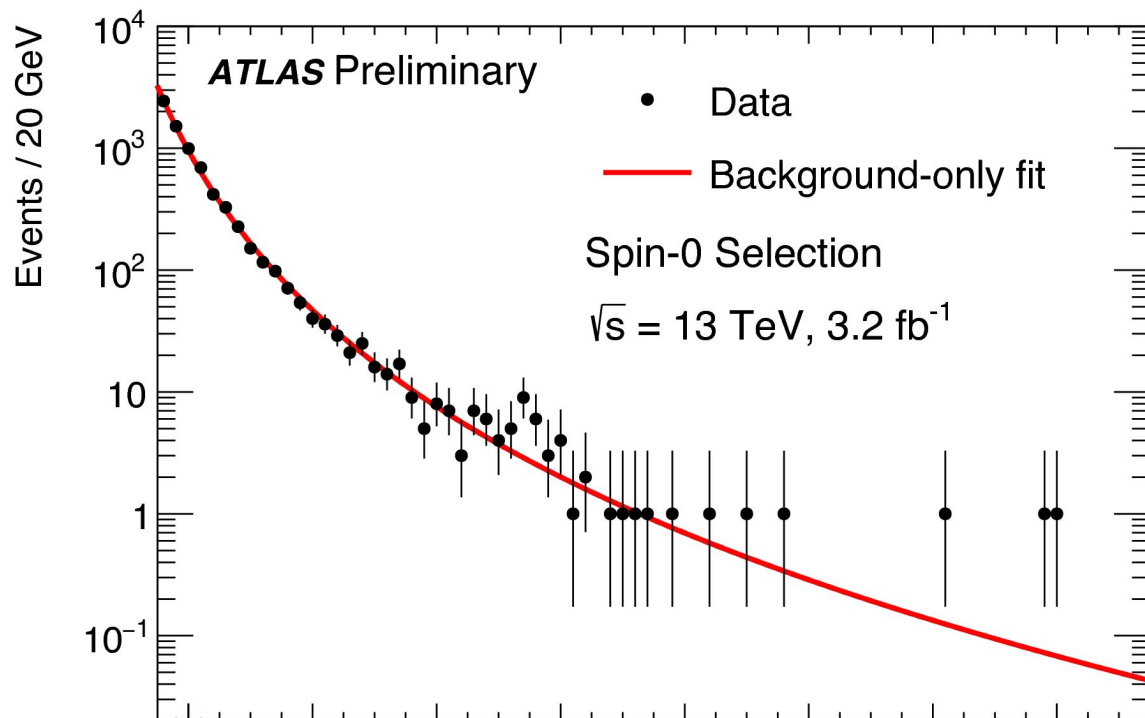
Re-analysis / extension of 8 TeV data

- Calculate local p_0 in 8 TeV around 750 GeV
 - Spin-0 \rightarrow **1.9 σ** (using 6% width)
 - Spin-2 \rightarrow **No excess observed** (using $k/M_{\text{Pl}} = 0.21$)
- Assuming both gg or qq scaling, consistent with 13 TeV result:
 - Spin-0 \rightarrow 1.2 σ (gg \times 4.7), 2.1 σ (qq \times 2.7)
 - Spin-2 \rightarrow 2.7 σ (gg \times 4.7), 3.3 σ (qq \times 2.7)



Summary

- Diphoton excess found around 750 GeV:
 - Spin-0 selections \rightarrow local $p_0 = 3.9 \sigma$, global $Z_0 = 2.0 \sigma$
 - Spin-2 selections \rightarrow local $p_0 = 3.6 \sigma$, global $Z_0 = 1.8 \sigma$
- No evidence (yet) for new physics
- Limits set on cross sections for both signal models



Moving forward

- In the process of preparing a paper presenting 2015 result
- LHC scheduled to begin collecting data again on April 25
- Goal: give a more definitive statement using 2016 data

| | Apr | | | May | | | | June | | | | | |
|----|---------------------------|-----------------------|----|---------|--|----|---------|------|-------------------|-----|----|----|----|
| Wk | 14 | 15 | 16 | 17 | 18 | 19 | 20 | 21 | 22 | 23 | 24 | 25 | 26 |
| Mo | 4 | 11 | 18 | ★ 25 | 2 | 9 | Whit 16 | 23 | 30 | 6 | 13 | 20 | 27 |
| Tu | | | | | | | VdM | | beta* 2.5 km dev. | | | | |
| We | | Injector TS (8 hours) | | | | | | | | TS1 | | | |
| Th | | | | | Ascension | | | | | | | | |
| Fr | Recommissioning with beam | | | | May Day comp | | | | MD 1 | | | | |
| Sa | | | | | Intensity ramp-up Scrubbing as required | | | | | | | | |
| Su | | | | 1st May | | | | | | | | | |

| | July | | | Aug | | | | Sep | | | | | |
|----|------|----|----|-------------------|----|----|----|-----|----|---------|-----|----|----|
| Wk | 27 | 28 | 29 | 30 | 31 | 32 | 33 | 34 | 35 | 36 | 37 | 38 | 39 |
| Mo | 4 | 11 | 18 | 25 | 1 | 8 | 15 | 22 | 29 | 5 | 12 | 19 | 26 |
| Tu | | | | | | | | | | | | | |
| We | | | | MD 2 | | | | | | MD 3 | TS2 | | |
| Th | | | | | | | MD | | | Jeune G | | | |
| Fr | | | | | | | | | | | | | |
| Sa | | | | beta* 2.5 km dev. | | | | | | | | | |
| Su | | | | | | | | | | | | | |

Backup

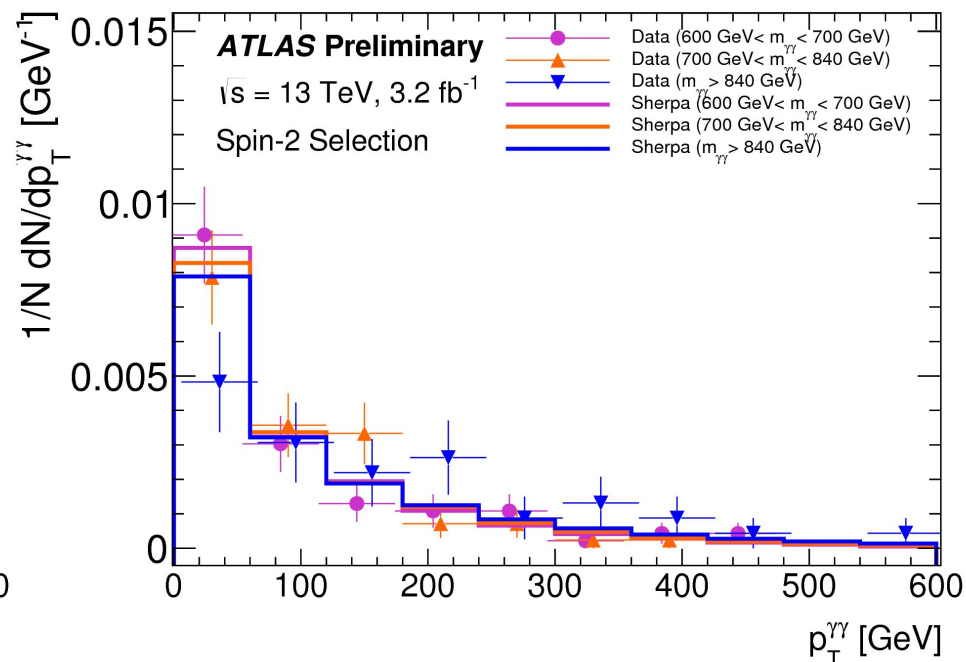
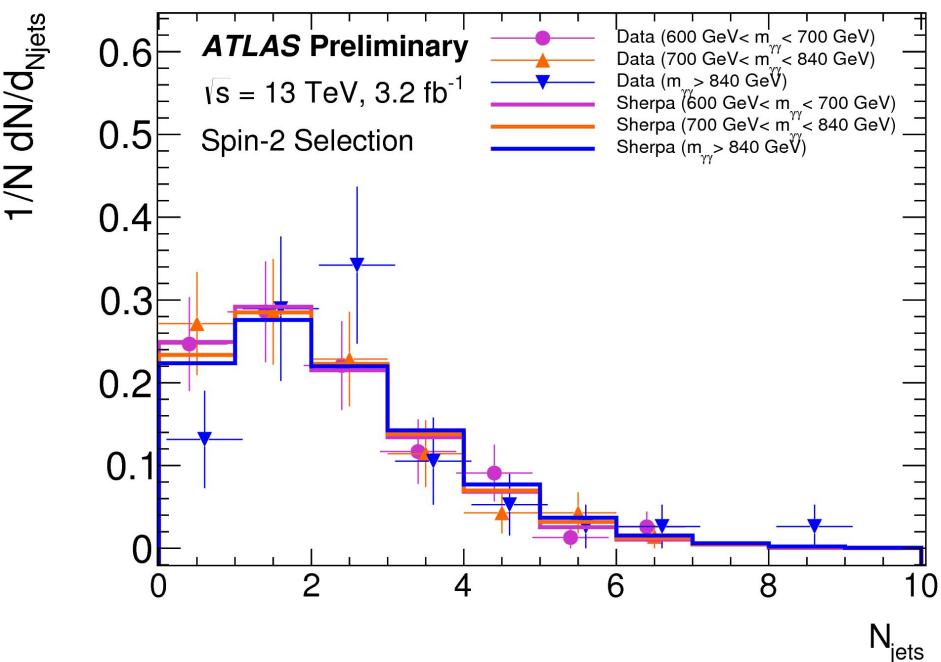
Systematic uncertainty

- Mass dependant range for:
 - Spin-0 resonance → 200 GeV to 2 TeV
 - Spin-2 resonance → 500 GeV to 3.5 TeV
- Spin-0 → 2878 events, spin-2 → 5066

| Uncertainty | spin-2 search | spin-0 search | |
|--|-------------------------|--|-----------------|
| Background (mass dependent) | $\pm 7\%$ to $\pm 35\%$ | spurious signal 20 – 0.04 events for $\Gamma/M=6\%$ | p_0 and limit |
| Signal mass resolution (mass dependent) | | $(^{+55}_{-20})\%$ – $(^{+110}_{-40})\%$ | p_0 and limit |
| Signal photon identification (mass dependent) | | $\pm(3 - 2)\%$ | limit |
| Signal photon isolation (mass dependent) | $\pm(3-1)\%$ | $\pm(4-1)\%$ | limit |
| Signal production process | N/A | $\pm(3-6)\%$ depending on Γ | limit |
| Trigger efficiency | | $\pm 0.6\%$ | limit |
| Luminosity | | $\pm 5.0\%$ | limit |

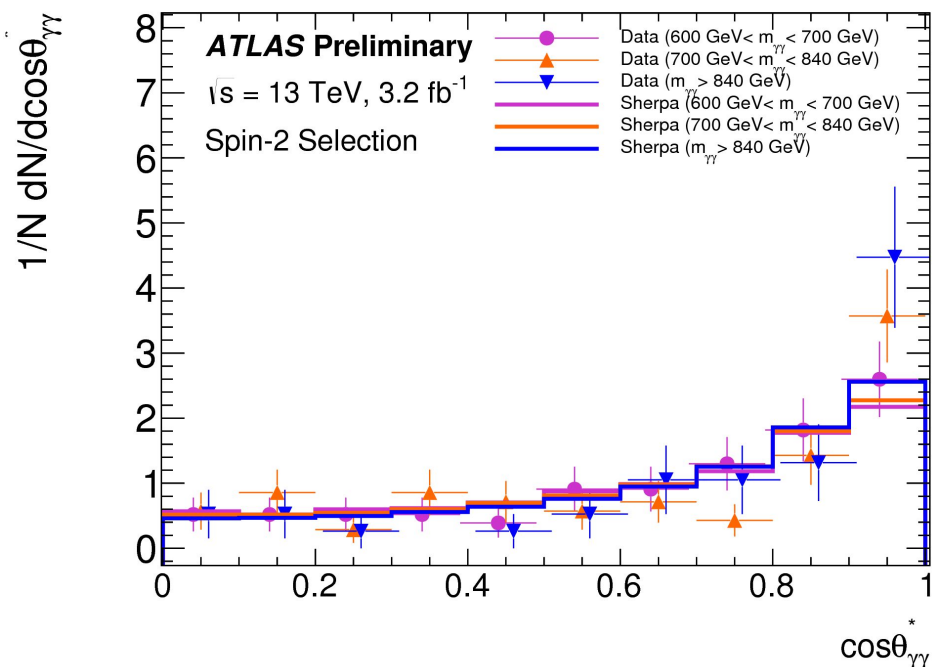
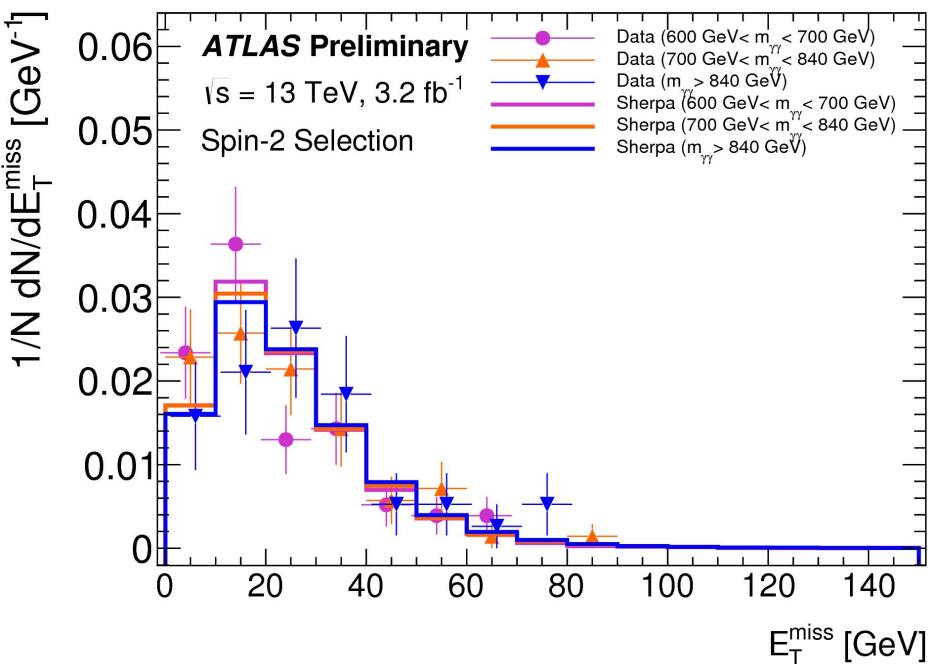
Kinematic distributions for spin-2

- Examine properties of events in different mass regions
 - Low side-band: 600-700 GeV
 - Excess region: 700-840 GeV
 - High side-band: >840 GeV
- No significant difference observed in different mass regions



Kinematic distributions for spin-2

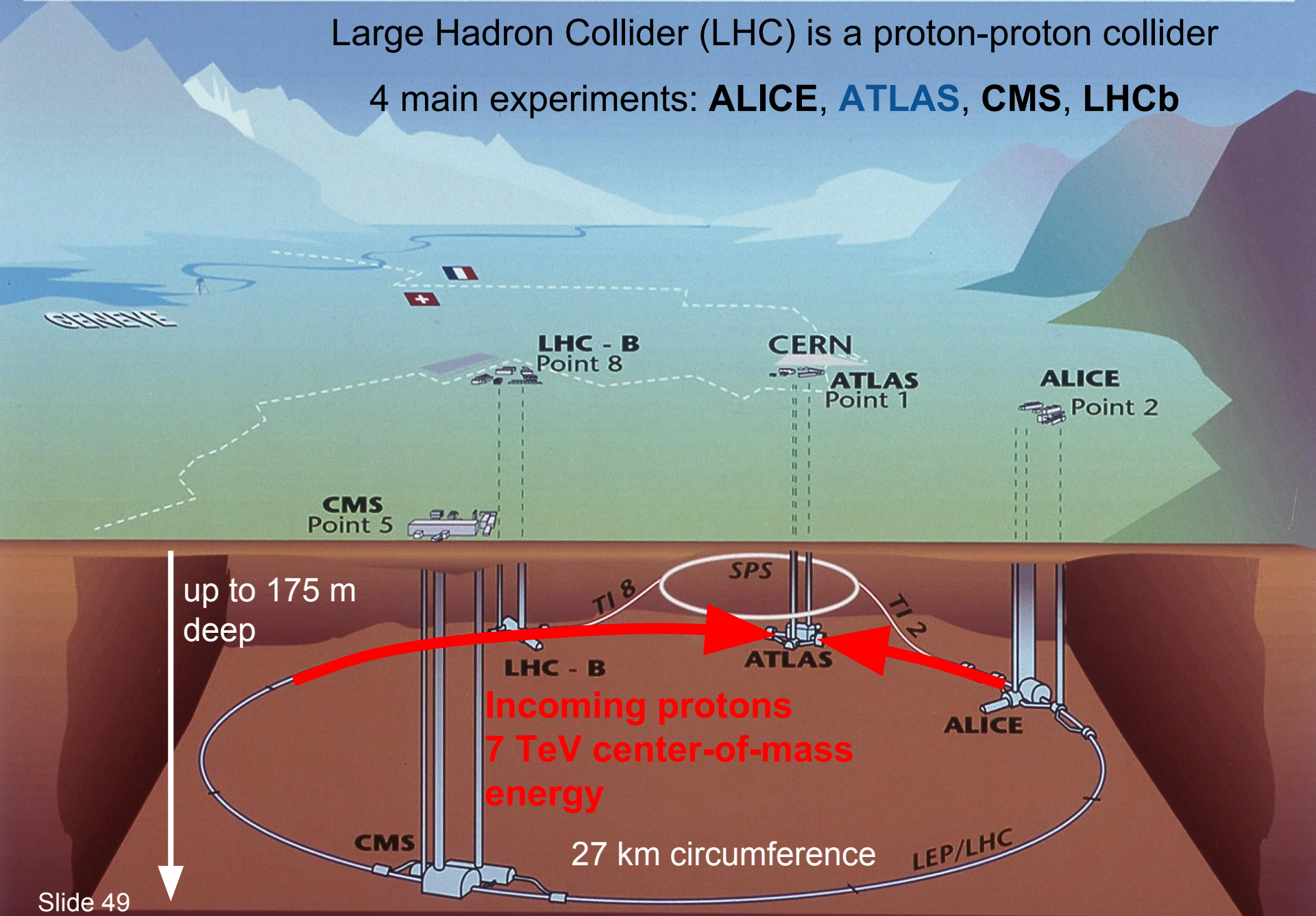
- Examine properties of events in different mass regions
 - Low side-band: 600-700 GeV
 - Excess region: 700-840 GeV
 - High side-band: >840 GeV
- No significant difference observed in different mass regions



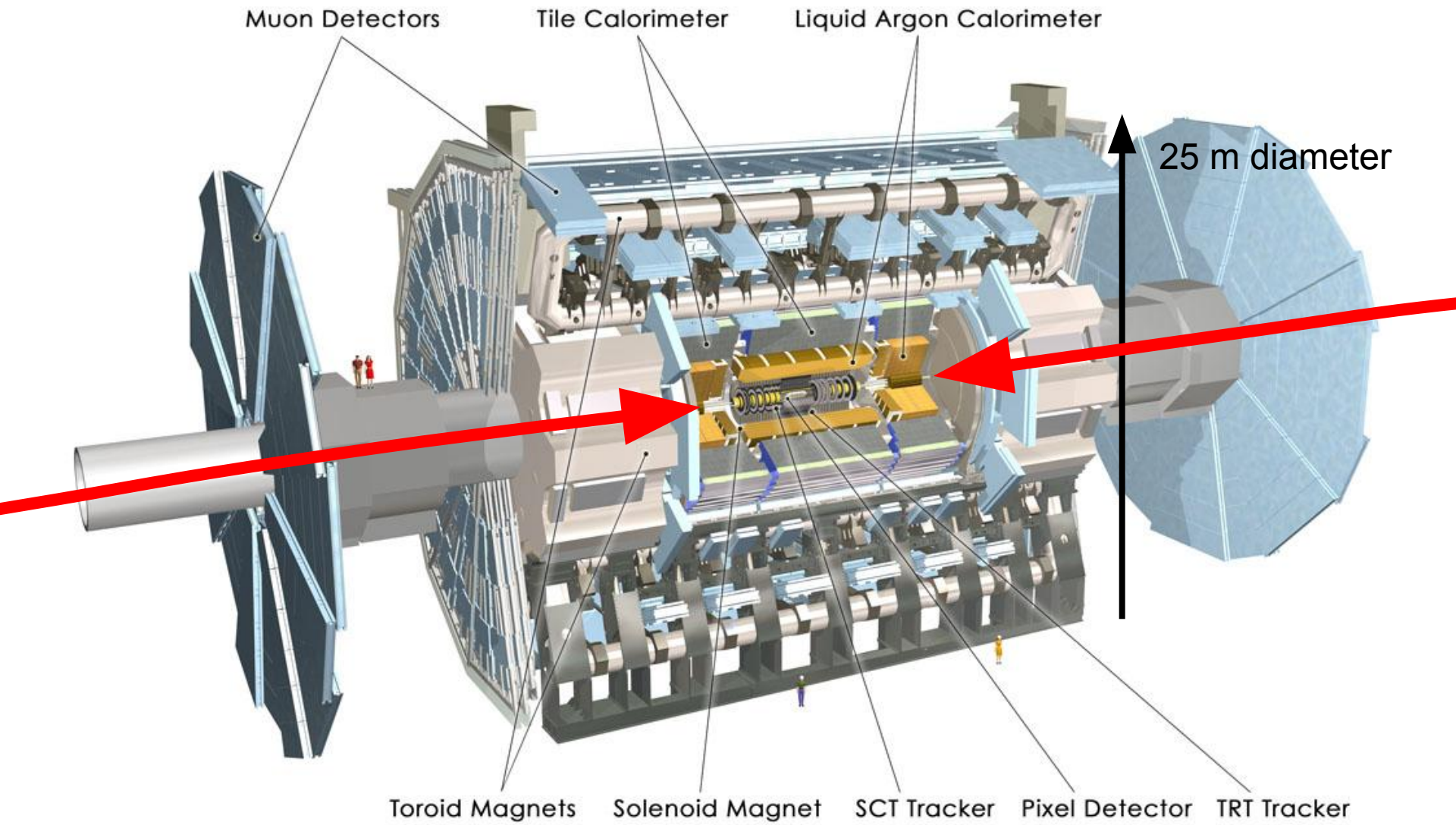
Overall view of the LHC experiments.

Large Hadron Collider (LHC) is a proton-proton collider

4 main experiments: **ALICE**, **ATLAS**, **CMS**, **LHCb**

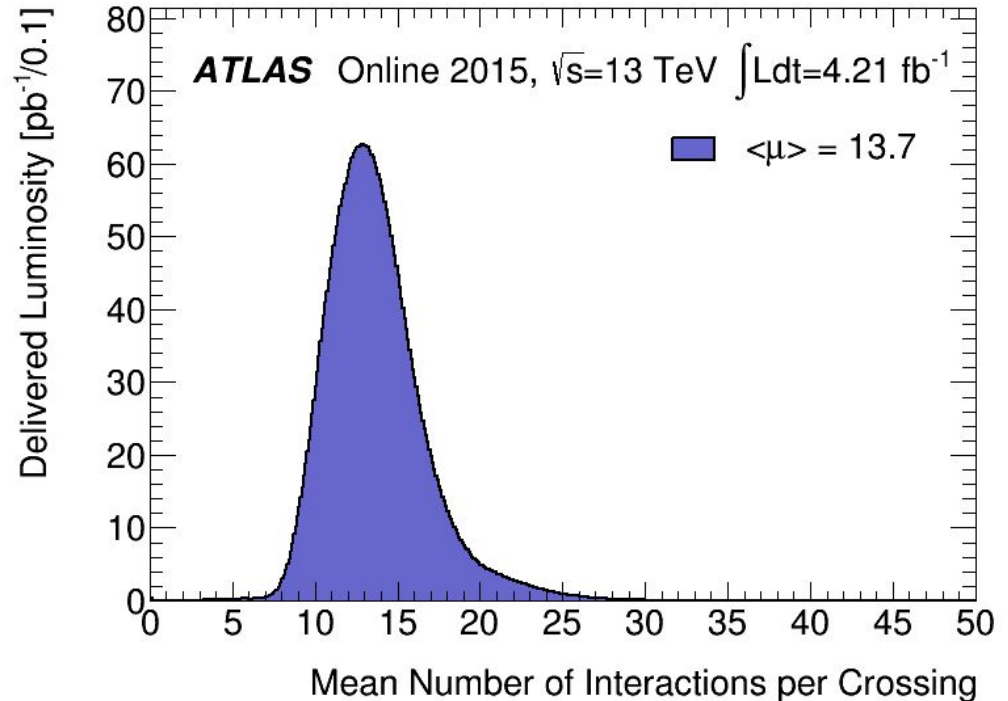


ATLAS: A Toroidal LHC ApparatuS



Data recording

- Proton-proton collisions at 13 TeV with 25 ns bunch spacing
 - Average interactions / bunch crossing: $\langle\mu\rangle = 13.7$



- Diphoton event trigger:
 - $E_{T,1} > 35, E_{T,2} > 25$ GeV
 - Loose photon shower criteria
 - Trigger is close to 99% efficient for events passing final selection

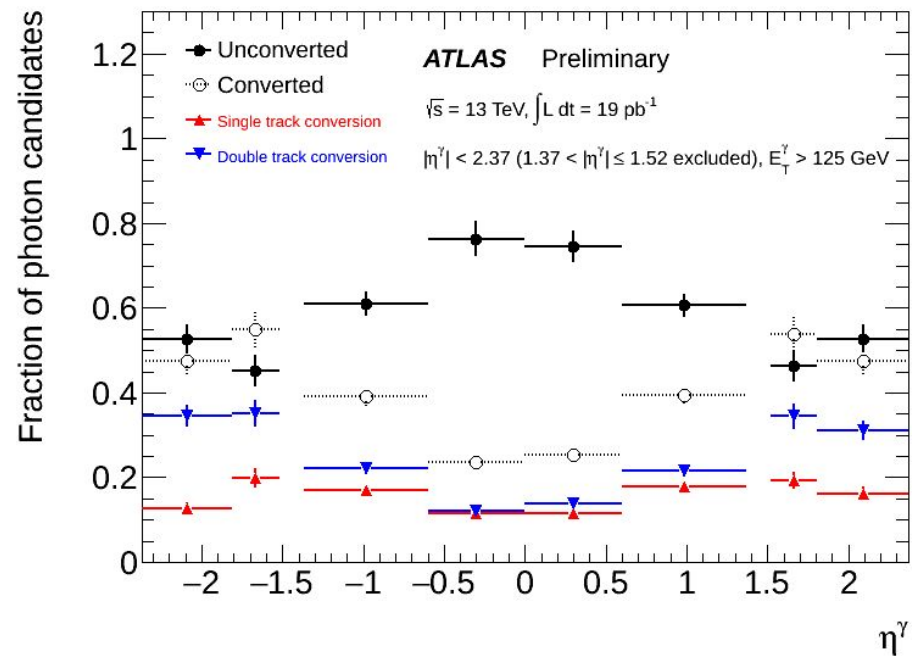
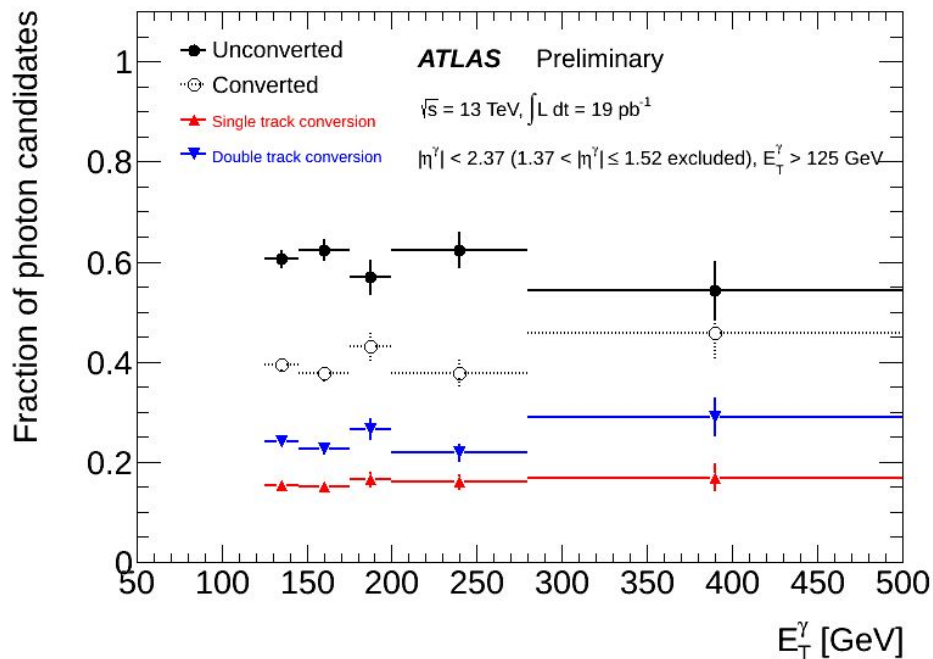


Photon reconstruction

- Create towers with $\Delta\eta \times \Delta\phi$ of 0.025×0.025
- Sliding window of 3×5 towers
 - Pre-cluster if $E_T > 2.5$ GeV, and local maximum
 - For close-by pre-clusters, remove smaller E_T pre-cluster
 - Position taken from barycentre of all attached cells
- Cluster formed starting in middle layer
 - First middle layer cells attached
 - Those within window, with centre taken as pre-cluster position
 - Then strip layer cells attached, using middle-layer barycentre
 - PS uses strip-layer barycentre to attach cells
 - Back layer uses mid-layer barycentre to attach cells
 - Different window sizes used for each type of particle
- Depending on attached tracks, electron or photon
 - Converted photon, unconverted photon, electron \rightarrow diff calibration

Photon conversion reconstruction

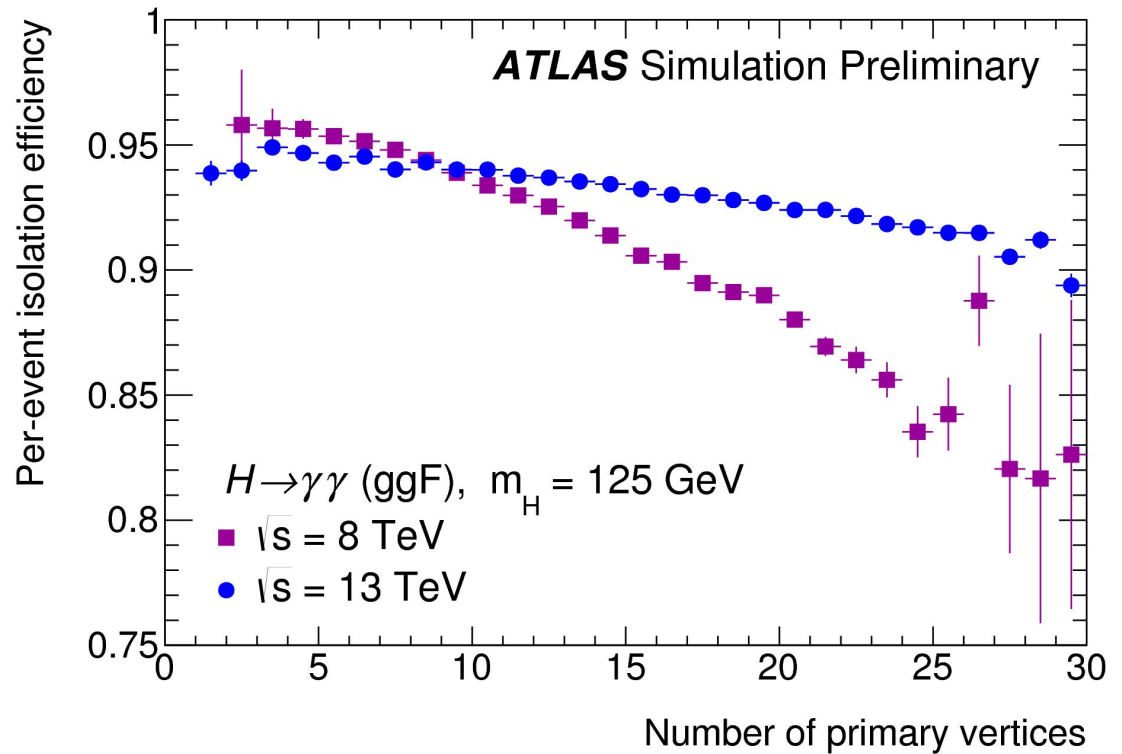
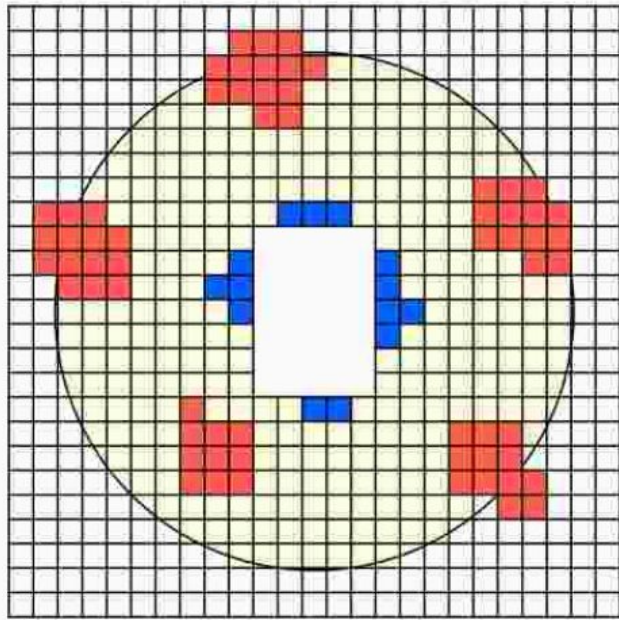
<https://atlas.web.cern.ch/Atlas/GROUPS/PHYSICS/PLOTS/EGAM-2015-004/index.html>



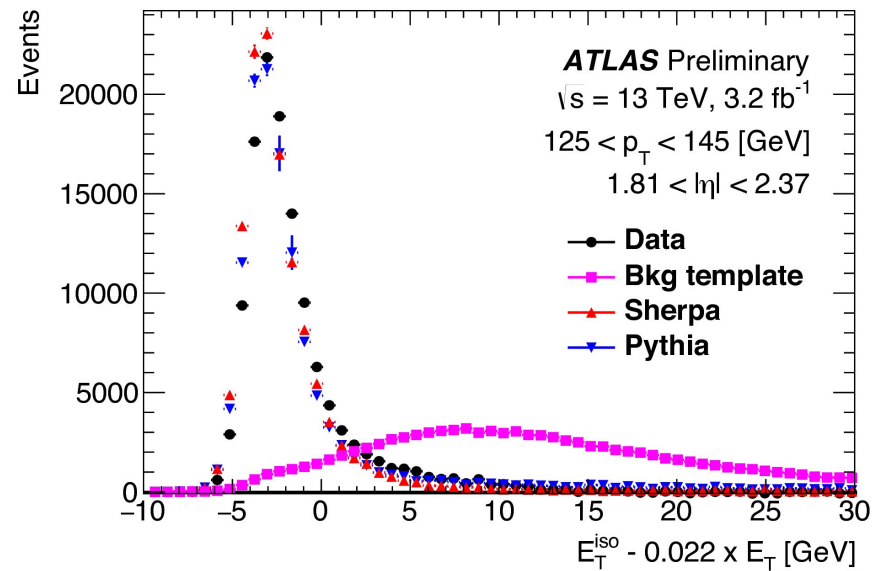
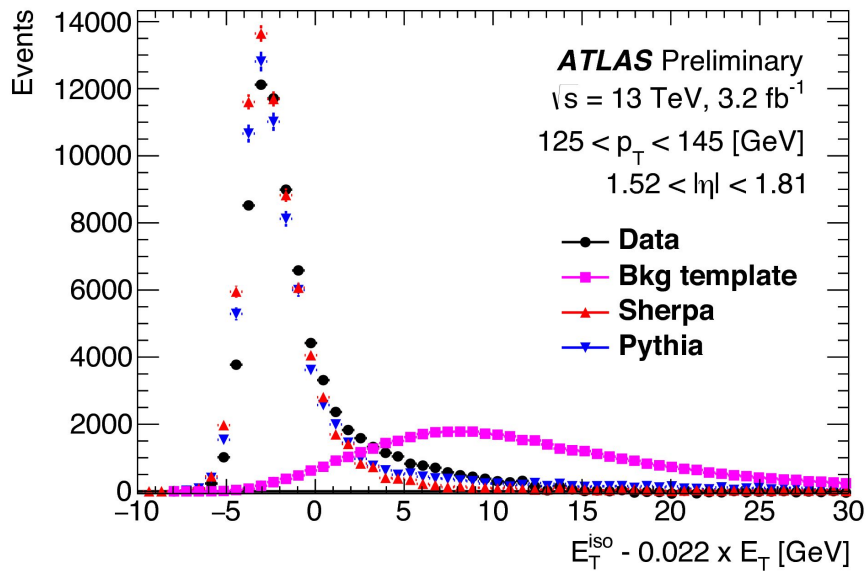
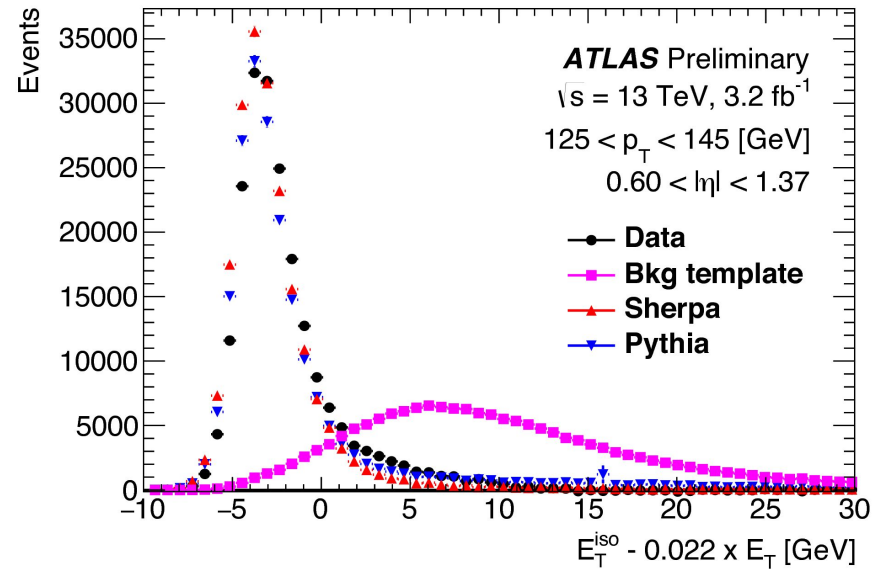
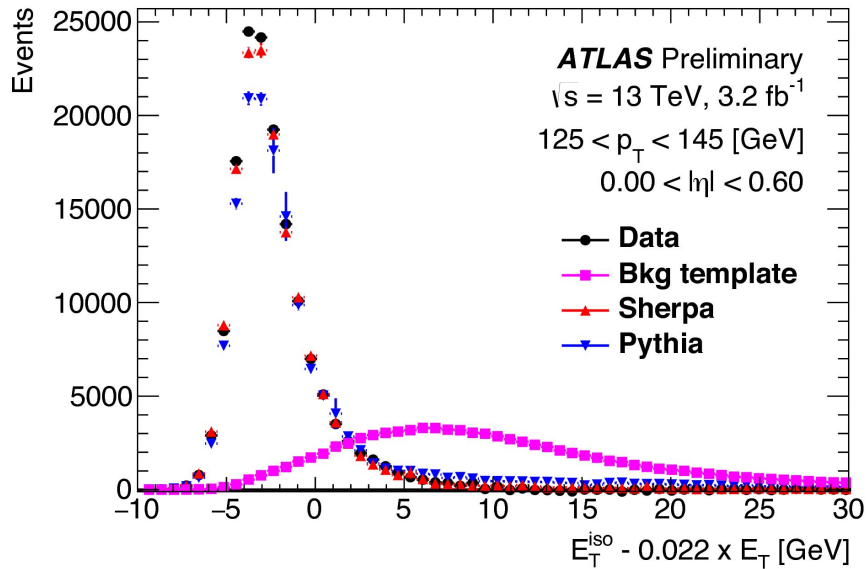
Photon isolation

- Both calorimeter and track isolation required
 - Calo isolation \rightarrow sum of E_T of energy clusters within $\Delta R = 0.4$
 - Ignore $\Delta\eta \times \Delta\phi = 0.125 \times 0.125$ centered on photon
 - Subtract out-of-cone energy from isolation
 - $E_{T,iso} < 0.022 E_T + 2.45 \text{ GeV}$
 - Track isolation \rightarrow scalar sum of track p_T within $\Delta R = 0.2$
 - Track $p_T > 1 \text{ GeV}$
 - Consistent with selected primary vertex
 - $p_{T,iso} < 0.05 E_T$
- Isolation efficiency uses tight definition, anti-tight definition
 - Shape of anti-tight definition normalized to tight
 - Anti-tight background subtracted from data
 - Compared with signal MC simulation

Photon isolation



Photon isolation

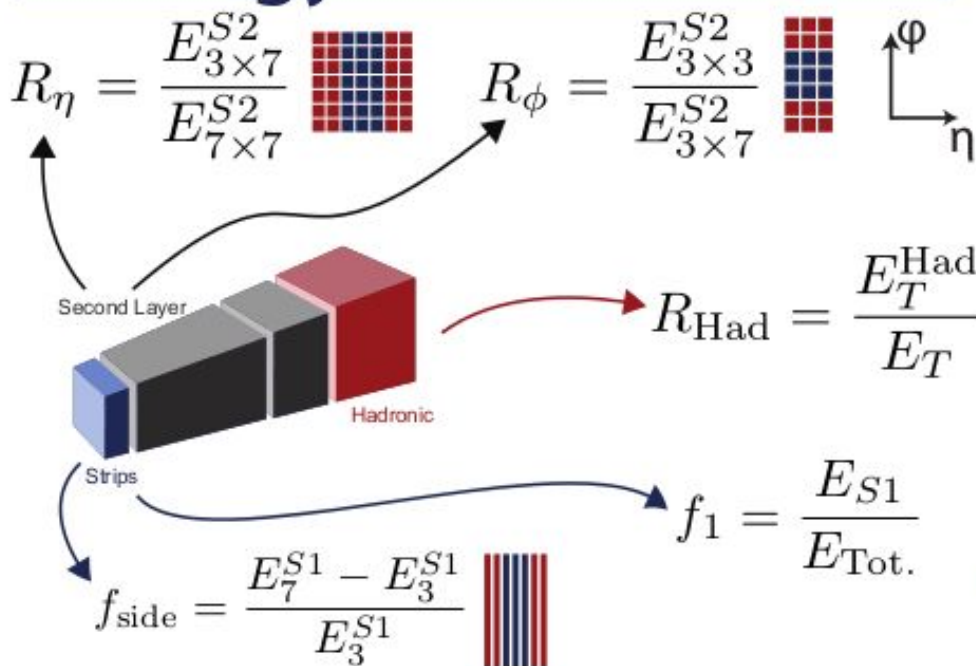


Photon identification variables

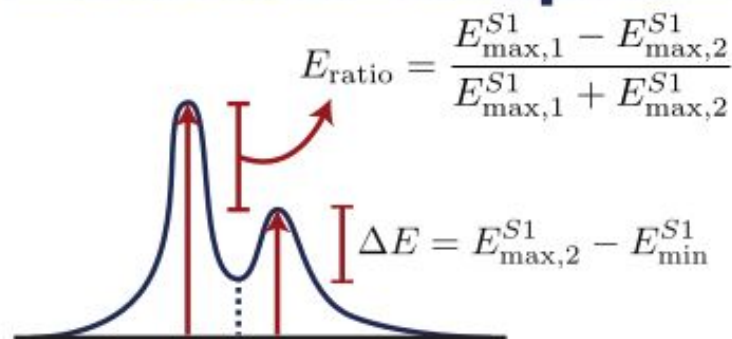
Variables and Position

| | Strips | 2nd | Had. |
|--------|------------------------|------------------------|---------------------|
| Ratios | f_1, f_{side} | R^*, R_ϕ | $R_{\text{Had.}}^*$ |
| Widths | $w_{s,3}, w_{s,t}$ | $w_{,2}^*$ | - |
| Shapes | Δ , ratio | * Used in PhotonLoose. | |

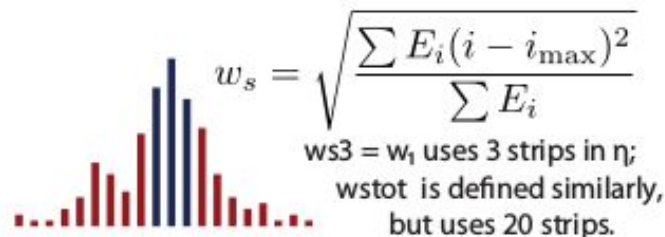
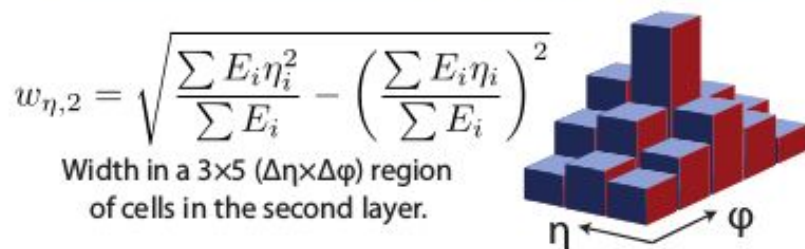
Energy Ratios



Shower Shapes



Widths



Slide by J. Saxon

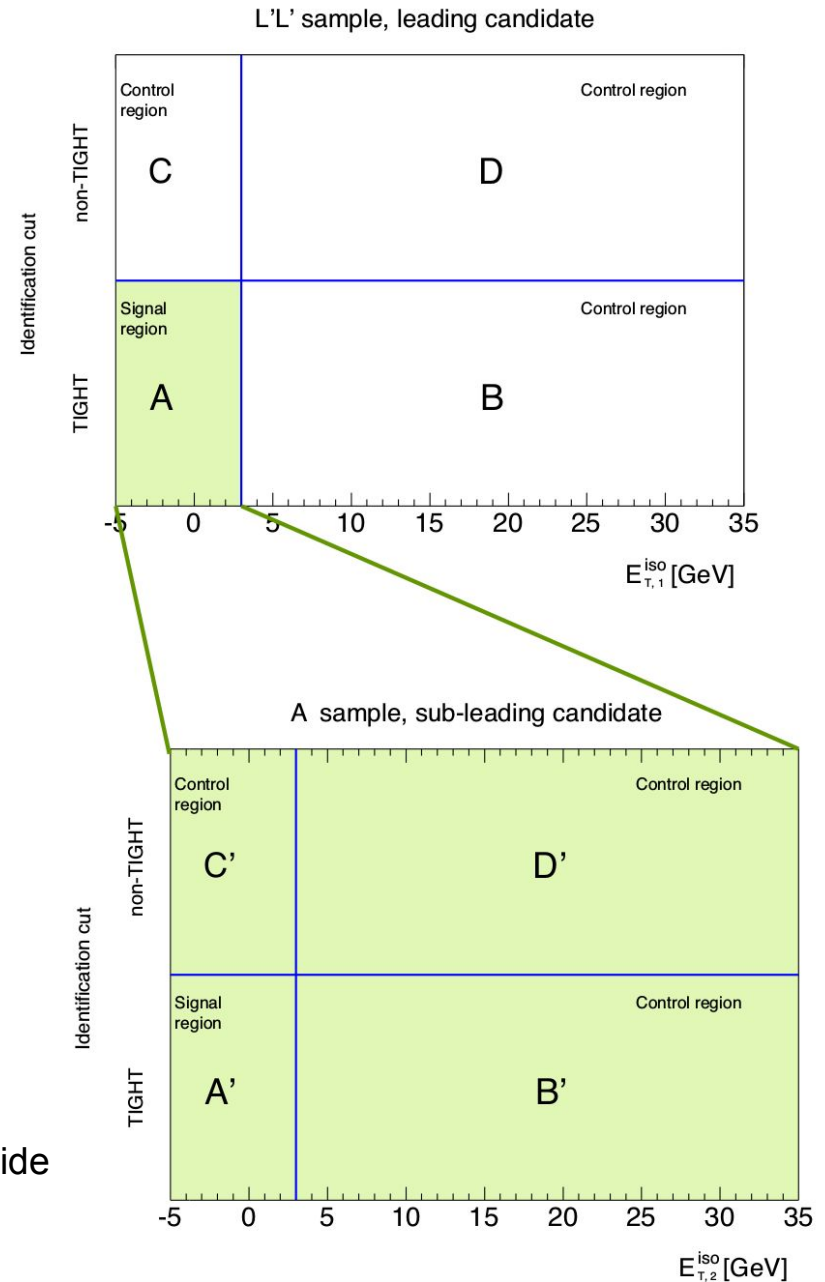
Photon calibration

- Multivariate analysis used for photon calibration
 - Optimized on MC simulation
- Correction for energy outside cluster, in front of calorimeter
- Accounts for variation of response vs calorimeter entry point
- Inputs for all photons:
 - Measured energy per layer
 - η of cluster, local position wrt cluster centroid
- Inputs for converted photons:
 - Track transverse momentum
 - Conversion radius
- Input layer energies calibrated using 2012 results
- Overall calibration estimated with $Z \rightarrow ee$ events

2x2D method

- Divide sample into 16 regions
 - Pass/fail photon identification
 - Pass/fail photon isolation
- Use isolation and identification efficiency from $\gamma\gamma$ simulation
- Solve a set of equations relating the regions
 - Provides number of $\gamma\gamma$, γj , jj events in the selected sample

Figure from M. Delmastro slide



Matrix method

$$\begin{pmatrix} \text{PP} \\ \text{PF} \\ \text{FP} \\ \text{FF} \end{pmatrix} = \begin{pmatrix} \epsilon_1 \epsilon_2 & \epsilon_1 f_2 & f_1 \epsilon_2 & f_1 f_2 \\ \epsilon_1 (1 - \epsilon_2) & \epsilon_1 (1 - f_2) & f_1 (1 - \epsilon_2) & f_1 (1 - f_2) \\ (1 - \epsilon_1) \epsilon_2 & (1 - \epsilon_1) f_2 & (1 - f_1) \epsilon_2 & (1 - f_1) f_2 \\ (1 - \epsilon_1)(1 - \epsilon_2) & (1 - \epsilon_1)(1 - f_2) & (1 - f_1)(1 - \epsilon_2) & (1 - f_1)(1 - f_2) \end{pmatrix} \begin{pmatrix} W_{\gamma\gamma} \\ W_{\gamma j} \\ W_{j\gamma} \\ W_{jj} \end{pmatrix}$$

Passes or Fails
isolation cut

ϵ_i = probability for a γ to pass isolation cut (data-driven)

f_j = probability for a jet to pass isolation cut (data-driven)

Event
weights

accounting for the correlation of the isolation energy of the 2 γ candidates

Figure from M. Delmastro slide

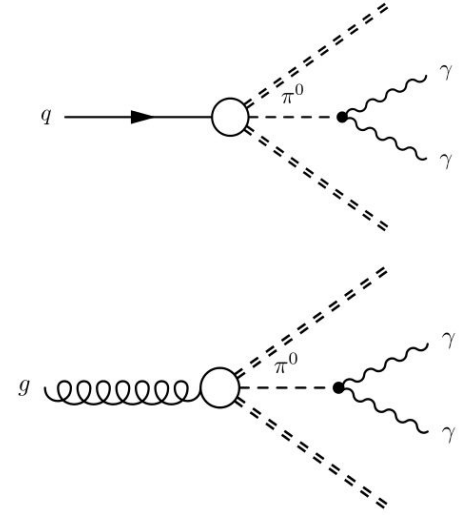
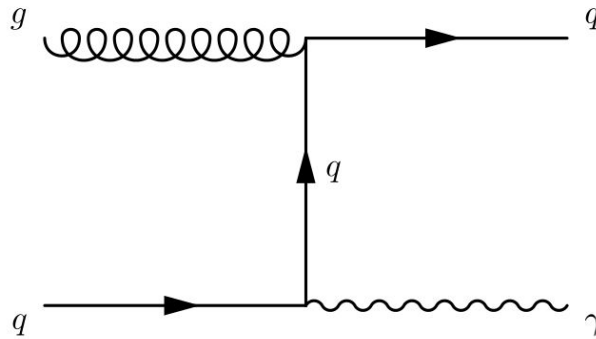
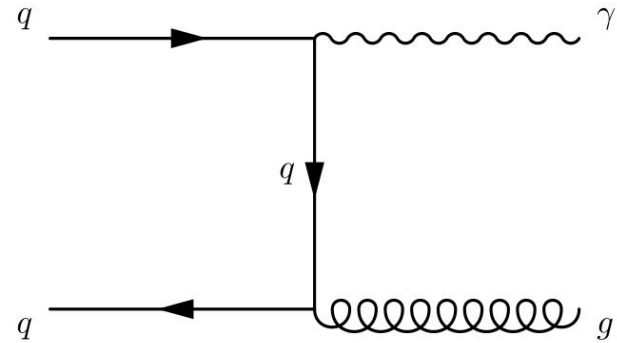
- Only invert isolation cut (2x2D also inverts identification)
- Consistent result with 2x2D method

Background MC simulation

- SHERPA generator (with GEANT4)
 - Irreducible background: two prompt photons
 - Up to two additional partons
 - Includes gluon induced box process
 - Reducible background: one prompt photon
- PYTHIA8 generator (with GEANT4)
 - Irreducible background: two prompt photons
 - qqbar t-channel annihilation
 - Gluon induced box processes
 - Pileup overlay events

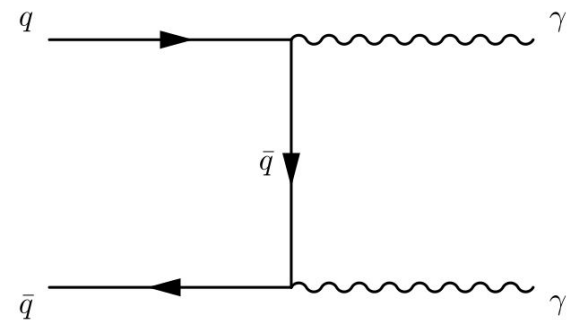
Background MC simulation

Reducible

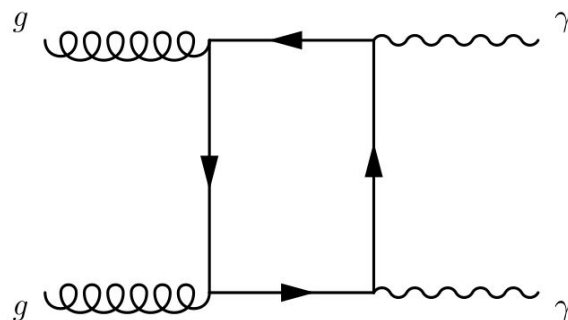


Irreducible

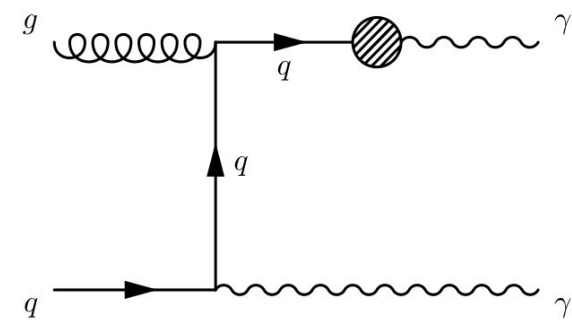
born



box



parton fragmentation



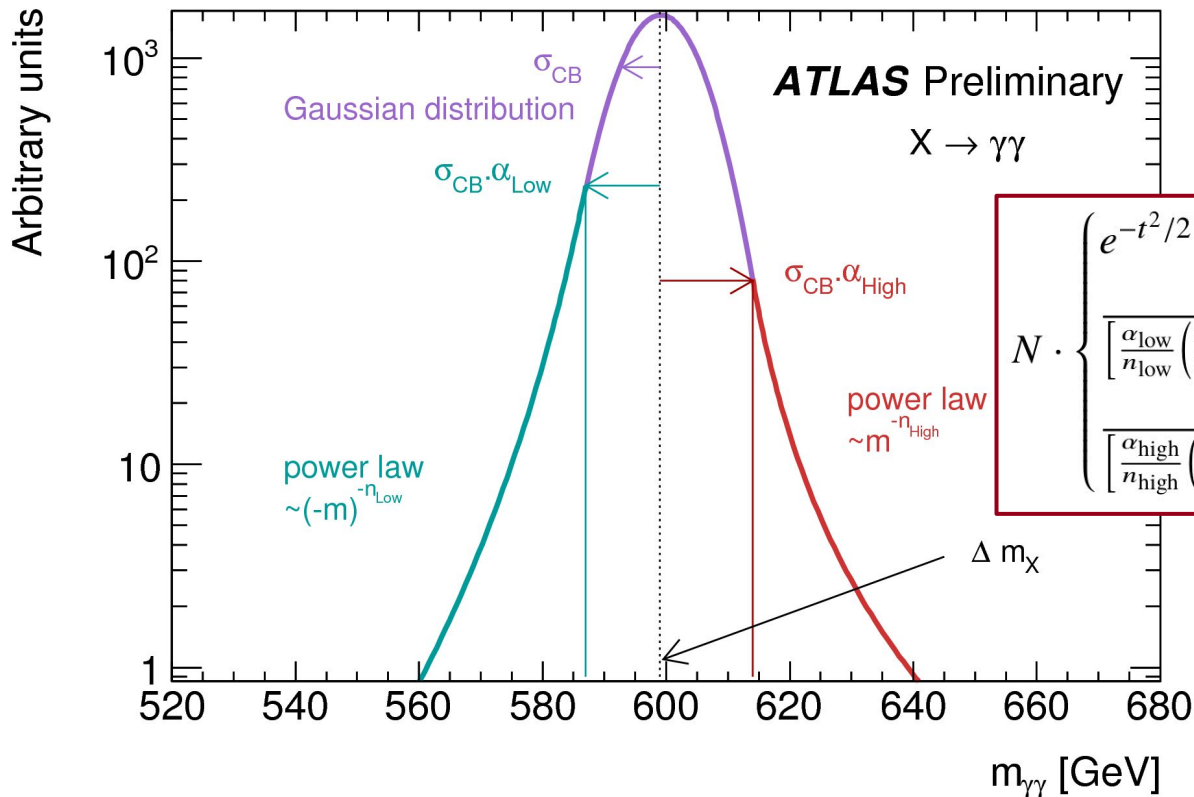
Figures from M. Delmastro slide

Signal simulation

- Spin-0 resonance samples
 - Production through gluon fusion is the default
 - Other production modes considered to impact signal modeling
 - POWHEG+PYTHIA8 used for all samples
 - Narrow width \rightarrow 4 MeV
 - Large width \rightarrow line shape modeled with Breit-Wigner distribution
 - Based on running-width scheme, xs dependence on gg luminosity
- Spin-2 resonance samples
 - PYTHIA8 from 500 GeV to 5 TeV, k/M_{Pl} from 0.01 to 0.3
 - Also a sample flat in mass \rightarrow reweight to any mass/width point
 - Graviton coupling increases with energy of decay products
 - Produces high-mass tail in spin-2, not present in spin-0
 - Full detector simulation using GEANT4

Signal modeling

- Double-sided Crystal Ball function
 - Peak near resonance mass, width from intrinsic decay and detector
- Spin-0 narrow width σ_{CB} varies from 2 GeV to 13 GeV
- Spin-2 convolutes detector resolution with theoretical line shape



$$N \cdot \begin{cases} e^{-t^2/2} & \text{if } -\alpha_{\text{low}} \geq t \geq \alpha_{\text{high}} \\ \frac{e^{-0.5\alpha_{\text{low}}^2}}{\left[\frac{\alpha_{\text{low}}}{n_{\text{low}}} \left(\frac{n_{\text{low}}}{\alpha_{\text{low}}} - \alpha_{\text{low}} - t\right)\right]^{n_{\text{low}}}} & \text{if } t < -\alpha_{\text{low}} \\ \frac{e^{-0.5\alpha_{\text{high}}^2}}{\left[\frac{\alpha_{\text{high}}}{n_{\text{high}}} \left(\frac{n_{\text{high}}}{\alpha_{\text{high}}} - \alpha_{\text{high}} + t\right)\right]^{n_{\text{high}}}} & \text{if } t > \alpha_{\text{high}}, \end{cases}$$

$$t = \Delta m_{\gamma\gamma} / \sigma_{CB}$$

$$\Delta m_{\gamma\gamma} = m_{\gamma\gamma} - \mu_{CB}$$

Spin-0 and spin-2 compatibility

- Events from spin-0 are a subset of those for spin-2
- A bootstrap method is used to assess compatibility
 - Union dataset is sliced into N blocks with 10 events in each block
 - N blocks are randomly picked regardless of possible duplication
 - i.e. the same block could be selected for more than one time
 - Pseudo-dataset will then pass spin-0 and spin-2 selections
 - Pseudo-dataset is fed into S+B fit assuming same signal hypothesis
 - Procedure is repeated many times until decent statistics are accumulated for compatibility check
- Spin-0 signal assumption $\rightarrow 0.2 \sigma$ compatibility
- Spin-2 signal assumption $\rightarrow 0.9 \sigma$ compatibility

Correction and acceptance

- Expected signal yield is: $\sigma \times \text{BR} \times A \times C$
 - $\sigma \rightarrow$ production cross section
 - BR \rightarrow branching ratio
 - A \rightarrow Acceptance (# particle-level / # total)
 - C \rightarrow Reconstruction / ID efficiency (# detector-level / #particle-level)
- Spin-0 reports limits on fiducial cross section ($\sigma \times \text{BR} \times A$)
 - Particle-level \rightarrow same kinematic selection + truth isolation
 - $E_{\text{Tiso}} < 0.05 E_{\text{T}} + 6 \text{ GeV}$
 - Also apply $\pm 2 \Gamma$ width cut on signal peak (reduce model dep)
 - A ranges from 75% to 85% (200 GeV to 1 TeV)
 - C ranges from 55% to 70% (200 GeV to 1 TeV)
- Spin-2 reports limit on total cross section ($\sigma \times \text{BR} \times A \times C$)
 - A \times C ranges from 45% to 60% (500 GeV to 3 TeV)

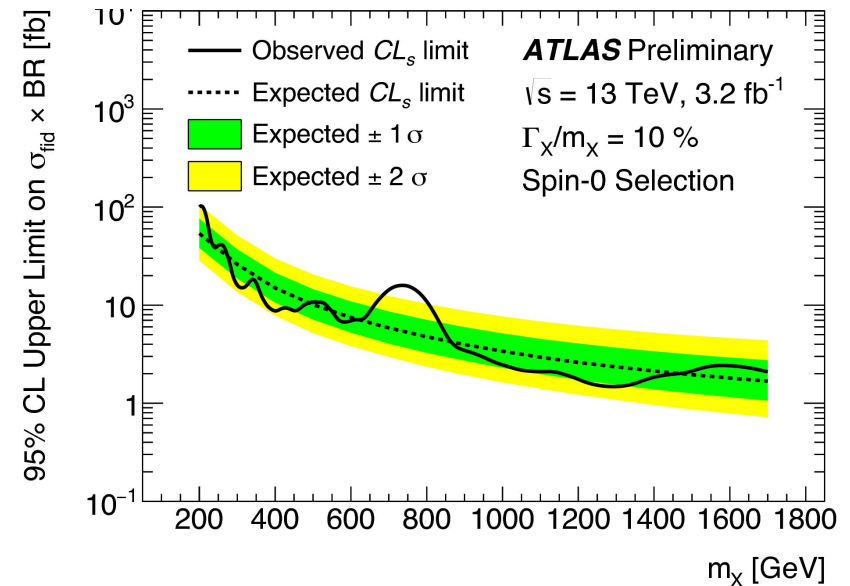
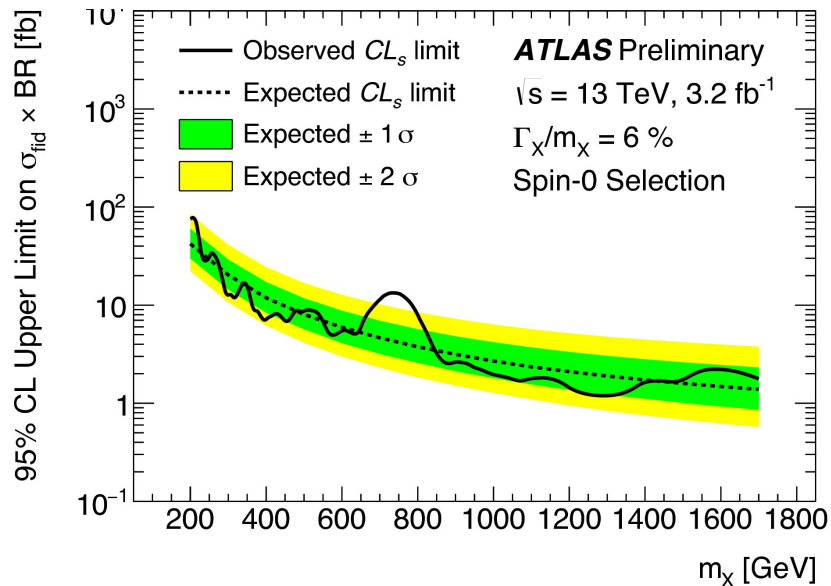
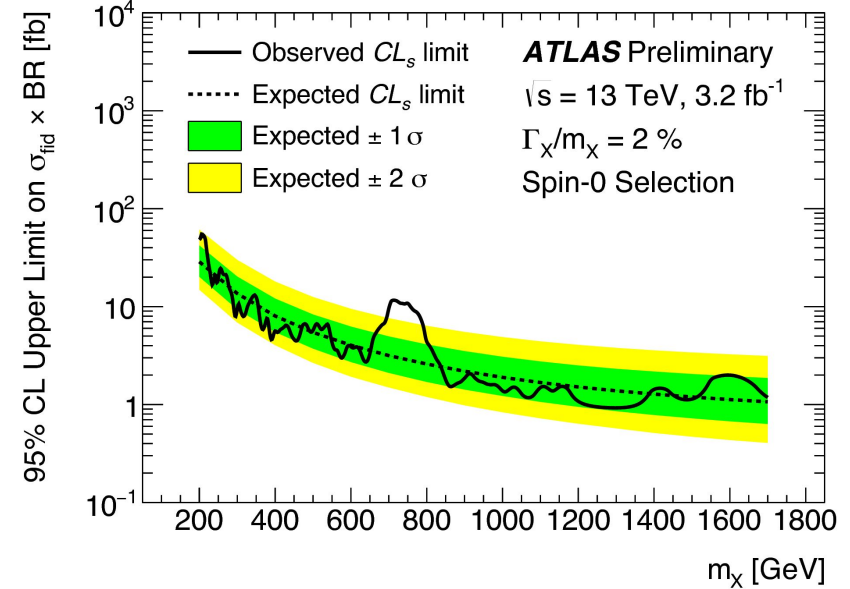
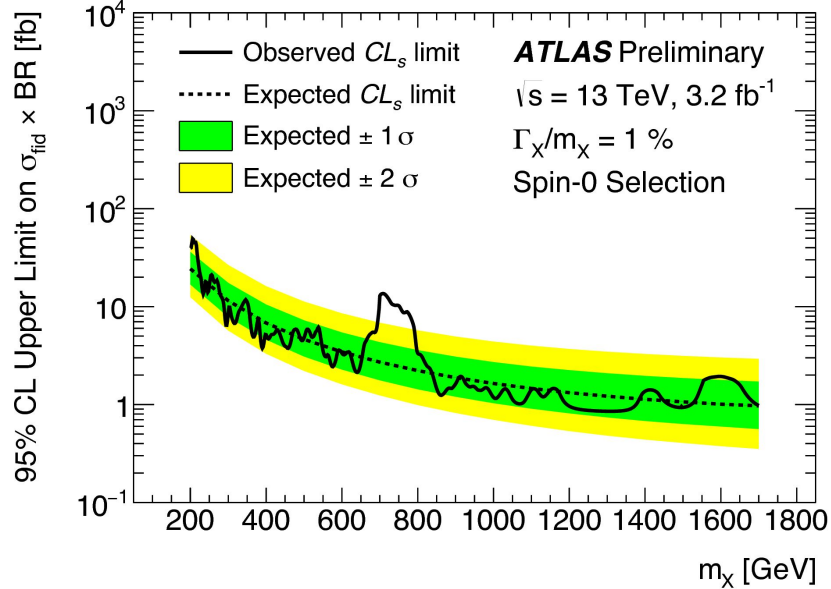
F-test

- Possibility that data needs more degrees of freedom in fit
- In the case that a more complex function f_2 embeds f_1
- Define a test statistic:

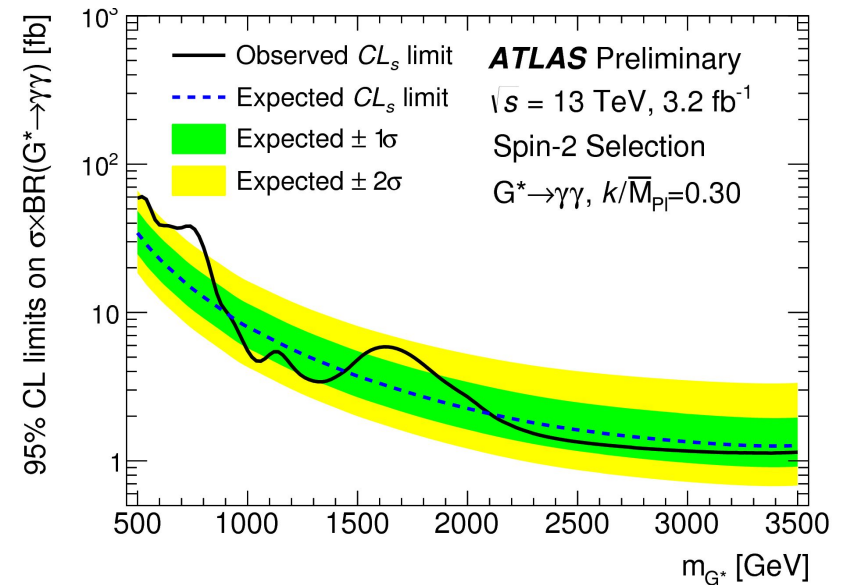
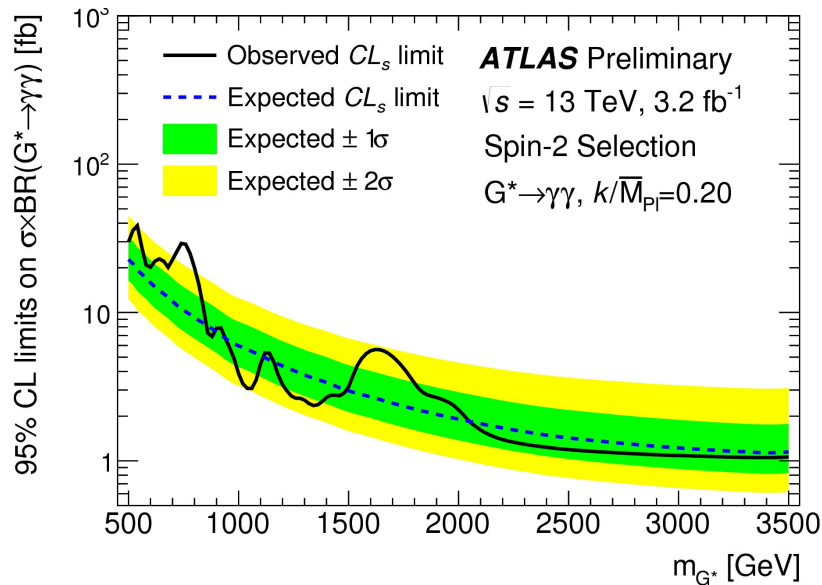
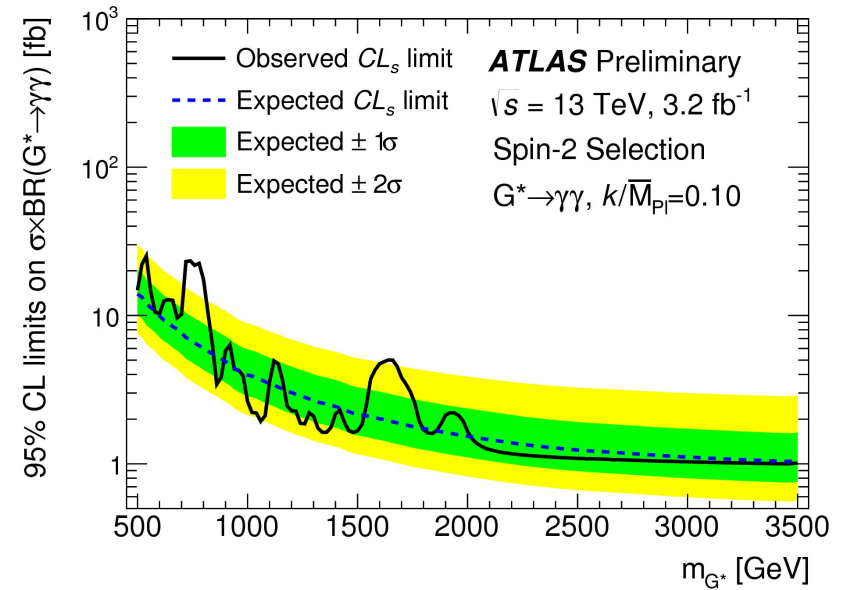
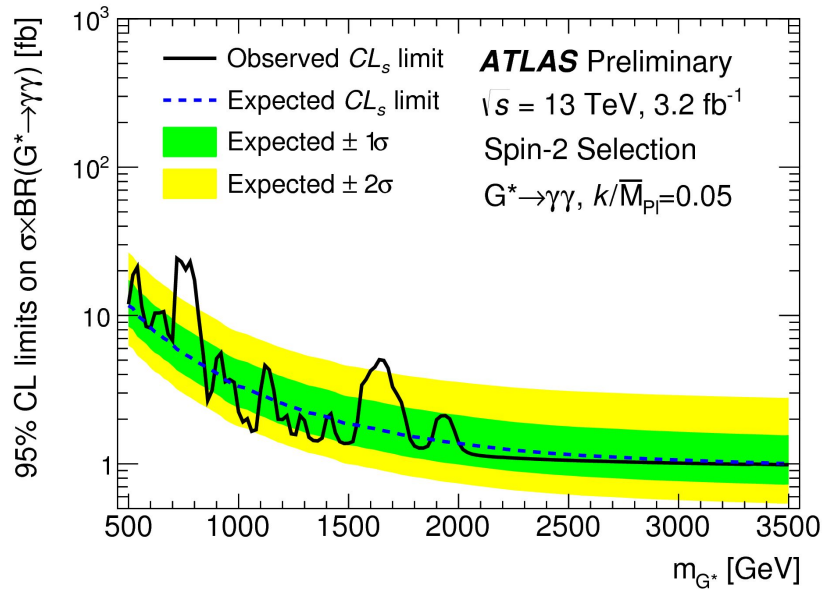
$$F = \frac{\frac{\sum_i (y_i - f_1(x_i))^2 - \sum_i (y_i - f_2(x_i))^2}{p_2 - p_1}}{\frac{\sum_i (y_i - f_2(x_i))^2}{n - p_2}}$$

- F has Fisher distribution $f(F; p_2 - p_1, n - p_2)$ if the added parameter is not improving the model
 - n is the number of bins in the distribution
- If $P < 0.05$, reject the hypothesis that an additional degree of freedom is useless

Cross section limits on spin-0 analysis



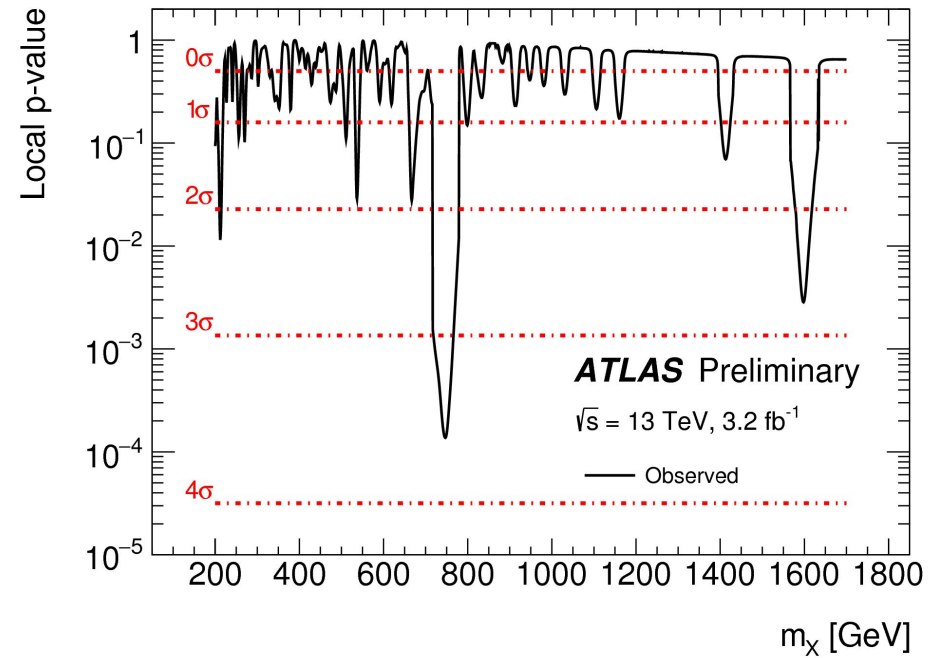
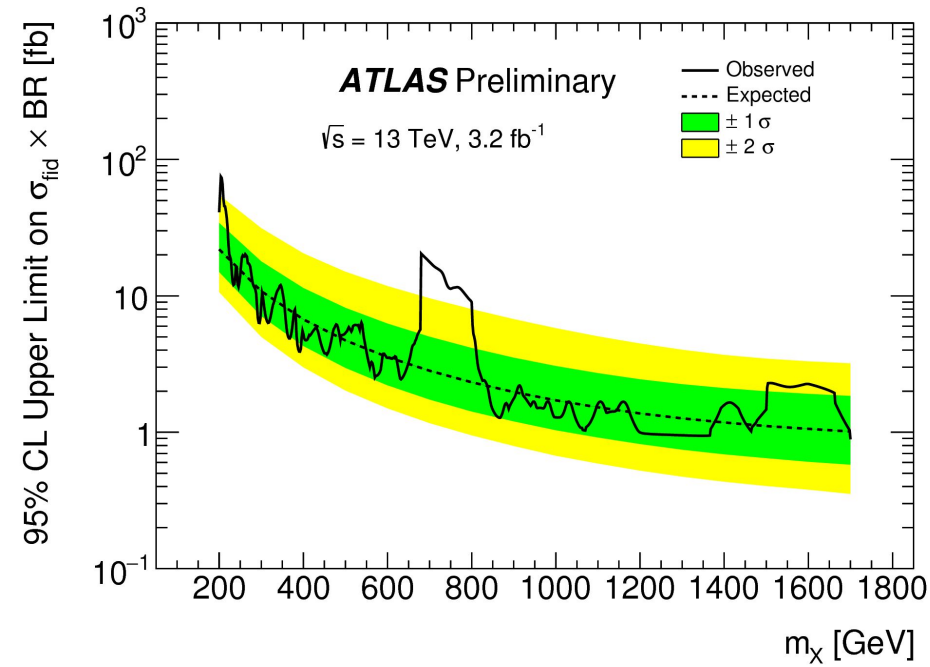
Cross section limits on spin-2 analysis



Analytic global significance

$$p_{\text{global}} \approx E[\phi(A_u)] = p_0 + e^{-u/2} (N_1 + \sqrt{u}N_2)$$

End of year results on spin-0

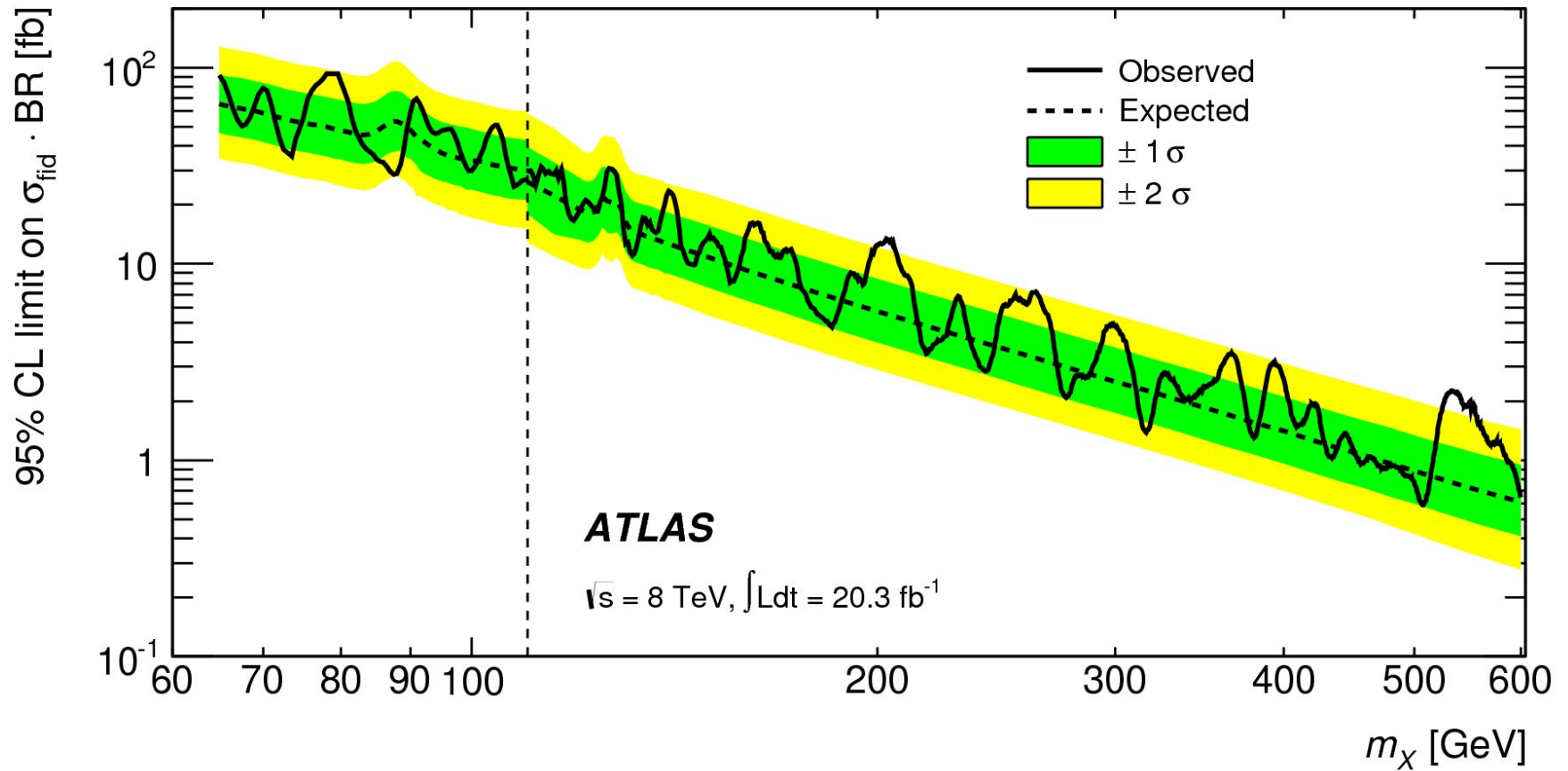


8 TeV selection

| Criteria | Scalar analysis | Graviton analysis |
|--------------------|---|---|
| Trigger | EF_g35_loose_g25_loose | |
| GRL | v61-pro14-02_DQDefects-00-01-00_PHYS_StandardGRL_All_Good | |
| LAr | LArError, TileError, event corruption | |
| vertex | At least one PV with 3 associated tracks or more | |
| Presel. | At least two photons passing loose ID, OQ, photon cleaning with $ \eta_{S2} < 1.37$ or $1.56 < \eta_{S2} < 2.37$ | |
| E_T cuts | $E_{T,1} > 0.4 \times m_{\gamma\gamma}$ and $E_{T,2} > 0.3 \times m_{\gamma\gamma}$ | $E_{T,1} > 50 \text{ GeV}$ and $E_{T,2} > 50 \text{ GeV}$ |
| Photon ID | Require both candidates to pass tight photon ID | |
| Isolation | $\begin{cases} E_T^{\text{iso,calo}} < 6 \text{ GeV} & \text{if } E_T < 80 \text{ GeV} \\ E_T^{\text{iso,calo}} < 6 \text{ GeV} + 0.7\%(E_T - 80 \text{ GeV}) & \text{if } E_T > 80 \text{ GeV} \end{cases}$ and $E_T^{\text{iso,track}} < 2.6 \text{ GeV}$ | $E_T^{\text{iso,calo}} < 8 \text{ GeV} - 0.07 \text{ GeV} + 4.8 \cdot 10^{-4} E_T + 2.6 \cdot 10^{-6} \frac{1}{\text{GeV}} E_T^2$ |
| $m_{\gamma\gamma}$ | $m_{\gamma\gamma} > 150 \text{ GeV}$ | |

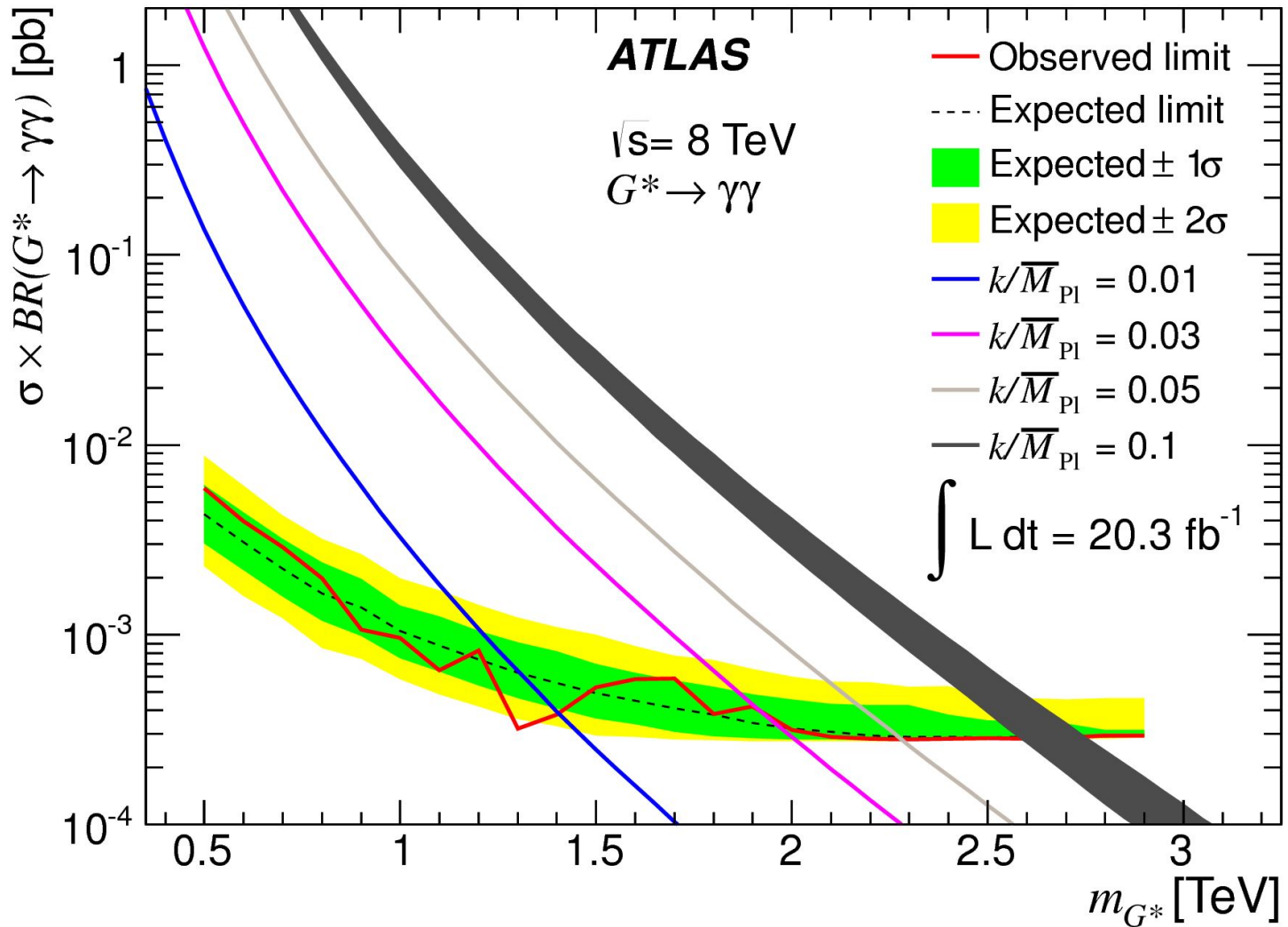
8 TeV scalar result

[Phys. Rev. Lett. 113, 171801](#)



8 TeV graviton result

[Phys. Rev. D 92, 032004 \(2015\)](#)



Andrey Loginov (1977-2016)

